Reliability of Engineering Materials

Edited by **Alrick L Smith,** BSc, HonsBSc, DPhil, DSc(Eng)

Butterworths
London Boston Durban Singapore Sydney Toronto Wellington

First published 1984

British Library Cataloguing in Publication Data

Reliability of engineering materials.
1. Strength of materials
I. Smith, Alrick L.
620.1'12 TA405

ISBN 0-408-01507-1

Library of Congress Cataloging in Publication Data

Main entry under title:

Reliability of engineering materials.

Papers from the First European Symposium on Materials Reliability held in Baden, Switzerland, Oct. 26, 1983, sponsored by EUREDATA (the European Reliability Data Banking Association)
Includes bibliographies.
1. Materials – Reliability – Congresses. I. Smith, Alrick L. II. European Symposium on Materials Reliability (1st : 1983 : Baden, Switzerland)
III. European Reliability Data Banking Association.
TA401.3.R45 1984 620.1'1 84-17618
ISBN 0-408-01507-1

Printed in England by Page Bros Ltd., Norwich, Norfolk

Preface

Engineering materials encompass a vast spectrum of characteristic types destined for performance in an equally vast spectrum of operating environments. Programmes aimed at new materials development, materials characterization and materials lifetime assessment are gaining impetus in the three geographic "units" of North America, Japan and Europe. A new discipline of "materials reliability", spawned from the application of reliability engineering techniques to materials science, is rapidly developing. In order to promote this discipline within Europe where, all too often, geographical barriers are compounded by language barriers, Motor-Columbus Consulting Engineers Inc., with headquarters in Switzerland, proposed hosting the "First European Symposium on Materials Reliability".

EUREDATA (the European Reliability Data Banking Association), an organisation of reliability data bank operators within Europe has, for some time, had an active working group investigating aspects of materials reliability data collection, storage and application. It was, therefore, agreed that EUREDATA would sponsor the Symposium with the objectives of bringing together a limited number of scientists and engineers, working in Europe on materials problems, to review and synthesize various fields of materials applications and thereby lay the foundations for the definition, assessment and applications of materials reliability in order to assist the furtherance of this discipline within Europe.

The chapters of this book represent the papers (some detailing work for the first time in the English language) presented at the First European Symposium on Materials Reliability, held in Baden, Switzerland, on 26 October 1983. The papers have been edited and arranged so as to constitute a logical and self-consistent presentation of the subject "Reliability of Engineering Materials". The comments expressed herein do not necessarily reflect the official policy of either Motor-Columbus or EUREDATA and any textual and related errors are the sole responsibility of the editor.

A.L. Smith
(Editor)

1 THE RELIABILITY OF ENGINEERING MATERIALS - INTRODUCTION AND OVERVIEW

A.L. Smith

Motor-Columbus Consulting Engineers, Baden, Switzerland

1.1 BACKGROUND

Engineering materials encompass a vast spectrum of characteristic types destined for applications in an equally vast spectrum of operating environments. It is useful, therefore, to categorize these materials into generic types, or classes, since reliability considerations regarding engineering materials are presently usually class-related.

Three broad classes of materials may be defined:

- Metals and metallic alloys
- Amorphous alloys (metallic glasses) and metallic composites
- Nonmetallics.

The latter class may be further subdivided, as follows:
. natural and synthetic rubbers
. plastics
. ceramics
. carbon and graphite
. natural composite materials.

The following comments are worth making in connection with some of these subdivisions:

Plastics

Plastics are that subclass of nonmetallics comprising thermoplastics and thermosetters. Thermoplastics (e.g. fluorocarbons, nylon, polyethylene, polypropylene, polystyrene, vinyls) all soften with increasing temperature and return to their original hardness when cooled. Most are meltable. Thermosetters (e.g. epoxy, polyesters, ureas) all harden when heated and retain their hardness when cooled. They "set" into permanent shape when heated under pressure.

Ceramics

Ceramic materials include brick, stoneware, porcelain, fused silica, glass, clay tile, concrete, abrasives, mortars and high-temperature refractories. In general, compared with metals, ceramics resist higher temperatures, have better corrosion and abrasion resistance (including erosion-corrosion resistance) and are better insulators. On the other hand, ceramics are brittle, weak in tension and subject to thermal shock.

Composite Materials

There is no really adequate definition of a composite material, but there are three main requirements for any acceptable composite material for use in engineering applications. These are /1/:

- It must consist of two or more physically distinct and mechanically separable materials.
- It should be able to be made by mixing the separate materials in such a way that the dispersion of one material in the other can be achieved in a controlled manner to ensure optimum properties.
- Its properties must be superior, and possibly unique in some specific respects, to the properties of the individual components.

Examples of natural composite materials are wood, bamboo, bone, muscle and other living tissue.

Metallic and amorphous alloys, metallic composites and thermoplastics constitute a group of synthetic composite materials termed microcomposite. (Natural composite materials also being microcomposites.) Engineered products such as galvanized steel, reinforced concrete, skis, etc. constitute a group of synthetic composite materials termed macrocomposite.

Most developmental work in engineering materials today is taking place with regard to composites (including plastic-based composites) and ceramics. Nevertheless, metals (and metallic alloys) and ceramics presently constitute over 90 % of world usage of engineering materials and, consequently, the chapters of this book will be primarily concerned with these two classes of materials.

1.2 FAILURE OF ENGINEERING MATERIALS

Engineering materials can be utilized for the construction of passive, active and what will here be referred to as "reactive" components and/or structures. Examples of the former include buildings, dams, storage tanks, containers, pipes (under cetain fluid-flow conditions), flanges, fasteners such as rivets, etc. Examples of the second class include pumps, motors, gears and all working machinery, etc. Examples of the latter class are basically passive components and/or structures which are subjected to continuously variable environmental stresses of a sufficiently large magnitude as to result in large-scale "response" of the structure. Specific examples which can be mentioned are pressure vessels, aircraft bodies, bridges and offshore oil platforms.

Sometimes passive components (e.g. pipes, tubing) can be combined to form a reactive component (e.g. oil platform) or even an active component (e.g. heat exchanger although it could be argued that this is a reactive component). A complete offshore oil-platform system, including topside equipment, actually constitutes a "composite structure" (not to be confused with a composite material) comprising passive (e.g. buildings), reactive (support structure) and active (e.g. pumps and other machinery) constituents. In the case of a heat exchanger (as will be discussed in Chapter 8) the failure of the active component is determined by the failure of its constituent passive components.

Applying the "bathtub", failure rate versus time, characteristic (Fig. 1.1) utilized in failure/reliability considerations on active components to reactive and passive components as well, one may make the following comments:

- In the case of reactive components/structures, design and testing (e.g. pressure tests on pressure vessels) ensure field operation of the component away from the infant mortality regime and design and in-service inspection ensure field operation of the component away from the wear-out regime.

- In the case of passive components, the same comments as made above are generally true, with the main difference being that more emphasis is placed on initial design and materials selection to ensure field operation in the useful life regime.

Whether one is dealing with active, reactive or passive components, engineering considerations strive to ensure that the plateau of the "bathtub" curve is as low and as long as possible. Cost considerations, naturally, limit both the extent and shallowness of the plateau. However, when safety considerations play an important role (such as in the case of a nuclear reactor pressure vessel, as will be discussed in Chapter 3) the shallowness of the plateau should lie in the region of 10^{-7} failures/year (a figure which is, however, still subject to intense international debate).

On the other hand, profit considerations relating to the industrial utilization of components require as long a plateau as possible. Only an optimization analysis can indicate whether the savings in cost (sometimes at the expense of increased risks) by not pushing for too long or too shallow a plateau are indeed not exceeded by expenditure on replacement parts. Broadly speaking, one might say that the subject of this book (the reliability of engineering materials) is concerned with deriving information on materials behaviour which can be used to maximize the useful life/minimize the failure rate of the components/structures fabricated from the material in question.

It is clear that reliability considerations of this nature can have important consequences for safety. Very often, however, the equally important cost consequences are often overlooked. Utilizing data available on the economic impact of materials failure in the USA /2,3/ and converting this to an inflation-adjusted per capita GDP figure, one can estimate that, for the EEC countries alone, the annual cost of materials failure and attendant conventional prevention efforts is in the region of SFr. 300,000 million. This figure is horrifying. (Its plausibility is substantiated by considering that the annual cost for zinc oxide painting to protect against rust, at just one particular European chemical plant, is over SFr. 5 million; also, the indirect cost, in losses due to one day's outage of a 1,000 MW class European nuclear power plant, caused by a failed condenser tube for example, is in the region of SFr. 1 million).

Efforts aimed at increasing existing knowledge about the failure of engineering materials in an effort to utilize this additional knowledge to reduce such failures are, without doubt, justified.

1.3 THE CLASSIFICATION AND SOURCES OF FAILURE IN ENGINEERING MATERIALS

When can an engineering material (or component/structure fabricated from the material) be considered to have failed? For instance, a support beam, when fractured and without additional struts or ties, can be regarded as having "failed". A waste-disposal storage tank containing highly toxic or radioactive liquid waste can be regarded as having "failed" when it begins to leak (although the consequences of the leak or failure will be dependent upon the magnitude of the failure and its capabilities for imparting damage).

However, with a toothed gear, for example, if the crown of one of the teeth fractures (and provided the broken-off portion is small and is ejected without causing seizure of the gear) the gear can continue functioning and cannot be considered to have "failed". On the other hand, even in the absence of fracture, when the teeth are sufficiently worn to prevent the gear from rotating at all, the gear can be regarded as having "failed". (Note that in both cases the material itself can be regarded as having "failed".) For this reason, one cannot speak of a failure of a component/structure without reference to either its intended function or use to which it is to be put. By including such reference, not only is it possible to talk of failure, but one can then readily define failures of even passive components. A definition of the "reliability" of an engineering material is then feasible (although inherent difficulties in achieving consistency in the use of any such definition in the various fields of materials applications will be highlighted throughout this book).

Generally, an engineering material can be considered to have failed when the component/structure fabricated from the material fails to perform its intended function with the required efficiency. One may, therefore, define the reliability of an engineering material (analogous to the definition of the reliability of an active component) as the probability of non-failure of the engineering material, in a specified use or application, in a specified interval of time in a specified environment. One may then say that the assessment of the reliability of a material is the assessment of the probable lifetime of the material before failure in a specified application. A related aspect, which is of considerable economic significance, is the assessment of the potential residual lifetime (lifetime beyond the

assessed probable life) of materials in various applications, for example high-temperature gas turbines, as will be touched upon in Chapter 5.

The following list /4/ provides a useful classification of failures:

- Yielding of the component material under static loading. Yielding causes permanent deformation which could result in misalignment or hindrance to mechanical movement.

- Buckling, which takes place in slender columns when they are subjected to compressive loading, or in thin-walled tubes when subjected to torsional loading.

- Creep failure, which takes place when the creep strain exceeds allowable tolerances and causes interference of parts. In extreme cases failure can take place through rupture of the component subjected to creep. In bolted joints and similar applications, failure can take place when the initial stressing has relaxed below allowable limits, so that the joints become loose or leakage occurs.

- Failure due to excessive wear, which can take place in components where relative motion is involved. Excessive wear can result in unacceptable play in bearings and loss of accuracy of movement. Other types of wear failure are galling and seizure of parts.

- Failure by fracture due to static overload. This type of failure can be considered as an advanced stage of failure by yielding. Fracture can be either ductile or brittle.

- Failure by fatigue fracture due to overstressing, material defects or stress raisers. Fatigue fractures usually take place suddenly without apparent visual signs.

- Fracture due to impact loading, which usually takes place by cleavage in brittle materials for example in steels below brittle-ductile transition temperature.

- Failure due to the combined effect of stresses and corrosion, which usually takes place by fracture due to cracks starting at stress concentration points, for example caustic cracking around rivet holes in boilers.

More detailed considerations of failure by corrosion will be presented in Chapters 7 and 8.

The sources of failure in engineering materials can be generally identified as one (or more) of the following:

- Design deficiencies (e.g. lack of engineering effort to avoid design features known to be conducive to failure, inadequate or erroneous stress analyses, etc.)
- Material selection deficiencies (e.g. specifying materials with inappropriate microstructure or with irremovable imperfections or flaws)
- Processing deficiencies (e.g. improper heat treatment)
- Assembly and installation errors (e.g. unsatisfactory welding, post-fabrication maltreatment - pitting resulting from electrolytic cleaning for instance, etc.)
- Operational and maintenance errors
- Environmental impacts (usually impacts resulting in previously unforeseen stresses or effects that can induce unforeseen failure mechanisms. The effect of the environment is clearly demonstrated in Table 1 which indicates the influence of three different environments on the fatigue strength of four mirror-polished steels of differing ultimate tensile strengths.)

Table 1: Environmental Effects on Fatigue Strength of Mirror-Polished Steels of Differing Ultimate Tensile Strength

Ultimate Tensile Strength (MN/m2)	Maximum Endurance Strength as a Percentage of Maximum Endurance for Steel in:		
	Air	Fresh Water	Salt Water
280	100	72	52
560	100	53	36
1,120	100	25	17
1,540	100	19	14

To reduce the overall impact of materials failure, the above sources (or causes) of failure must be eliminated or reduced through:

- Improved designer/manufacturer/installer/operator reliability

- Improved knowledge concerning materials properties and behaviour (including improved storage of, and access to, relevant data) under different circumstances

- Improved methods for forecasting materials behaviour, and greater accuracy in lifetime assessment, under environmental uncertainties

- Improved materials technology and manufacturing/processing techniques (including the use of "superior" materials, wherever applicable). An example is hot isotatic pressing (HIP). Fig 1.2/5/ depicts the stress-rupture properties of cast, hafnium modified B-1900 alloy at 760 °C and 650 MPa without and with HIP and the improvements as a result of the improved technology are clearly apparent.

1.4 ASPECTS CONSIDERED IN THIS BOOK

An attempt has been made in the chapters which will follow to consider in greater detail the various aspects referred to above. One particular aspect which has not, however, been considered is the impact of the radiation environment on materials, since this has not too long ago received sophisticated treatment elsewhere /6/.

Whilst one may readily appreciate that it is not meaningful to attempt to talk about the reliability of a material without reference to the applicable environment, what is often forgotten is the fact that this implies reference to structural properties since it is these which determine the "contact" between the material and its environment. This can clearly be understood by considering that a solid cube of iron in a corrosive environment will support an object placed on top of it for a longer period of time before failure of the support than will the same mass of iron in the same environment when the iron is a thin-walled hollow cubic structure. Thus, structural aspects should not be forgotten in any considerations on materials reliability.

In this book, structural aspects such as have already been treated in /7/ for example, will not, however, be considered. Instead, in Chapter 2, a novel method for modelling component structural integrity, with the objective of determining failure probability, is presented. Problems relating to data distributions for toughness and defect size are discussed and the fracture mechanics approach is fully employed. These metallic materials fracture mechanics considerations are followed on in Chapter 3 by the development of a mathematical definition of materials reliability and the application of an international benchmark exercise to the assessment of the failure probability of a light-water reactor pressure vessel. The influences of the selection of, and dispersion in, input data are considered in more detail and implications for non-destructive examination (NDE) are assessed. In Chapter 4, fracture mechanics considerations, together with strength distribution and critical flaw size aspects, are applied to non-metallic (cementitious) materials. The role of the microstructure as a factor in reliability considerations is emphasized.

In Chapter 5, high-temperature behaviour of metallic materials is treated, once again emphasizing the importance of microstructure. A novel approach to interpreting the term "reliability" is adopted through a careful consideration of the dispersion in data measurements. Chapter 6 takes the question of data in high-temperature applications a stage further by considering storage, retrieval and interchange of such data using computerized data banks. A specific European high-temperature materials data bank is described. Materials reliability data banking in the chemical industries is discussed in Chapter 7, where corrosion problems are highlighted. The possible use of zirconium as a material in urea reactors is also given attention and it is interesting to note improved component reliability obtained elsewhere /8/ through the utilization of this metal. Teledyne Wah Chang, amongst other interesting results, report that whereas malleable iron flanges for stripper columns and impervious graphite heat-exchanger tubes in a particular chemical process had a lifetime of a few years, replacement by substitutes fabricated from zirconium R60702 resulted in the flanges lasting the life of the column and the heat-exchanger tubes showing no signs of corrosion after even eight years' service.

The final chapter extends the corrosion considerations of Chapter 7 to heat exchangers, primarily from the standpoint of large power plant condensers. An expression for the mean time between failures of the condenser, in terms of number of tubes, is established and the modes and causes of tube failure are discussed in detail, together with methods for combatting such failure. This work complements the discussion on heat-exchanger reliability recently presented in /9/.

REFERENCES

/1/ Hull D. - An Introduction to Composite Materials, Cambridge University Press, Cambridge, 1981.

/2/ Duga J. - The Economic Effects of Fracture in the United States, Parts 1 and 2, US Department of Commerce, Washington, 1983.

/3/ Fontana M.G. and Greene N.D. - Corrosion Engineering, McGraw-Hill Kogakusha, Tokyo, 1978.

/4/ Forag M.M. - Materials and Process Selection in Engineering, Applied Science Publishers, London, 1979.

/5/ Hanes H.D. and McFadden J.M. - HIPing of Castings: An Update, "Metal Progress", April 1983.

/6/ Roberts J.T.A. - Structural Materials in Nuclear Power Systems, Plenum Press, New York, 1981.

/7/ Thoft-Christensen P. and Baker M.J. - Structural Reliability Theory and its Applications, Springer-Verlag, Berlin, 1982.

/8/ Materials Progress News, "Metal Progress", November 1983.

/9/ Collier J.G. - Reliability Problems of Heat Transfer Equipment, "Atom", August 1983.

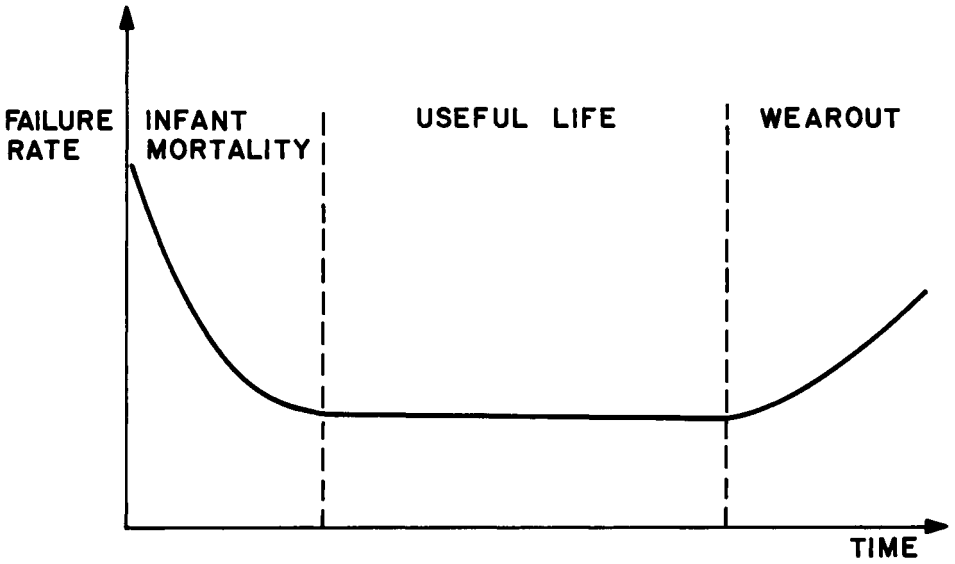

Figure 1.1: The Failure Rate-Age "Bathtub" Curve

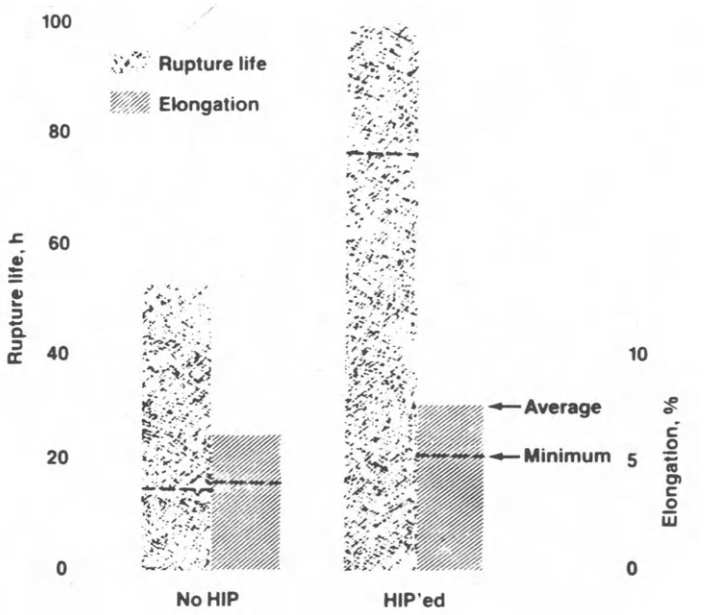

Figure 1.2: Stress-Rupture Properties of Cast, Hafnium Modified B-1900 Alloy /5/

2 STRUCTURAL INTEGRITY MODELLING

V. Pistone, S. Venzi and G. Re

SNAM S.p.A., S. Donato Milanese, Italy

2.1 INTRODUCTION

The prevention of structural failures (ensuring structural integrity) naturally assumes an important role in industrial safety philosophy. Appropriate plant design, suitable material production and present-day manufacturing procedures for the pressure vessels, tanks and pipes generally used in, for example, the chemical industry, all contribute towards ensuring satisfactory levels of safety against structural failures. In fact, the data gathered on accidents show trouble to be due to occasional errors, rather than to faulty design or procedures.

Because of possible errors arising during production and manufacturing, the material may be less tough than required; the welding process, for example, may even cause defects or cracks which eventually grow, in-service, under fatigue or by stress corrosion cracking. If such a situation occurs, it is necessary to decide whether or not the structure in question should be removed and replaced, when inspection has indicated the presence of flaws, for example.

Since the decision process is related to cost, as well as safety considerations, it contains an element of chance. One is, therefore, ultimately concerned with assessing the failure probability of the particular structure. For present purposes, the structure considered will be a pressure vessel and failure probability, in this context, is an index of the soundness of the structure. To determine the failure probability, a suitable modelling procedure must be developed and tested against historical failure data. Such a procedure is here presented. Caution, of course, is essential when comparing model results against the failure probability obtained from historical data.

2.2 FRACTURE MECHANICS MODEL

Here, the failure probability is calculated with the aid of a simple fracture mechanics model which considers three main factors: defect size, applied stress and material toughness. The temporal variation of the input parameters is not considered - failure probability is calculated at a given moment of the vessel's life, the material characteristics and defect size at that moment being known.

Unfortunately, the available elastic-plastic fracture mechanics formulae are not as precise as those for linear-elastic fracture mechanics. Therefore, either an existing method for the verification of defect tolerability is chosen, or a new one has to be developed and verified. At SNAM, a model has been proposed that distinguishes toughness-governed from plastic collapse-governed failure. This approach, despite being essential for thin-walled structures, has not been employed in other models.

When the material toughness, measured by the crack opening displacement (COD), exceeds a certain limiting value

$$COD_{lim} = \alpha \pi \varepsilon_y a(1-a/t)^2 = \delta$$

where α is a constant, ε_y the yield strain, a the depth of a surface defect and t the thickness, the ligament underneath the defect fails by plastic collapse; otherwise, brittle fracture occurs. (This procedure is also used for measuring material toughness of small test specimens.)

Fig. 2.1 shows the flow diagram for the model calculation procedure; Fig. 2.2 gives the formulae used to calculate the critical stresses and symbols are defined in Fig. 2.3. A comparison is made between the critical and applied stresses and the 'safety factor' subsequently calculated.

2.3 MODEL ACCURACY

Model acceptability has been verified on the basis of literature data concerning tests made on pressure vessels with a longitudinal notch and on plates with a central notch.

The coefficient α in the COD_{lim} formula depends on the geometry considered; in this case it was assumed to be constant and set equal to 2.5, by optimizing a first set of 378 data.

To date, 691 tests have been recorded and incorporated; the results are shown graphically in Fig. 2.4 and demonstrate a fair overall agreement between model and test results. It should be noted that scattering is due partly to uncertainties in the formulae and partly to toughness variations; this scattering would also occur when using more correct formulae.

Table 1: Predicted Results from Model Compared with Test Measurements

	Surface Defects			Through-Thickness Defects		
	Total Number of Measurements	Incorrectly Predicted	Error (%)	Total Number of Measurements	Incorrectly Predicted	Error (%)
Plates						
Ductile	83	18	22	45	37	82
Brittle	47	3	6	253	55	22
Pipes and Vessels						
Ductile	152	53	35	44	8	18
Brittle	7	0	0	60	5	8
Total	289	74	26	402	105	26

Table 2: Modes of Fracture (B = Break, L = Leak) Compared with Experimental Data

Predicted	Experimental	Number of Instances	% of Total Instances
L	L	36	22
L	B	11	7
B	B	84	52
B	L	29	18

Tables 1 and 2 provide a summary of predicted results compared with test measurements and acceptability of the model output results is evident, although there is some non-conservativeness in predicted through-thickness defects for ductile failure of plates. However, the number of cases when a leak was predicted instead of a break is low.

When calculating failure probability, the greatest uncertainties concern material toughness and defect size. Factors to account for the uncertainty in both of these are therefore taken into consideration and the procedure is demonstrated by reference to a simple calculational exercise concerning the flaws caused by an automatic welding process, discussed below.

2.4 TOUGHNESS MEASUREMENT

British Standard 5762 of 1979 /1/ sets forth the procedure for COD measurement on a test piece, the COD being taken as an index of the material's fracture toughness.

The variation in toughness of carbon steels with temperature follows a typical S-shaped pattern, going from low toughness brittle fracture to high toughness values, which ensures that the material will tolerate rather large defects and which can easily be detected by non-destructive examination (NDE). Fig. 2.5 is typical of such a situation; additionally, it shows that when the number of tests at the relevant temperature increases, scattering becomes quite large with low COD values appearing and indicating possible brittle fracture. This scattering is an intrinsic characteristic of all materials and becomes more severe at a weldment, since this is a non-homogeneous zone where toughness varies almost from spot to spot. (The usual COD test-piece is rectangular and its height equals plate thickness; the notch is perpendicular to the surface and thus affects all welding passes.)

A notch nominally located at the heat affected zone (HAZ) affects three metallurgically different zones. If sufficient information on defect orientation is available, the fatigue notch tip can be located in the area where the defect tip lies, using a square test piece notched parallel to its surface. However, if this area is very narrow, accurately locating the tip might not be possible because of the curvature of the fatigue front.

When faced with such a significant scattering the question arises whether a suitable statistical distribution for the COD data can be determined so as to be able to evaluate the parameters, given a small number of tests. In practice, the two functions mostly used are the lognormal function and Weibull two-parameter function /2,3/. Both are defined for values greater than zero only and have no upper limit. From the authors' experience, there is no reason to believe that the COD values will preferably follow either distribution.

COD readings taken at the weld metal and HAZ for a welding process adopted for pipeline girth welds are given in Figs. 2.6 and 2.7. These measurements are presented in Fig. 2.8 on Weibull probability paper and in Fig. 2.9 on lognormal paper. Without recourse to any statistical tests, it can be seen that the weld metal data are much more inconsistent and do not follow either distribution. When the number of tests is increased, scattering does not increase proportionally because of a physical limitation to toughness values. For the materials and thicknesses concerned, the lower limit COD can be set at 0.01 mm and the upper limit at 2 mm.

2.5 DEFECT SIZE DETERMINATION

With regard to defect size, either one of the following two situations will apply:

1) The material has low toughness and the actual or possible defects occurring in service need to be assumed.

2) Defects have been detected and data on their size are available. This situation will evidently also supply information for the former.

To be able to evaluate failure probability, the following really need to be known:

- Defect density (number of defects per metre of weldment)

- Position of the defect across the thickness

- Defect depth and length distribution.

When data on size are obtained by NDE, account needs also to be taken of defect detection uncertainty. Studies carried out on behalf of the nuclear

industry indicate a fairly high probability for a defect going undetected or, when detected, for its size being misjudged /4/. At small thicknesses, certain researchers draw a far from encouraging picture. As an example, no correlation of defect size with ultrasonic echo amplitude appears in Fig. 2.10 (although slightly better correlation was found when averaged over several NDE operators) /5/.

For the weldment considered in this exercise, defect depth was measured on the fracture surfaces of test pieces welded by a similar process and fractured by fatigue. As proposed in /6/, the depth data (plotted in the histogram of Fig. 2.11) were assumed to follow a Weibull distribution as presented in Fig. 2.12. Fig. 2.13 shows the length of the defects detected by NDE in 30 weldments; the data are presented on lognormal paper in Fig. 2.14. Since this inspection was very carefully performed in the laboratory, with both ultrasonic and X-ray equipment, inspection uncertainty can be neglected as a first approximation. Note that field use of NDE would have eliminated a portion of the cracks over 50 mm in length.

The authors have no information at their disposal to permit an assessment of the probability of rejecting a defect depending upon its size; this naturally affects both the derived number of weld defects and the fracture mechanics calculation. For the type of defect being considered here, length and depth can be assumed to be uncorrelated and since length is secondary for defect tolerability, the consequences of NDE for length distribution determination may be disregarded. Defect density in this case is 44/30 = 1.47 defect per weldment (18 thereof being X-ray detected - X-rays also being used in field inspection - and having length greater than 50 mm). By prior use of field inspection, defect density would drop to (44 - 18)/30 = 0.87 per weldment.

2.6 FAILURE PROBABILITY CALCULATION

Failure probability is calculated by the Monte Carlo method: For each procedure, a value is extracted from each random variable and a final count of failure causes is made at the end. For the type (lack of fusion) and position of the defects considered, failure occurs along the less tough of either the weld metal or the HAZ.

The applied stress is the nominal design stress, 334 MPa, thickness is 19 mm, yield strength 448 MPa and ultimate tensile strength 531 MPa. Any variation of these values is assumed to be negligible with respect to uncertainties concerning toughness and defect size. (In the program, any COD value below 0.01 mm is set at this value.) The number of extractions was limited to 10^4.

Failure probability, calculated assuming a lognormal COD distribution, is 2×10^{-3} per defect. By multiplying by crack density, one obtains a probability of failure of 1.7×10^{-3} per weldment. With a Weibull distribution, the failure probability becomes 5.1×10^{-3} per weldment. All are brittle failures, according to the model, and cause breakage. The straightforward use of the experimental histograms of toughness values (Figs. 2.6 and 2.7), assuming that no lower COD values would be found when increasing the number of tests, results in no failures in 10^4 extractions.

2.7 EXAMPLE OF APPLICATION TO A THIN-WALLED TANK

The model has been used to calculate the failure probability for a population of stress-corrosion cracked thin-walled tanks /7/.

Crack length had been obtained with fair precision by magnetoscopic inspection; the depth was assumed to follow an exponential distribution. The cracks were subdivided into those lying parallel to the weld bead and those lying transversal (Fig. 2.15), since they differed in their shape and average size and were submitted to a different pattern of residual stresses.

Failure probability was calculated separately for both cases, in this instance raising the number of extractions to 10^6; the results were combined according to the fault-tree shown in Fig. 2.16 yielding an overall probability of 4.65×10^{-4}.

2.8 CONCLUSIONS

The simple exercises presented here illustrate the difficulty of suitably describing the failure of a structural element when account is taken of the

statistical variability of the governing parameters. Specifically for toughness, neither of the considered probability functions accounts for the limits of the COD range and correctly represents the COD distribution.

The Monte Carlo method, when utilized with a simple fracture mechanics model, does provide results in terms of failure probability of the structural element. It is felt that, the current unreliability of the results notwithstanding, no other approach can be taken in view of the wide variation in values such as fracture toughness in the transition range and defect size. An expanded effort to refine the mathematical tools and to enhance data collection might lead to better results and to the specification of failure probabilities that would actually indicate the reliability of the structure concerned.

REFERENCES

/1/ BS 5762 - Methods for Crack Opening Displacement Testing, BSI, London, 1979.

/2/ Johnston G.O. - Toughness Distributions in Two Steels, Weld. Inst. Research Report 106, 1979.

/3/ Johnston G.O. - Interim Progress Report on Toughness Distributions in a Submerged Arc Weld, Weld. Inst. Research Report 110, 1980.

/4/ Dufresne J. - Probabilistic Application of Fracture Mechanics, Advances in Fracture Research, pp. 517 - 581, 1981.

/5/ Førli O., Pettersen B. - Reliability of Ultrasonic and Radiographic Testing, Fitness for Purpose Validation of Welded Constructions, London, 17 - 19 November 1981.

/6/ Rogerson J.H. - Weld Defect Distributions in Offshore Structures and their Influence on Structural Reliability, OTC 9237, Offshore Technology Conference, 1982.

/7/ Venzi S., Sinigaglia D., Pistone V. - Modello per la valutazione della tollerabilità dei difetti e sua applicazione al calcolo della affidabilità di serbatoi in pressione, Affidabilità nella progettazione meccanica, Roma 31 maggio 1982.

/8/ Dawes M.G. - The Crack Opening Displacement (COD) Design Curve Approach to Crack Tolerance, Tolerance of Flaws in Pressurized Components, I. Mech. 5, pp. 21 - 36, 1978.

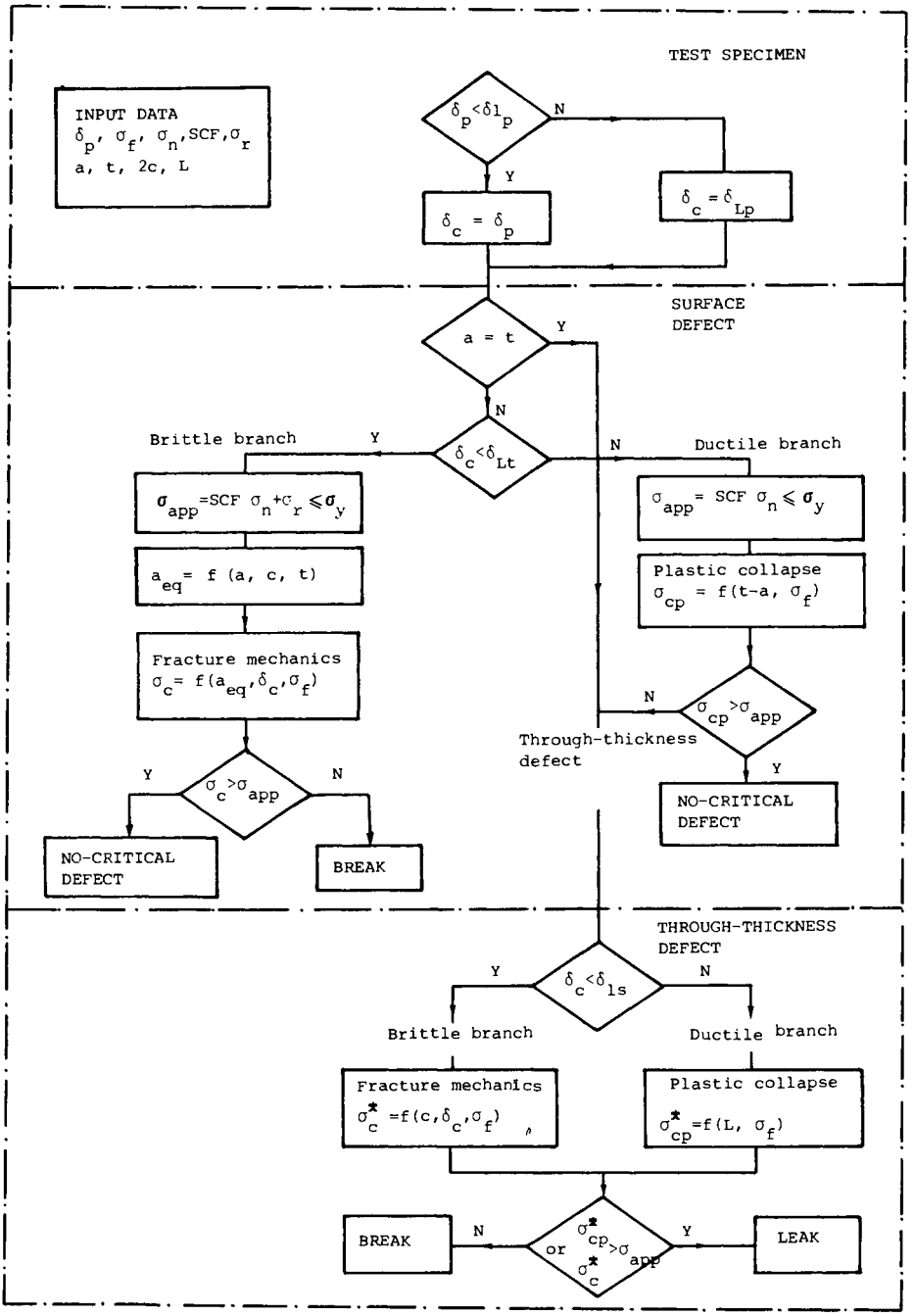

Figure 2.1: Flow Diagram for Model Calculational Procedure

PLASTIC COLLAPSE

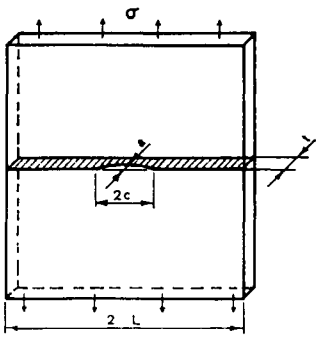

FRACTURE MECHANICS

$$\sigma_{cp} = \sigma_f \left[1 - \frac{\pi\, ac}{2t(2c+t)}\right] \frac{1-a/t}{1-a/(1.1\,t)}$$ SURFACE DEFECT

$$\sigma_c = \frac{2}{\pi}\sigma_f \arccos\left[\exp\left(-\frac{\pi E \delta_c}{8\sigma_f\, a_{eq}}\right)\right]$$

$$\sigma^*_{cp} = \sigma_f\left(1 - \frac{c}{W}\right)$$ THROUGH THICKNESS DEFECT

$$\sigma^*_c = \frac{2}{\pi}\sigma_f \arccos\left[\exp\left(-\frac{\pi E \delta_c}{8\sigma_f\, c}\right)\right]$$

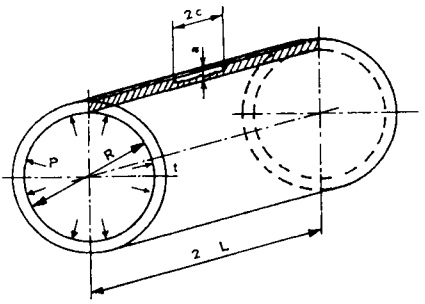

$$\sigma_{cp} = \sigma_f \left[\frac{1-a/t}{1-a/(Mt)}\right]$$ SURFACE DEFECT

$$\sigma_c = \frac{2}{\pi}\sigma_f \arccos\left[\exp\left(-\frac{\pi E \delta_c}{8\sigma_f\, a_{eq}}\right)\right]$$

$$M = \left(1 + 1.61\,\frac{c^2}{Rt}\right)^{1/2}$$ THROUGH THICKNESS DEFECT

$$\sigma^*_c = \frac{1}{M}\sigma_f \frac{2}{\pi} \arccos\left[\exp\left(-\frac{\pi E \delta_c}{8\sigma_f\, c}\right)\right]$$

$$\sigma^*_{cp} = \frac{\sigma_f}{M}$$

Figure 2.2: Formulae for Critical Stress Calculation

a	depth of a surface defect
a_{eq}	equivalent depth of a defect
$2c$	length of a defect
L	residual ligament for a through-thickness defect
SCF	stress concentration factor
t	thickness
α	constant of the limiting COD formula
δ	crack tip opening displacement (COD)
δ_c	critical COD
δ_{Lp}	limiting COD for the test specimen
δ_{Ls}	limiting COD for the structure (through-thickness defect)
δ_{Lt}	limiting COD for the structure (surface defect)
δ_p	COD measured on the test specimen
ε_y	yield strain
σ_{app}	applied stress
σ_c	critical stress for brittle fracture
σ_{cp}	critical stress for plastic collapse
σ_f	flow stress
σ_n	nominal stress
σ_r	residual (internal) stress

Figure 2.3: List of Symbols

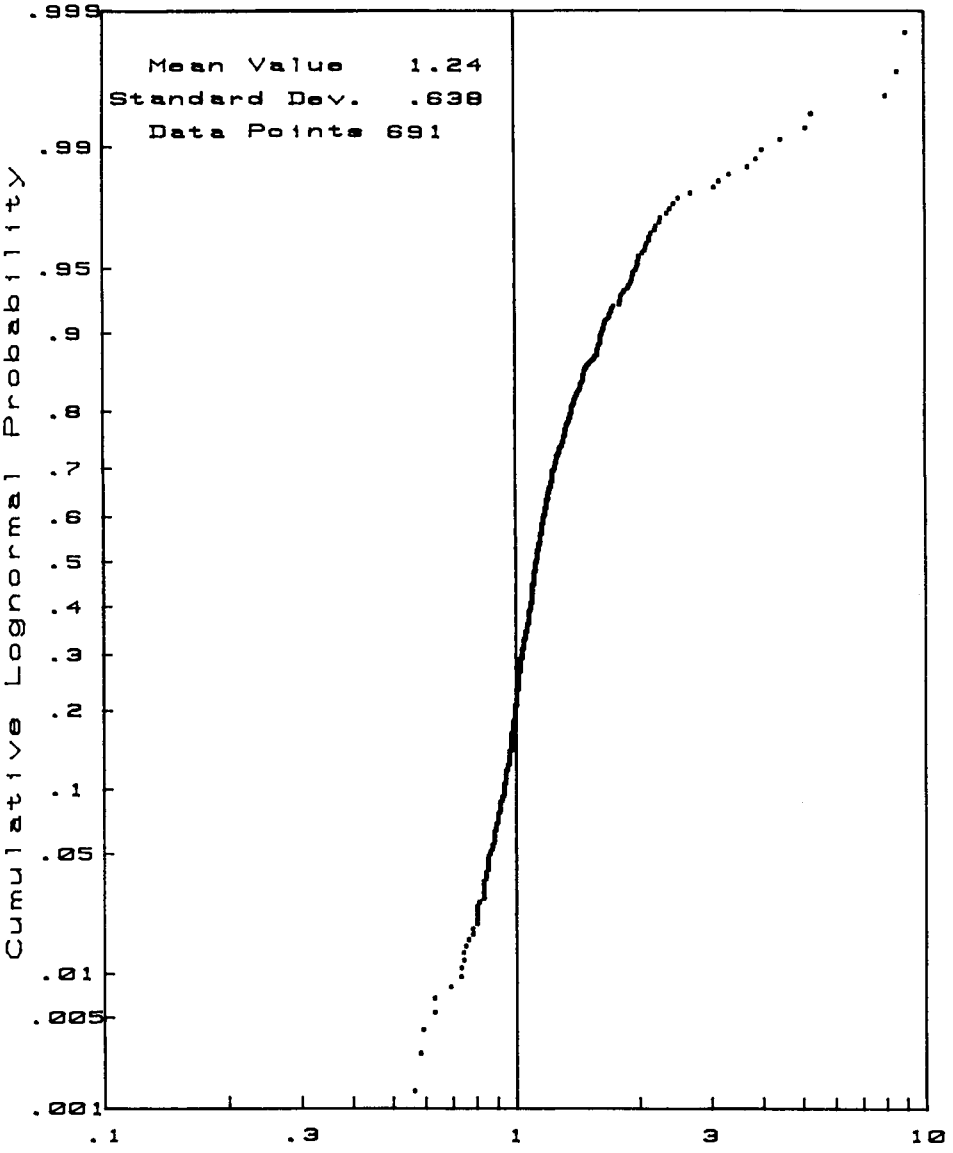

Figure 2.4: Cumulative Lognormal Plot of the Safety Factor Values Calculated According to the Model, Based on 691 Tests on Vessels and Wide Plates

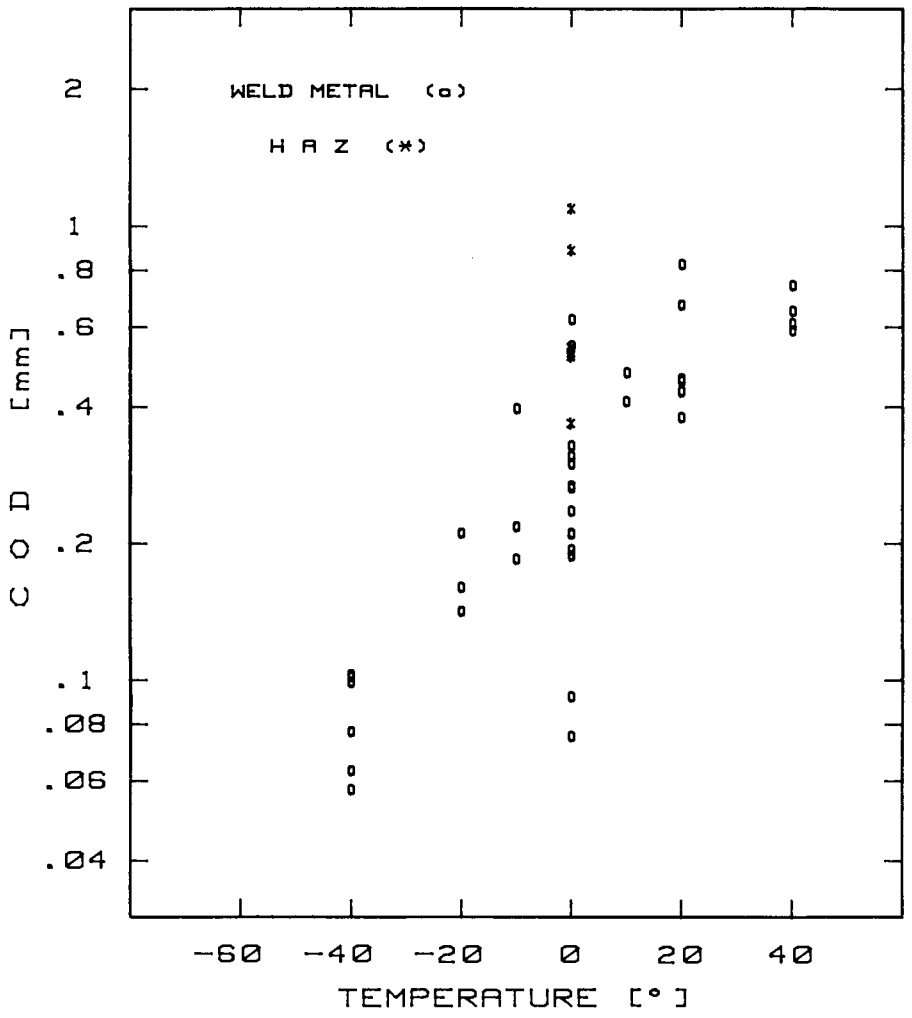

Figure 2.5: Transition Curve of COD Values of a Welding Process

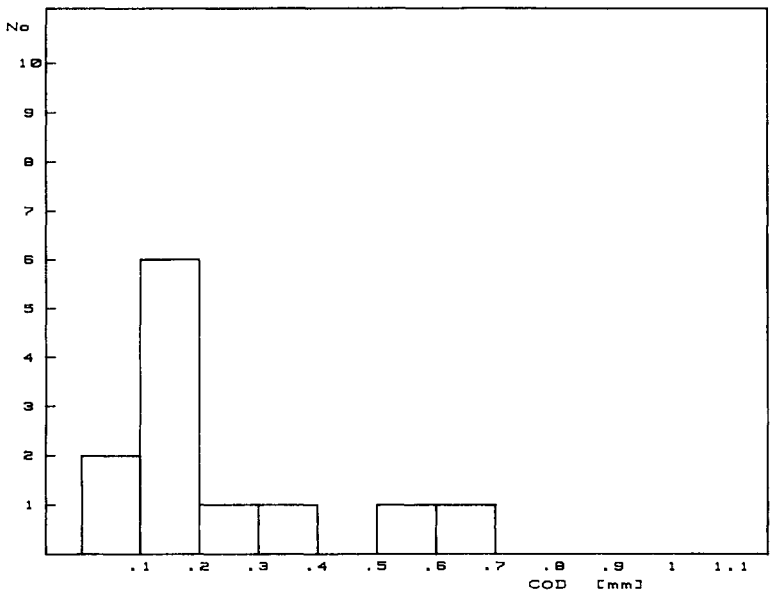

Figure 2.6: Histogram of COD Values of a Welding Process (Weld Metal)

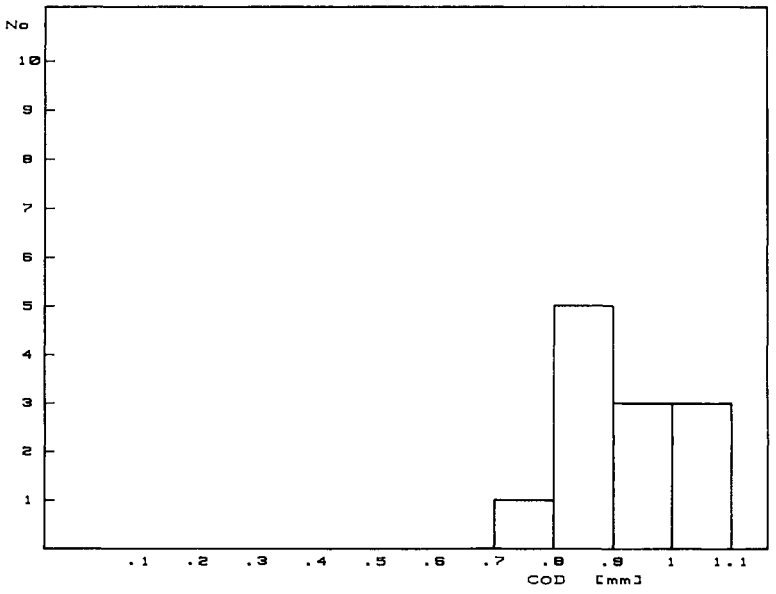

Figure 2.7: Histogram of COD Values of a Welding Process (HAZ)

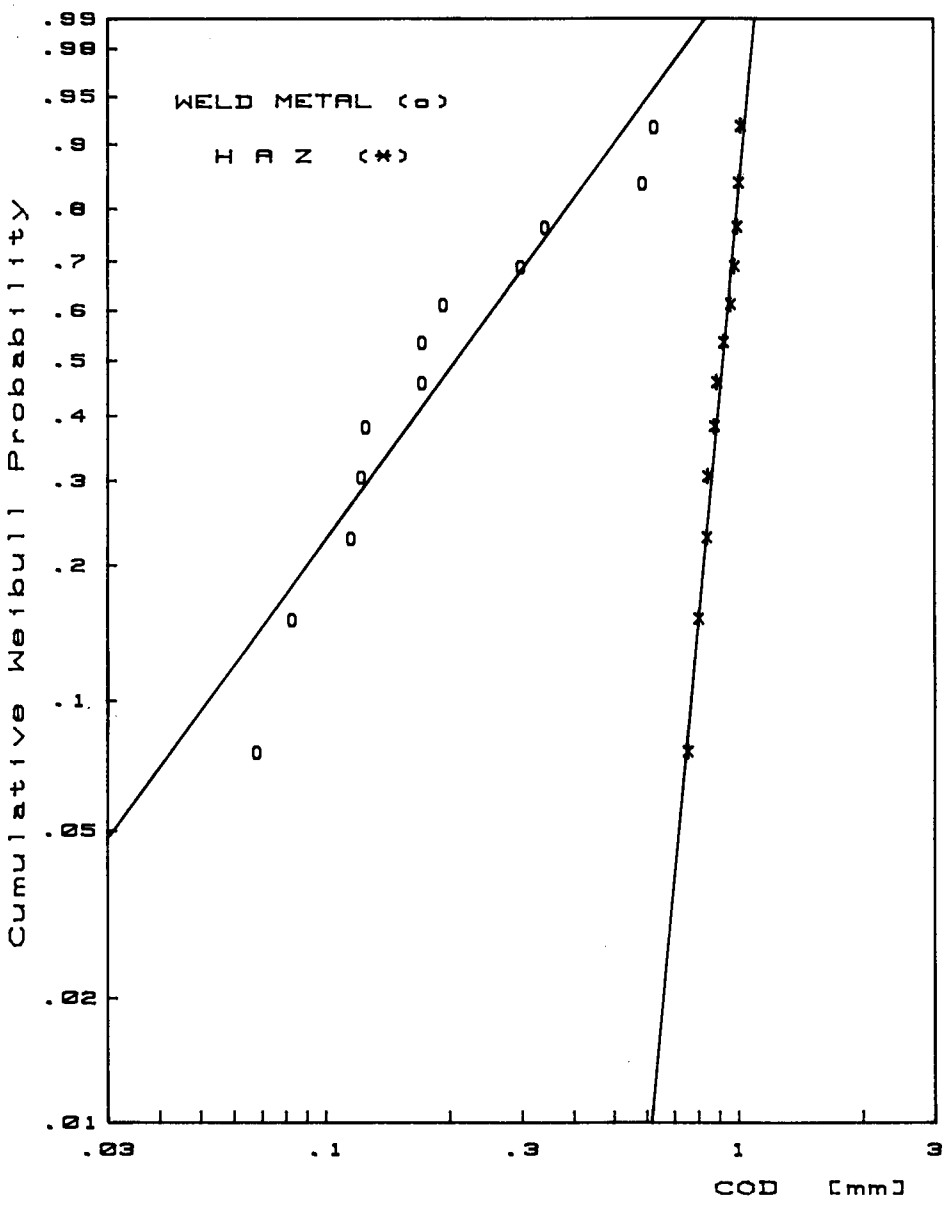

Figure 2.8: Cumulative Weibull Plot of COD Values Shown in Figures 2.6 and 2.7

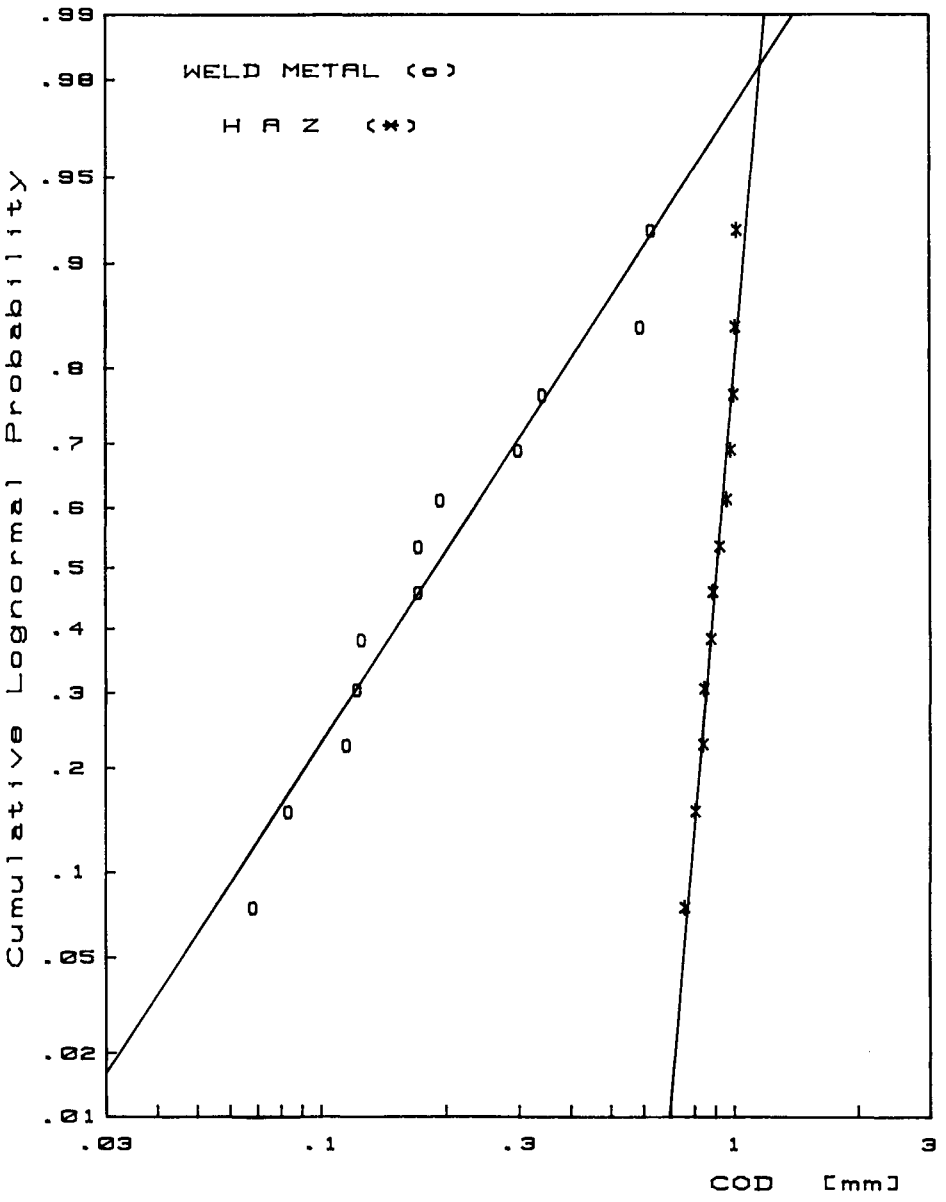

Figure 2.9: Cumulative Lognormal Plot of COD Values Shown in Figures 2.6 and 2.7

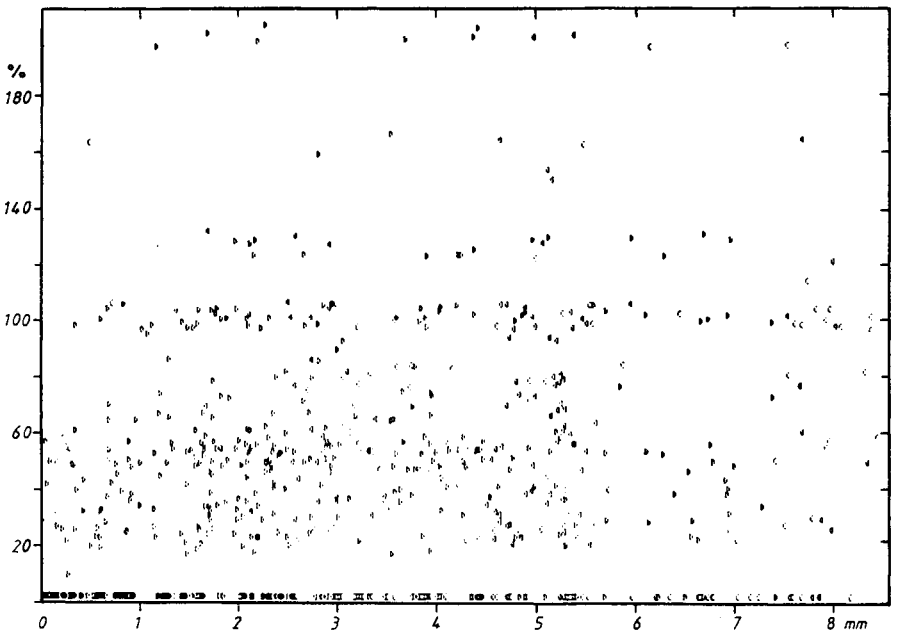

Figure 2.10: Comparison Between Real Depth and Ultrasonic Echo Amplitude for Lack of Fusion and Lack of Penetration Defects /5/

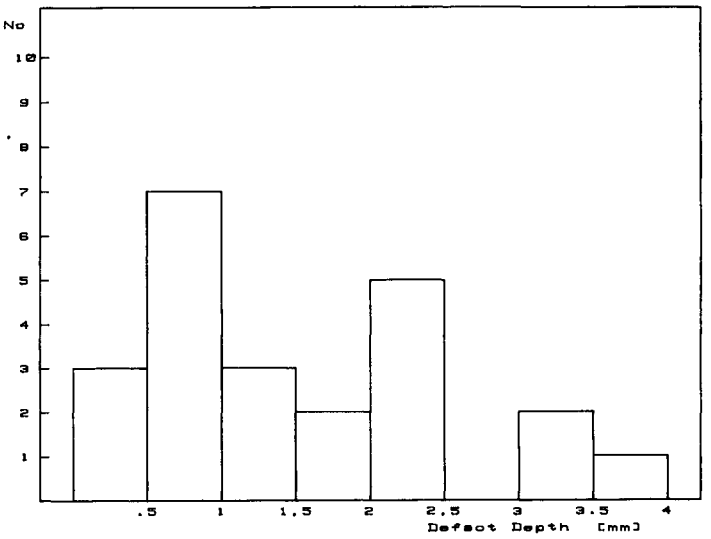

Figure 2.11: Histogram of the Defect Depth in Pipeline Girth Welds

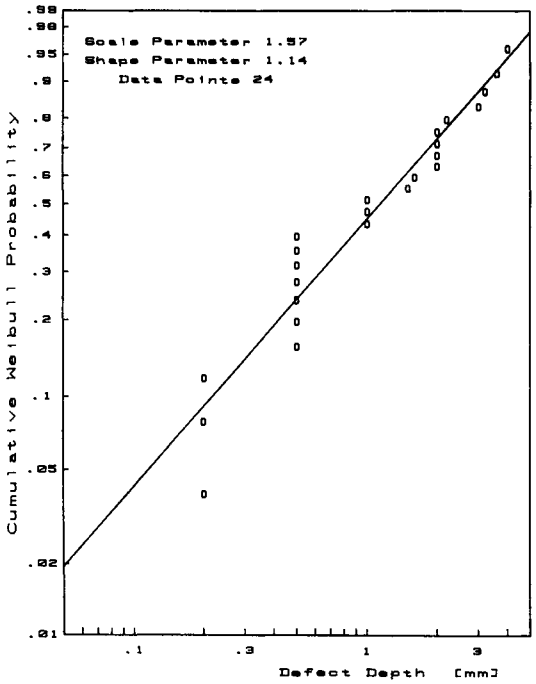

Figure 2.12: Cumulative Weibull Plot of the Defect Depth Data Shown in Figure 2.11

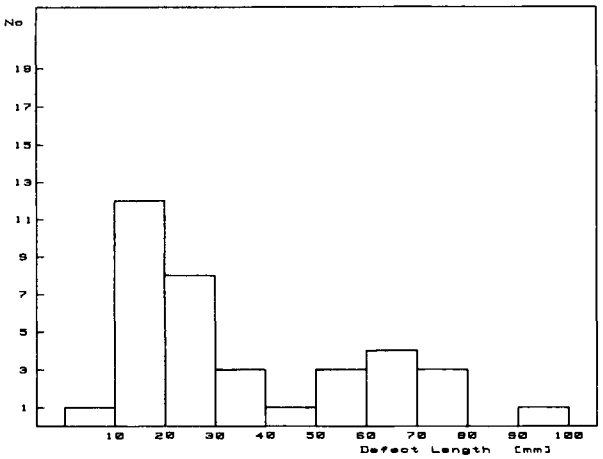

Figure 2.13: Histogram of Defect Lengths

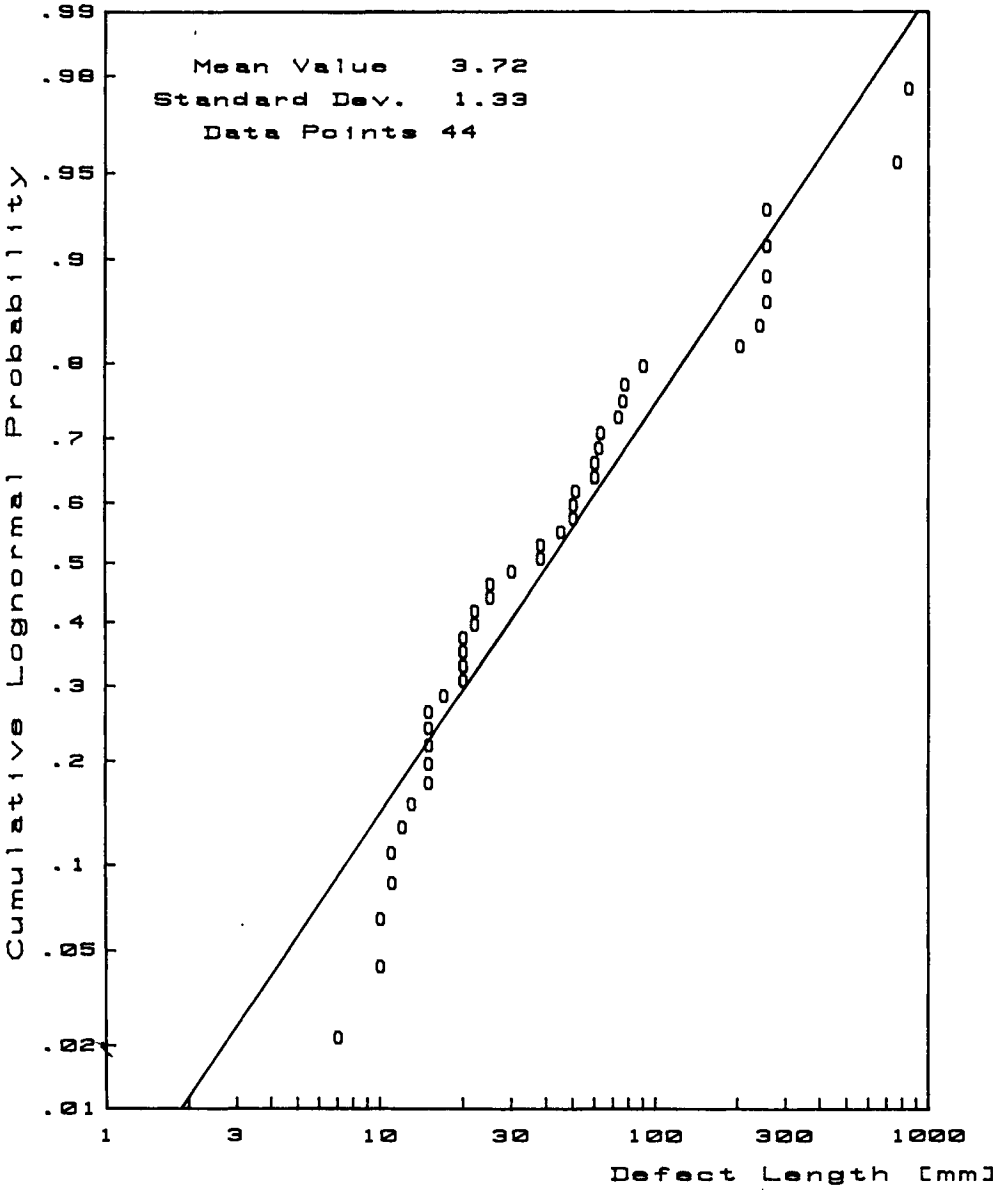

Figure 2.14: Cumulative Lognormal Plot of the Defect Length Data Shown in Figure 2.13

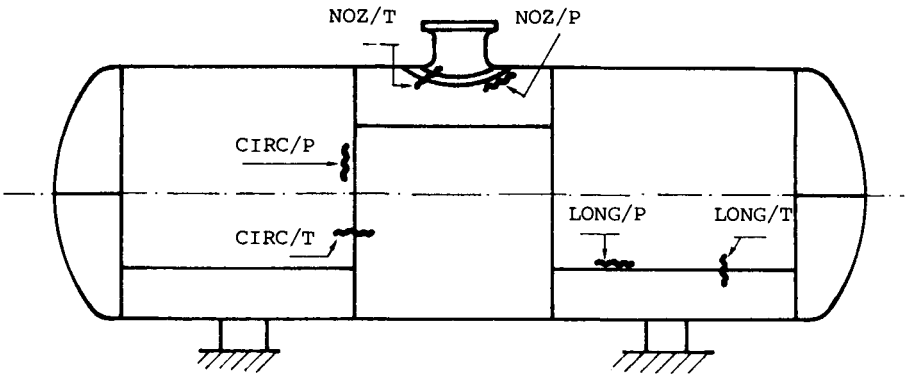

Figure 2.15: Schematic Drawing of the Vessel Showing Position of the SCC Flaws

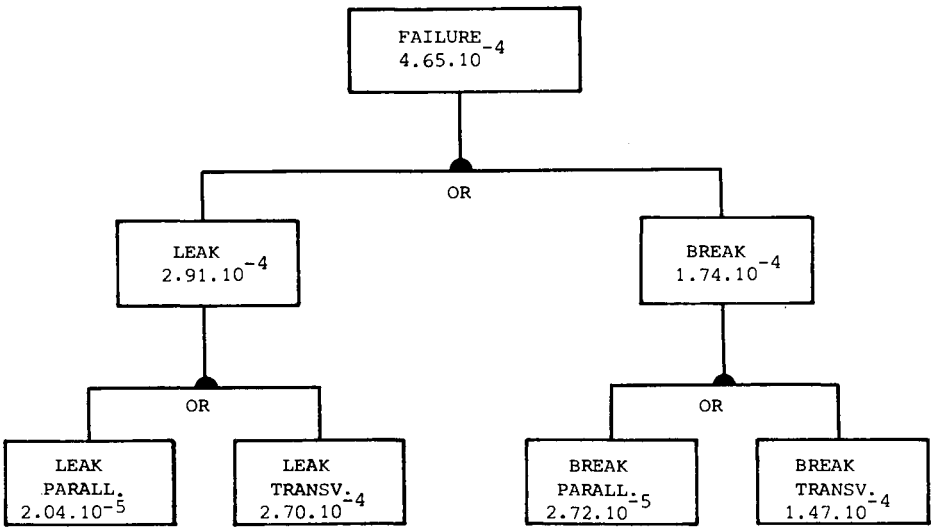

Figure 2.16: Fault Tree Applicable for the Failure of the Vessel Shown in Figure 2.15

3 ASSURING THE RELIABILITY OF STRUCTURAL COMPONENTS - EXPERIMENTAL DATA AND NON-DESTRUCTIVE EXAMINATION REQUIREMENTS

A.C. Lucia

Commission of the European Communities
Joint Research Centre, Ispra, Italy

3.1 INTRODUCTION

The probability of failure of a structural component can be estimated, as is well-known, by either statistical methods (i.e. collection of failure data over a representative population of components) or a probabilistic structural reliability approach (where the failure is seen as a level crossing of a damage stochastic process which develops in space and in time).

One great advantage of the probabilistic approach is constituted by the deeper insight gained about the structure itself in the reliability assessment procedure. Probabilistic methods will, in fact, make available not only an absolute value of the failure probability (limitations as discussed in the chapter by Pistone, Venzi and Re notwithstanding), but also a lot of additional information, such as that providing:

- Possibilities for the comparison of the failure probabilities caused by different accident conditions or different assumptions on the behaviour of the same accident;

- Quantitative estimates (via sensitivity analysis methods) of the influence of the main variables on the final result;

- Estimates of the dispersion of the final result as a function of the dispersion of the input variables;

- Possibilities for the ranking of structural zones according to their failure probability;

- Possibilities for the definition of more rational and better justified inspection strategies.

The disadvantage of the probabilistic approach is its complexity, a consequence both of the need for

identifying and correctly modelling degradation and failure processes and of the need for large amounts of data.

3.2 RELIABILITY OF A STRUCTURAL COMPONENT

Structural reliability is a dynamic characteristic which results from the statistical interference, in time and space, of the capacity of the component for performing a given function with the corresponding demand made on that component. The reliability can be thought of as the probability of the absence of crossings of a "safe level" by accumulated damage processes. The best approach to structural reliability problems would appear to be one based upon the theory of stochastic processes.

Assume that all possible failure modes of a structural component have been identified so that the set of failure criteria can be expressed as:

$$\underline{F} = \{ F_1, \ldots, F_a, \ldots, F_N \} \qquad - (1)$$

Given a failure criterion F_a, the absence of failure can be expressed by the following functional relation:

$$^a\underline{f} = J_a\{ \, ^a\underline{q} \, \} > {}^a\underline{\alpha} \qquad - (2)$$

where J_a is an operator, $^a\underline{q}$ is a set of parameters or characteristics determining the behaviour of the system, $^a\underline{f}$ is a set of damage accumulation functions, $^a\underline{\alpha}$ is a set of constants.

When J_a is expressed by an analytic relationship expression (2) can be rewritten as:

$$^a\underline{f}(\, ^a\underline{q} \,) = {}^a\underline{f}(\, ^aq_1, \ldots, {}^aq_\ell, \ldots, {}^aq_L \,) > {}^a\underline{\alpha} \qquad - (3)$$

All variables $^aq_\ell$ should be treated as stochastic processes, defined in time period T (life of the structure) and in euclidean space zone $\underline{X}$ (space domain of the structure). This means that $^a\underline{f}$ is a stochastic multidimensional process.

The reliability of the component can thus be expressed by:

$$R(T,\underline{X}) = \sum_{a=1}^{A} {}_{T,\underline{X}}P\{ {}^{a}\underline{f}({}^{a}\underline{q}) > {}^{a}\underline{\alpha} \}.P\{ F_a \} \qquad - (4)$$

where the ${}_{T}{}^{P}{}_{\underline{X}}$ is the conditional reliability with reference to failure criterion F_a and $P\{F_a\}$ is the probability that criterion F_a holds. However, it is in practice difficult to estimate the reliability, R, using the general expression (4). It is difficult to even define the structure of ${}^{a}\underline{f}$ and simplifying assumptions have to be made.

Component performance capacity and demand are not statistically independent. Loads indeed tend to activate ageing and damaging mechanisms that have a definite effect on the capacity of the structure. Modifications of strength may in turn influence loads. A simplified scheme might be to decompose loads into two parts: fatigue loads, affecting the resistance, and those arising from accidents but not adversely affecting the capacity. As far as the variation in space of structural reliability is concerned, the component can be segmented into a number of regions whose failure characteristics can be studied independently. The realiability is, therefore, reduced to a statistical interference, in time, of capacity and demand processes which are, in general, complex processes and which have to be decomposed into simpler ones. Additionally, these simple processes have to be quantitatively specified both by experimental techniques and by statistical inferences on data obtained by these techniques.

It will be worthwhile to consider some examples of the problems connected with statistical inference from data. Reference will here be made to the work constituting the background of the COVASTOL computer code which has been developed for use in determining pressure vessel failure probability in light water reactors. The main simplifying assumptions are that the load and resistance are statistically independent; that the vessel is subdivided into regions analysed independently; that fatigue and neutron embrittlement are the only two damaging processes; that brittle failure (K_{1c} criterion) is the only failure mechanism considered.

3.3 MATERIAL PROPERTIES DATA FOR FATIGUE CRACK GROWTH EVALUATION

The fatigue crack growth (FCG) process is very appropriate for highlighting two types of difficulties which have to be overcome in the modelling process: the first difficulty is the dependence of the process on many parameters (which, in turn, implies either a reduction to simpler and less accurate models, or the development of complex models with the corresponding need for very large amounts of experimental data to obtain statistical significance in every region of the experimental space); the second difficulty is the scattering of data.

Parameters which might influence fatigue crack propagation rate are the following:

- Stress parameters (maximum stress, mean stress, frequency and shape of the load signal, ratio of minimum to maximum stress);
- Material parameters (chemical composition, heat treatment, presence of cracks or flaws);
- Environmental parameters (relating to corrosion, irradiation, temperature, etc.);
- Geometric or structural parameters.

The model(s) attempting to describe the FCG should endeavour to take all these parameters into account. In fact, no such complete model exists. About a hundred different models (empirical, semi-empirical or theoretical) are suggested in the literature. They can be classified as follows:

1) Phenomenological models.
2) Models based on the dislocation theory (e.g., Bilby-Cottrel-Swinden).
3) Models based on the material behaviour at the crack tip (e.g., McClintock, Pook-Fiort).
4) Models based on cyclic properties of the material (e.g., Schwalbe).

Theoretical models often introduce parameters which, in practice, are not readily measurable and their complexity makes them difficult to use, except in the precise situation with regard to which they were established. Hence, in the development of the COVASTOL computer code, phenomenological models have mainly been considered, for validation by comparison

with experimental data. Specifically, the Paris, Priddle, Forman and Walker relations (this latter one, unlike the preceding three empirical models, relies on the physical concept of effective stress intensity factor) were selected. Their validity has been assessed by the use of a population of about 3,000 experimental points pertaining to A533B steel /1/.

The four models have been compared by determining the four coefficients C_i, n_i, r^2 and e, as defined in Fig. 3.1, for a limited number of "classes" or domains specified for the most relevant factors selected from those influencing FCG. For this purpose a series of experiments on specimens have been undertaken to investigate the influence of the following:

- Material:
  . base material (laminated SA533B Cl.1 steel or forged SA508 Cl.3 steel)
  . weld material
  . heat affected zone (HAZ)

- Stress orientation:
  . combined loads on specimens (modes I and II, modes I and III, modes I, II and III)

- Environmental conditions:
  . dry environment
  . wet environment, with nominal water composition
  . wet environment with polluted water (oxygen, chlorine, fluorine content above nominal values)

- Frequency of the loading cyle (f, in cycles per minutes)

- ΔK range (MPa$\sqrt{m}$)

- Value of ratio of minimum to maximum stress R*

- Effect of the 3D stress field when passing from specimen to structure

- Irradiation.

From the experimental data collected to study these different factors, and according to the real conditions pertaining for a light water reactor pressure vessel, the "classes" or domains were specified according to ΔK, frequency of the loading cycle, environment and ratio of minimum to maximum stress. Appropriate values or distribution for C_i and n_i then had to be selected and all necessary coefficients in Fig. 3.1 calculated.

When dealing with two distributions of experimental data with a given confidence level, the student test was used in order to decide whether or not to mix the data of the two distributions. The end result was the selection of the following four "classes":

- 3 corresponding to 3 ranges of ΔK:
  . $0 \leqslant \Delta K < 20$ MPa$\sqrt{m}$
  . $20 \leqslant \Delta K < 90$ MPa$\sqrt{m}$
  . $90 \leqslant \Delta K < 170$ Mpa$\sqrt{m}$
  in a dry environment for any value of f and ratio of minimum to maximum stress

- 1 for a wet environment, with $f \leqslant 10$ cpm and $\Delta K \geqslant \Delta KTR^*$

For each "class", one histogram of C_i and one value for n_i were selected on the basis of analysing 4,150 experimental points.

Fig. 3.2 groups together all the results obtained for the different models. Even though the Priddle, Forman and Walker formulas can - in certain cases - lead to slightly better theoretical forecasts than that of Paris, this latter relationship was chosen for the entire complex of experimental conditions considered.

The application of different data treatment methods (graphic, method of differences, secant method and method of the total polynomial) has led to the important conclusion that the main cause of dispersion is a consequence of the experimental techniques; data treatment methods contribute far less to the overall dispersion.

3.4 A BENCH-MARK EXERCISE ON REACTOR PRESSURE VESSEL FAILURE PROBABILITY COMPUTATION

A simple bench-mark exercise has been undertaken to compare the results obtained using the probabilistic computational methods developed at Westinghouse on the one hand, and by a CEC-CEA-Framatome group whose work is reported here, on the other.

Common pressure vessel input data used were:

- Inside radius: 1,994 mm
- Wall thickness: 200 mm
- Flaw geometry: surface flaw 12 mm deep, 72 mm long
- Operating pressure: 157 bar
- Coolant water temperature: 10 °C and 20 °C
- Fluence: 5.10^{19} (Ω/cm^2>1 MeV)
- Reactor age: 40 years.

Input data used specifically by only one or the other participant in the exercise, where W refers to Westinghouse and C refers to CEC-CEA-Framatome:

- Cladding thickness: W, 4 mm; C, 7.5 mm

- Reference transition nil ductility temperature (RTNDT): W, base mat. = 0 °C, weld = -20 °C; C, distribution in Fig. 3.3

- Impurities: W, normal distributions for P and Cu content; C, histograms shown in Figs. 3.4 and 3.5

- Loading case: large loss of coolant accident (LOCA).

A variety of computations were carried out and some are summarized in Table 1 (page 42).

In general, it was found that the failure probability obtained by the CEC-CEA-Framatome approach is higher (but by a factor less than 10) than that obtained by the Westinghouse approach. Comparison of Cases 1 and 7, 6 and 10, 9 and 11 indicates that using the C stress and temperature data results in a value of failure probability that is 20 to 40 times higher than that obtained by using W data. The influence of the K_{1c} and K_{1a} distributions can be seen by comparing Cases 6 and 9, 10 and 11. The distributions used by C result in lower values of probability. As far as the copper and phosphorous contents are concerned, comparison of Cases 1 and 4, 3 and 6, and 2 and 5 shows that the W data give rise to a more pessimistic result. Particularly astonishing is the discrepancy between Cases 2 and 5.

In conclusion, it is possible to say that not only are the experimental data important in their own right but, equally important, the way in which they are utilised can also affect the end result. This is particularly true when the result is determined by the tails of the relevant distributions.

3.5 NON-DESTRUCTIVE EXAMINATION (NDE) FOR ASSURING A GIVEN LEVEL OF STRUCTURAL RELIABILITY

Using the COVASTOL computer code as a basis, a sensitivity analysis has been performed on all the parameters considered in the code. One of the inferences from this analysis is the high sensitivity of failure probability to the position of defects in the thickness and in the various regions of the vessel. This aspect of the sensitivity analysis is given further attention here and is also discussed elsewhere /2/.

Figs. 3.6 and 3.7 show the failure probability (unconditional) of the belt-line weld and of the nozzle-attachment welds, as a function of reactor age and of crack distribution in the thickness. From the situation "cracks in the whole thickness" to the situation "no cracks in the first 6 mm of thickness (from the cladding-ferritic interface)" the failure probability decreases by a factor of nearly 10^3.

Fig. 3.8 shows the conditional failure probability (assuming a specified defect and accident) for the belt line weld, at the 40th year of reactor operation, for a large LOCA, as a function of crack width (2a) and for different locations (d). The location is expressed by the distance, d, of the crack centre from cladding-ferritic interface and a is one half of the minor axis of the crack. The crack length is here always assumed equal to 512 mm. The stress and temperature evolution during LOCA are evaluated assuming an emergency core coolant supply water temperature of 20 °C.

It can be seen that a 12 mm defect leads to a failure probability lower than 10^{-6} if its inner tip is 12 mm distant from the interface, while the probability can increase to 10^{-3} if this distance is only 3 mm. Fig. 3.8 indicates that a surface defect of 3 mm could still yield a failure probability of 10^{-4} during a large LOCA.

Fig. 3.9 shows the conditional failure probability caused by an 8 mm undercladding defect (length 64 mm) during an intermediate-size breach LOCA (40th year of operation). In each zone (A, B, C, D) the given probability is the average of the values estimated on four sections (one meridian to vessel, one circumferential to vessel, two at 45°). The distances of B, C and D from nozzle corner A are about 270, 460 and 790 mm, respectively.

Fig. 3.10 shows the conditional failure probability (average values on four sections) for the nozzle attachment weld, in the case of a large LOCA (40th year of operation). Defects smaller than 7 mm appear to make no contribution to the probability of failure. However, calculations carried out on the most stressed section only would have given more pessimistic results. This is indicated by Fig. 3.11, where the most stressed section only, meridian to vessel, is considered for undercladding defects in the inner corner of the nozzle. The results refer to the case of cladding broken from the beginning of reactor life.

Figs. 3.12 and 3.13 show isoprobability curves in coordinates representing the crack width (2a) and the distance of crack inner tip from cladding-ferritic interface. These curves provide a rapid indication of the degree of resolution that should be reached with NDE, as a function of crack position, in order to assure ability for ascertaining a certain level of structural reliability. For example, in the case of an intermediate breach LOCA, to assure ability for ascertaining a conditional probability of failure lower than 10^{-4} it is necessary to detect, on the belt-line weld, defects as small as 3 mm in the first millimetres (inner side) of the wall.

3.6 CONCLUSIONS

A few concluding statements can be made:

- The estimation of the structural reliability of a component by a probabilistic approach can be made only by starting from simplifying assumptions on the stochastic processes representing loads and resistance.

- The implications of these assumptions should always receive preliminary investigation.

- Results can be strongly affected by data available on parameters and variables.

- In the case of the reactor pressure vessel here considered, the inner layer (thickness not larger than 50 mm) of the wall determines the whole pressure vessel failure behaviour.

- Cladding integrity is of utmost relevance.

- If the final goal of NDE is to assist towards keeping the failure probability of a reactor pressure vessel below a predetermined level, one should relate requirements on NDE reliability and resolution to the specific region to be inspected.

The presently discussed exploratory study suggests the need for deeper investigations of the directions into which the development and validation of NDE techniques should be channelled.

Table 1: Computational Results

Comp. No.	Data Str-esses & Temp	Coolant Temper-ature °C	Cu,P Con-tent	RTNDT °C	K_{1c}	K_{1a}	Failure Prob-ability	
							Model W	Model C
1	W	10	W	0	W	W	10^{-3}	$8x10^{-3}$
2	W	10	W	-20	W	W	$4x10^{-3}$	$2x10^{-2}$
3	W	10	W	C	W	W		$2.3x10^{-3}$
4	W	10	C	0	W	W		$2x10^{-3}$
5	W	10	C	-20	W	W	$2x10^{-7}$	$<10^{-7}$
6	W	10	C	C	W	W		$3.5x10^{-4}$
7	C	10	W	0	W	W		$1.5x10^{-1}$
8	C	10	W	0	C	C		$2.3x10^{-3}$
9	W	10	C	C	C	C		$5.4x10^{-5}$
10	C	10	C	C	W	W		$1.6x10^{-2}$
11	C	10	C	C	C	C		$2.6x10^{-3}$

REFERENCES

/1/ Dufrense J., Lucia A.C., Grandemange J., Pellissier Tanon A. - Etude Probabiliste de la Rupture de Cuve de Réacteur à Eau sous Pression. Final Report EUR 8682 Fr, 1983.

/2/ Lucia A.C., Volta G. - Requirements for NDI Reliability as a Function of the Size and Position of Defects in RPVs. IAEA-OECD Specialist Meeting on Defect Detection and Sizing, Ispra, May 3 - 6, 1983.

PARIS: $\frac{da}{dN} = C_1(\Delta K)^{n_1}$

FORMAN: $\frac{da}{dN} = \frac{C_2(\Delta K)^{n_2}}{(I-T)K_c - \Delta K}$

PRIDDLE: $\frac{da}{dN} = C_3(\Delta K - \Delta K_s)^{n_3}$

WALKER: $\frac{da}{dN} = C_4(K_{eff})^{n_4}.\exp C_4'(\log K_{eff})^2 + C_4''(\log K_{eff})^3$

r^2 IS THE DETERMINATION COEFFICIENT AND MEASURES THE CORRELATION BETWEEN THE CALCULATED CURVE AND EXPERIMENTAL DATA POINTS

$$e = \frac{1}{t} \sum_{i=1}^{t} \{((\frac{da}{dN})_{cal} - (\frac{da}{dN})_{ex})/(\frac{da}{dN})_{ex}\}_i$$

WHERE t IS THE TOTAL NUMBER OF DATA POINTS

Figure 3.1: Models Considered for the Benchmark Exercise

ΔK (MPa√m)	f (cpm)	Environment	No. Data	PARIS C_1	PARIS n_1	PARIS r_1^2	PARIS e_1 (%)	FORMAN C_2	FORMAN n_2	FORMAN r_2^2	FORMAN e_2 (%)
0 to< 20	any	air	720	3.3E-27	2.64	0.99	+1.3	2.1E-19	2.68	0.99	+1.1
20 to< 90	any	air	821	4.8E-25	2.32	0.98	-1.5	7.2E-15	2.09	0.98	+0.4
90 to<170	any	air	98	7.0E-20	1.65	0.73	+1.7	9.5E-04	0.69	0.68	+4.1
≥ΔKTR*	≤10	water	858	2.3E-14	1.04	0.87	-6.0	9.2E-02	0.48	0.47	-0.4

ΔK (MPa√m)	f (cpm)	Environment	No. Data	PRIDDLE C_3	PRIDDLE n_3	PRIDDLE r_3^2	PRIDDLE e_3 (%)	PRIDDLE ΔK_s
0 to< 20	any	air	720	1.5E-14	0.82	0.86	-9.0	3.8E-06

ΔK (MPa√m)	f (cpm)	Environment	No. Data	WALKER C_4	WALKER C_4'	WALKER C_4''	WALKER n_4	WALKER r_4^2	WALKER e_4 (%)
90 to<170	any	air	98	7.0E-20	2.8E-03	-1.4E-04	1.65	0.69	+2.3
≥ΔKTR*	≤10	water	858	2.3E-14	2.2E-03	-9.3E-05	1.04	0.89	+0.9

Figure 3.2: Numerical Results

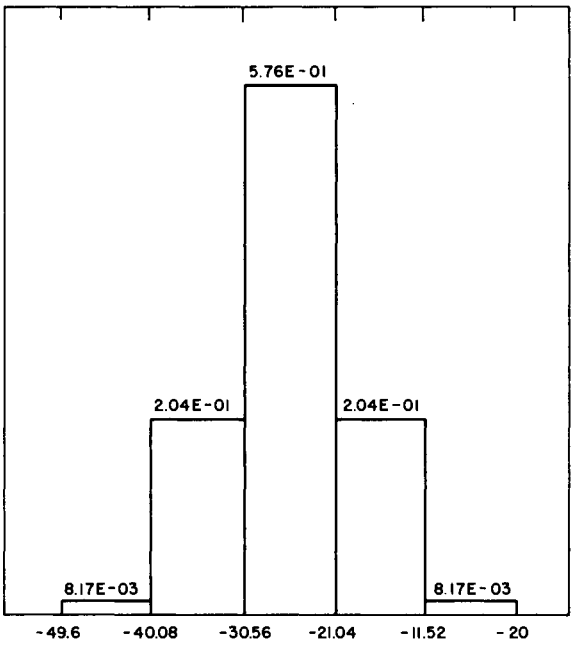

Figure 3.3: RTNDT Distribution

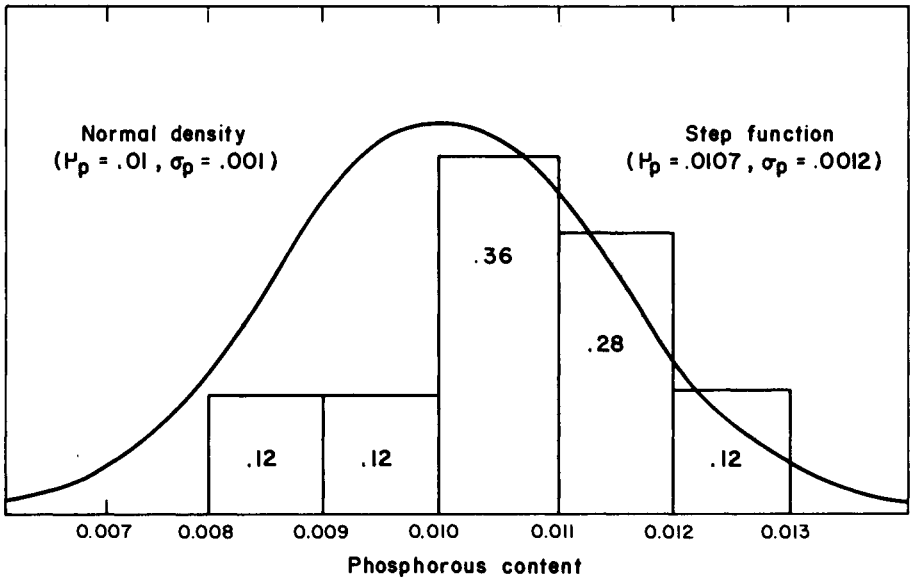

Figure 3.4: Phosphorous Content Probability Density Functions Suggested by Westinghouse (NORMAL) and CEC-CEA-Framatome (STEP FUNCTION)

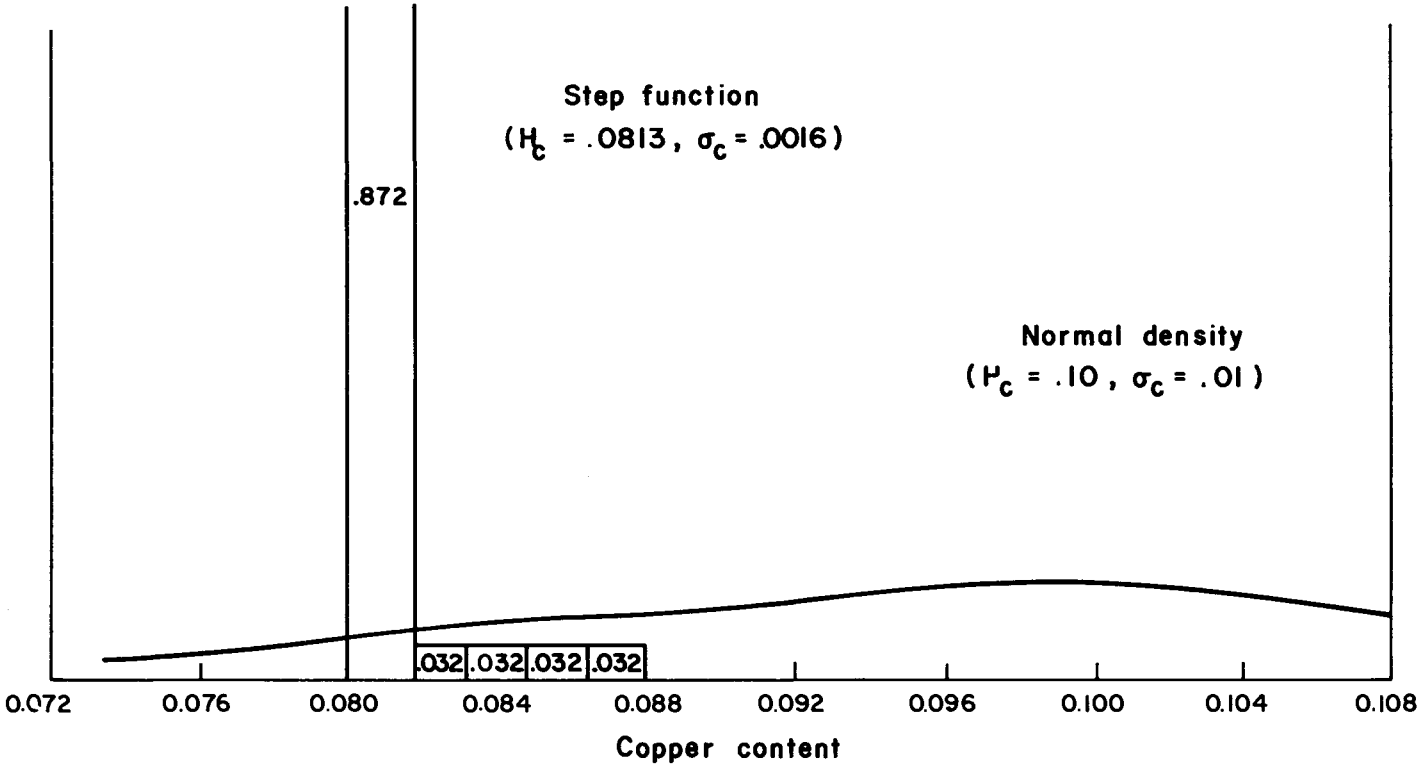

Figure 3.5: Copper Content Probability Density Functions Suggested by Westinghouse (NORMAL) and CEC-CEA-Framatome (STEP FUNCTION)

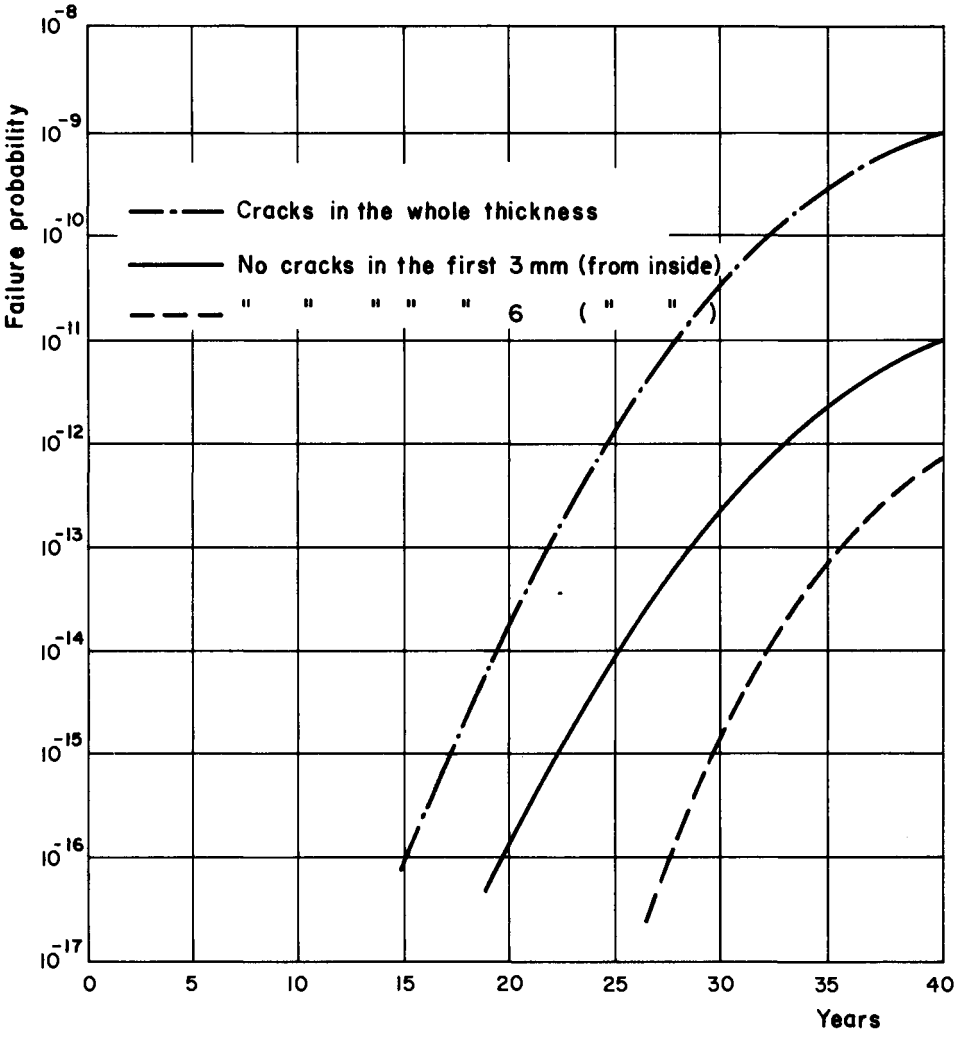

Figure 3.6: Failure Probability of the Belt Line Weld as a Function of Age and of Crack Distribution

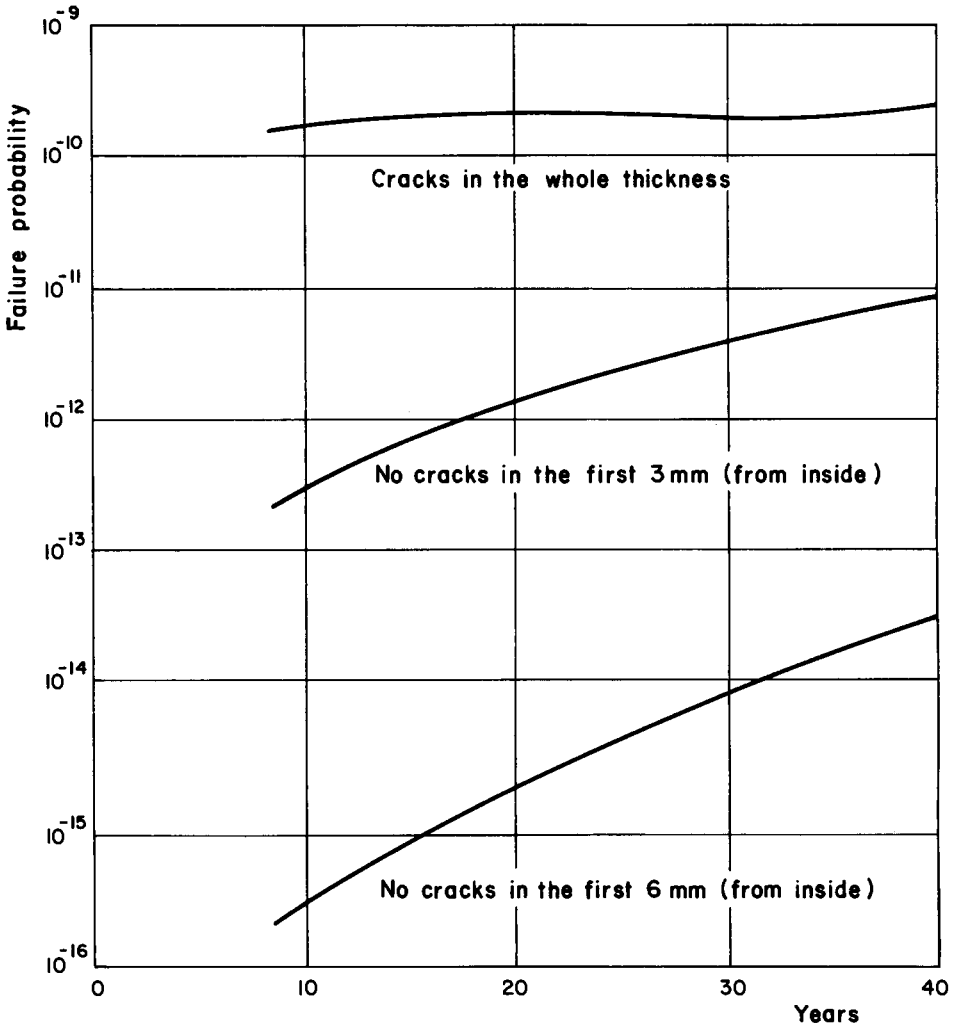

Figure 3.7: Failure Probability of Nozzle Attachment Welds as a Function of Age and of Crack Distribution

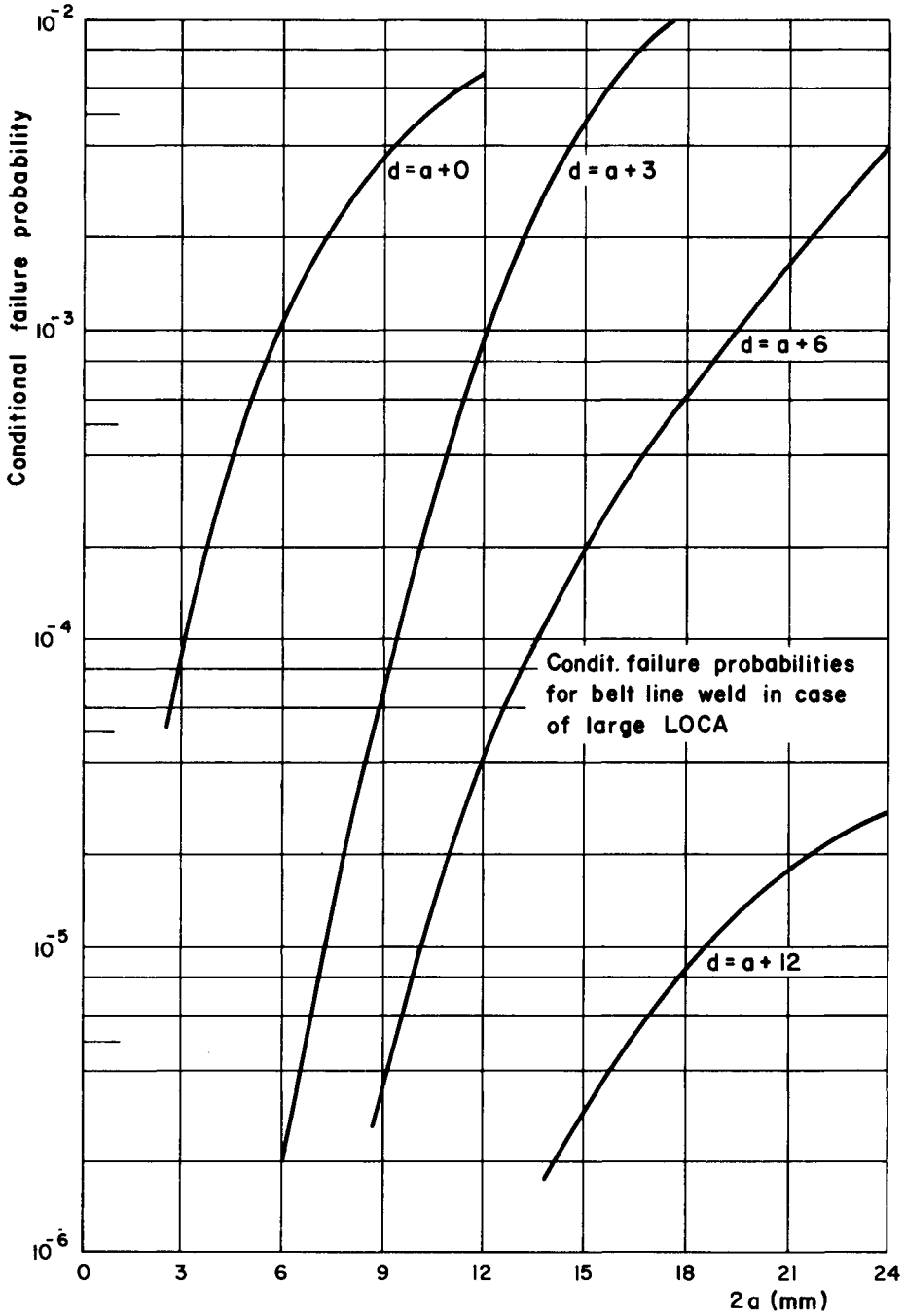

Figure 3.8: Conditional Failure Probabilities for Belt Line Weld in the Case of a Large LOCA

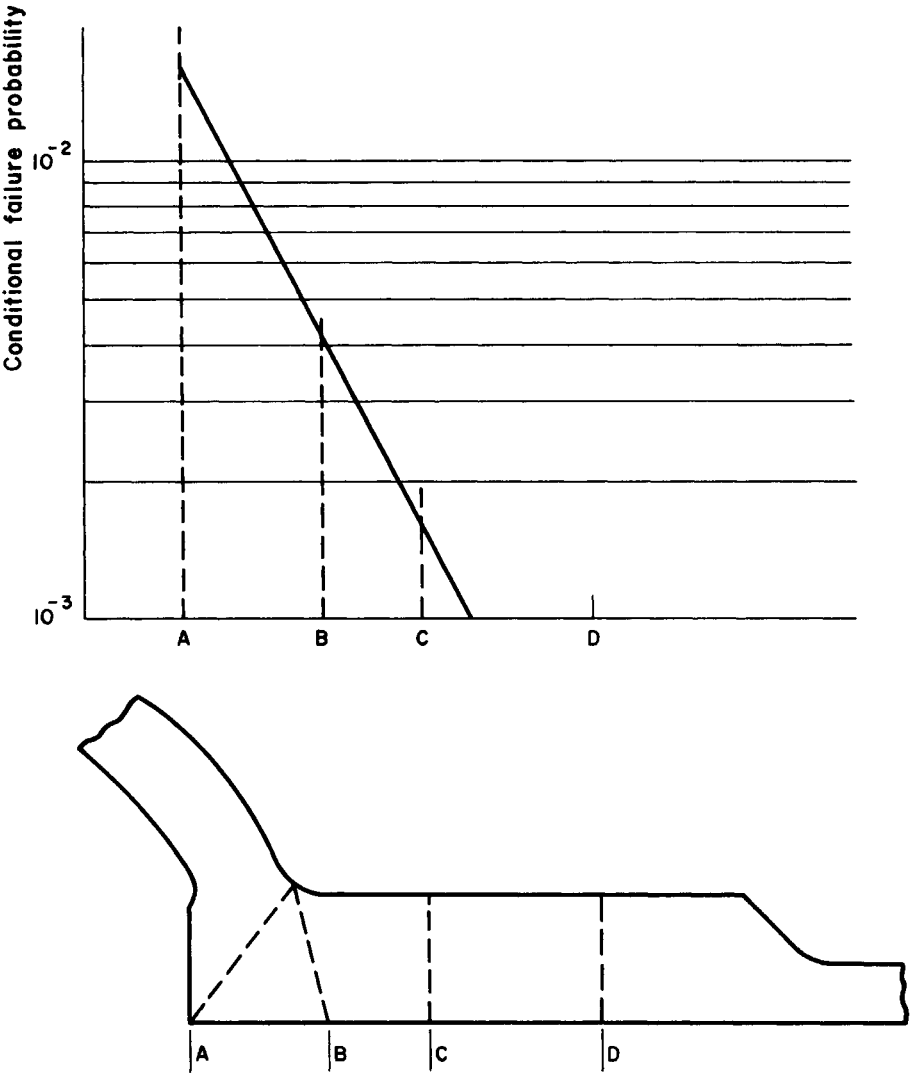

Figure 3.9: Conditional Failure Probability Caused by an 8 mm Undercladding Defect in Different Nozzle Regions in the Case of an Intermediate Breach LOCA

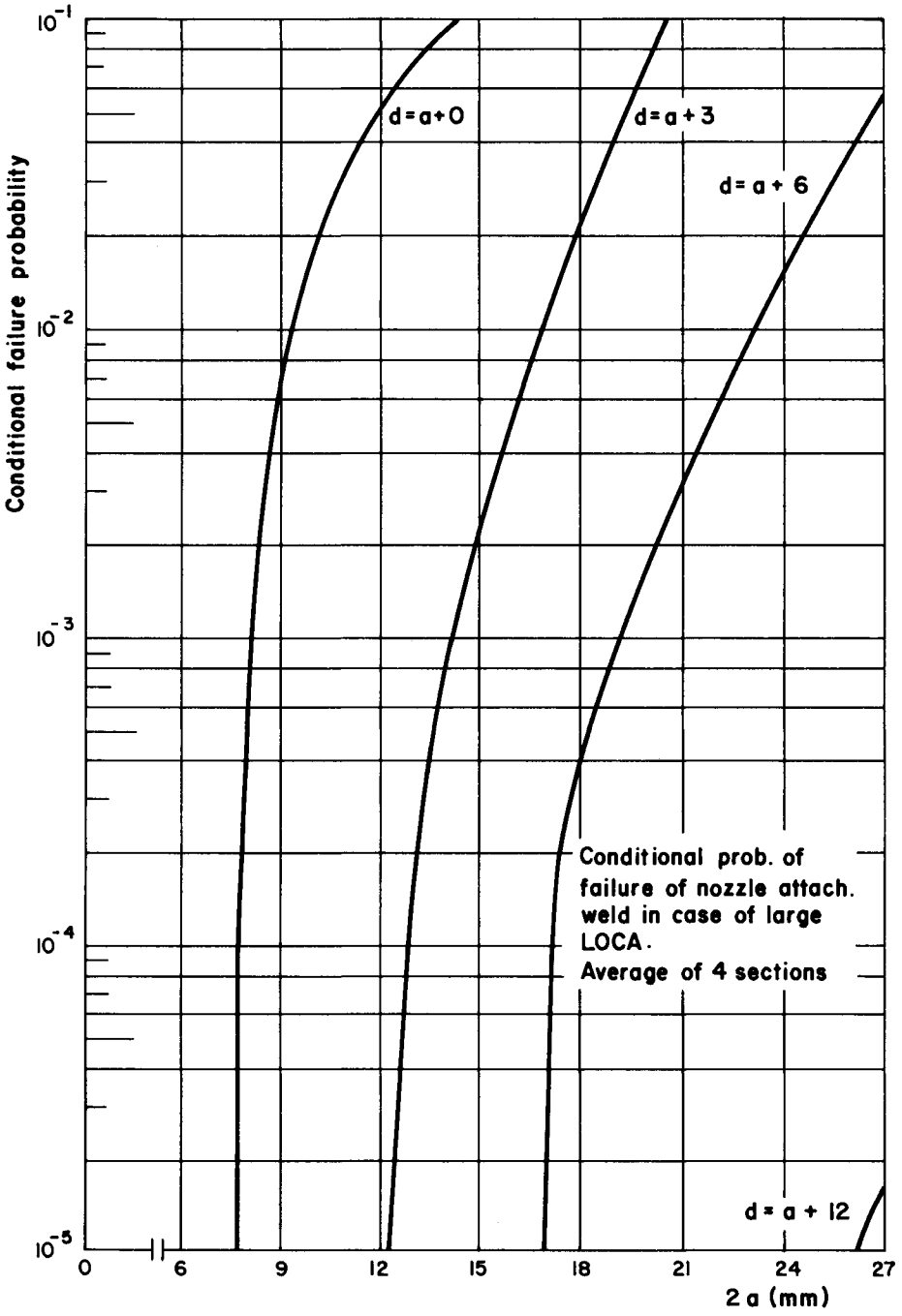

Figure 3.10: Conditional Failure Probability of Nozzle Attachment Weld in the Case of a Large LOCA

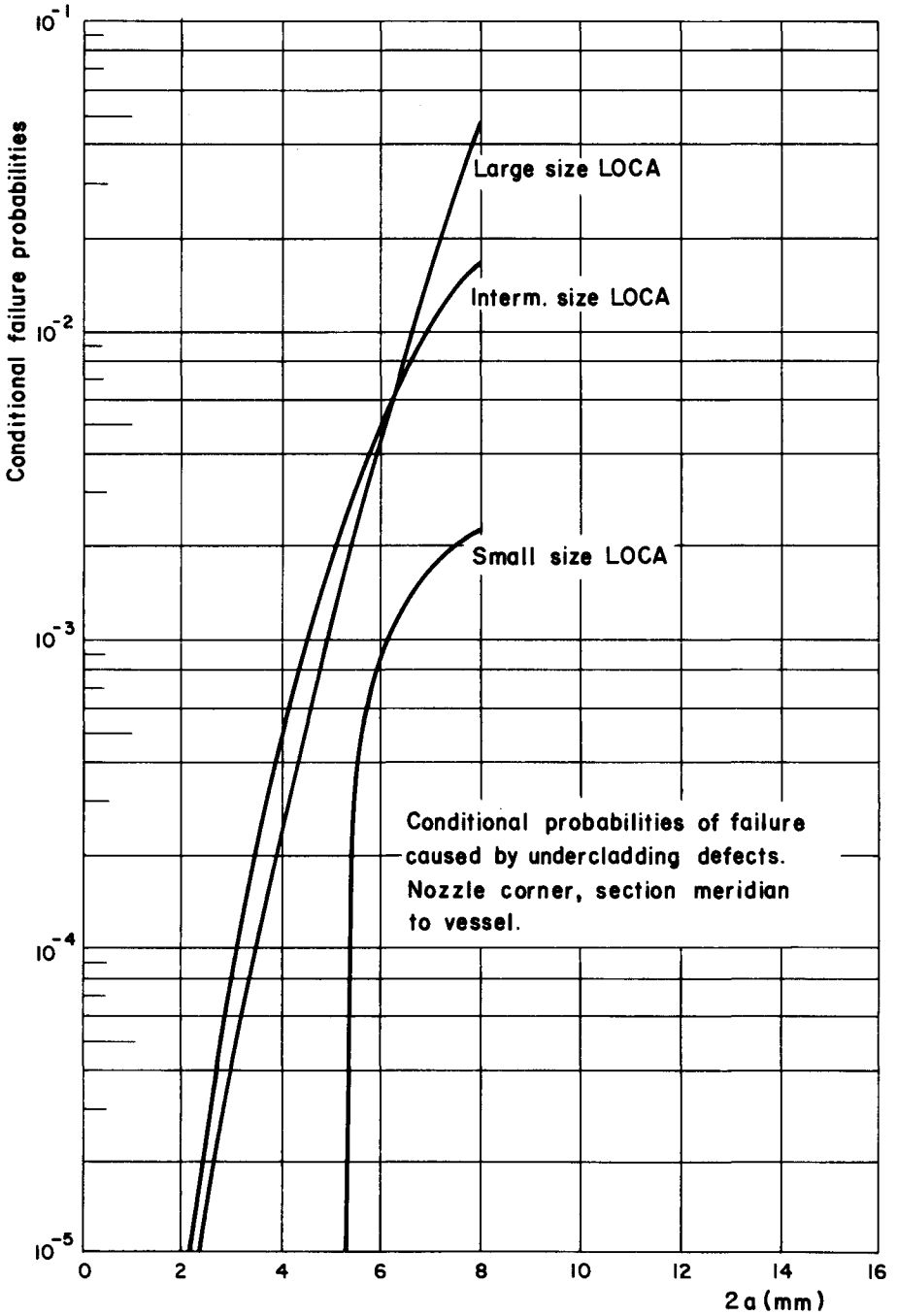

Figure 3.11: Conditional Failure Probabilities Caused by Undercladding Defects in the Inner Corner of the Nozzle (Section Meridian to Vessel)

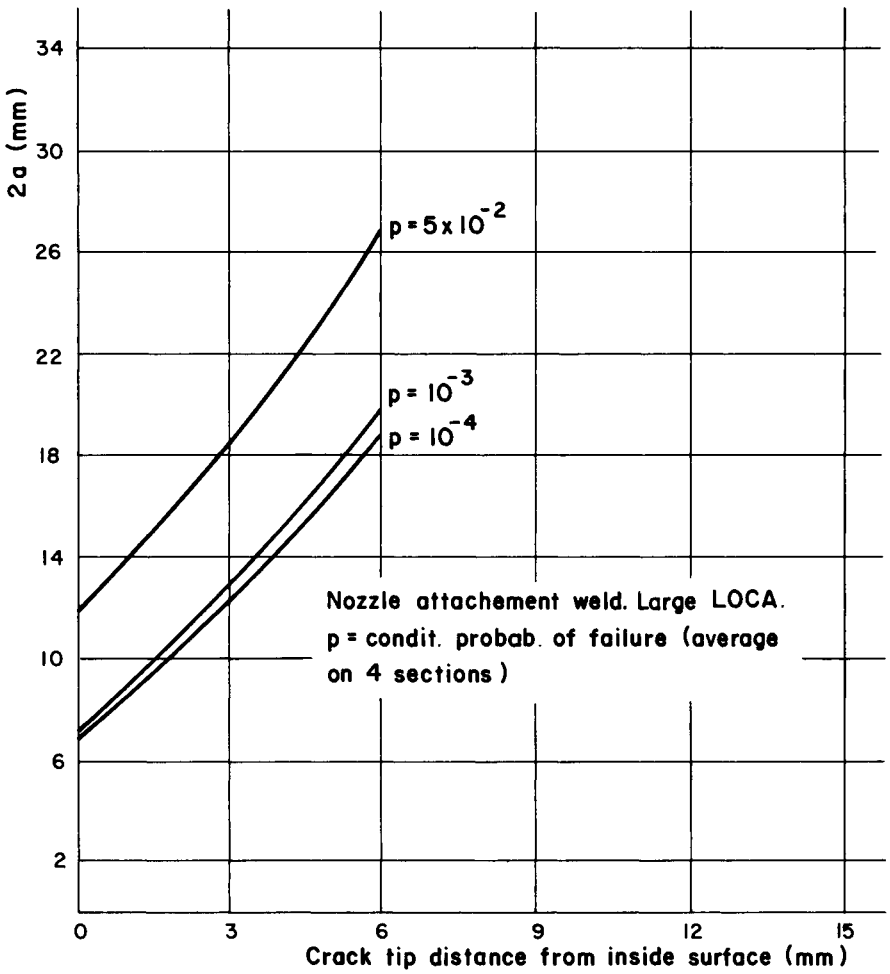

Figure 3.12: Conditional Failure Probabilities for Nozzle Attachment Weld in the Case of a Large LOCA

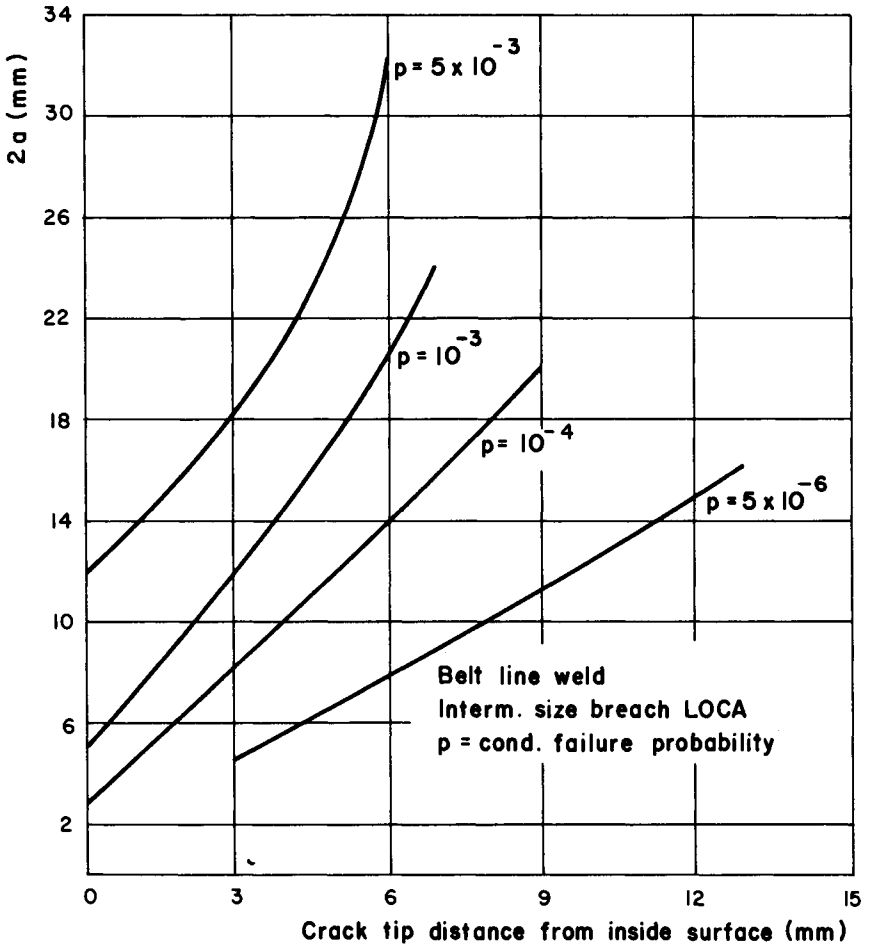

Figure 3.13: Conditional Failure Probabilities for Belt Line Weld in the Case of an Intermediate Breach LOCA

4 RELIABILITY ASPECTS OF NON-METALLIC STRUCTURAL MATERIALS

F.E. Buresch

Kernforschungsanlage Jülich, FRG

4.1 INTRODUCTION

Concrete, ceramics and glass are the most important structural materials having been used for more than two thousand years in building and in the first technological processes, such as iron smelting in blast furnaces. The performance of some of these materials, such as roofing pantiles, has been outstanding over thousands of years. However, in previous centuries the reliability of these non-metallic materials was often unsatisfactory due to deficiencies arising during manufacturing processes.

It is well known that in modern technology concrete, ceramics and glass have an important impact on the engineering design of large constructions, examples which might be cited being television towers or the structural components of energy generation and conversion plants, such as gas turbine power stations, high-temperature gas-cooled reactors or liquefied-natural-gas storage containers. Ceramics offer great potential as structural materials because of their high strength-to-weight ratio, high corrosion resistance, excellent high temperature properties, and abundant availability.

It was very quickly recognized that high reliability is an important prerequisite for the application of concrete and related materials in modern technology. Such reliability depends upon proper fabrication conditions and on well-defined service conditions. The goal of proper fabrication conditions is a tailored microstructure which should be optimized for the special intended service conditions. Since the constituents of a structural material's microstructure, such as the phases or the grain and pore size distribution, are characteristic and determine its ultimate technological properties, characteristic properties of the microstructure finally determine structural reliability.

On the other hand, the reliability of a component also depends on relations between microstructure and service conditions, especially on factors governing

damage to the material. To be able to assess the lifetime of a component, therefore, these damage mechanisms must be quantified in terms of service conditions. In the following, technological and microstructural parameters which charaterize the reliability of concrete and related materials will be discussed and, finally, some factors affecting damage mechanisms will be considered.

4.2 TECHNOLOGICAL PARAMETERS OF RELIABILITY - CRITICAL FLAW SIZE AND DISTRIBUTION OF STRENGTH

Ceramics and related materials are not only characteristically brittle, often exhibiting low fracture strength, but they do not yet possess the high standards of uniformity and reproducibility that is required of structural materials under certain applications. One of the major obstacles to the extensive use of ceramics as structural entities, devices, or component parts in, for example, the high-temperature gas-cooled reactor has been a distinct lack of design data; and the reliability of available design data on ceramics is generally conceded to be of relatively low order as compared with such materials as metals. Part of this problem can be traced to the lack of standardization for test methods for this group of materials.

Design data for safety assessment of structural components are based on the mechanical and fracture parameters of the constitutive law of the material. Values of these parameters under service conditions must be used. Most important are the distribution of strength in the case of static loading, which is considered here, and the changes in mechanical properties after thermal or mechanical cycling which is considered in the next section.

The characteristic brittleness of concrete, ceramics and glass has its origin in the non-yielding nature of these materials' constituents. They cannot deform with a homogeneous plasticity such as is the case with metals. Critical flaws of different sizes, therefore, act as stress concentrators and the strength of these materials is governed by a distribution function of a stochastic flaw size, a, which is given as

$$F(a) = \exp\text{-}1/\checkmark(a/a_K)^m \qquad \text{- (1)}$$

Here

$$a_K = (V_K/V_o)^{2/m} \cdot a_n \qquad - (2)$$

where V_K and V_o are the stressed volume of the component or specimen and the unit volume, respectively. a_n and m are material property and scale parameters. With the stress intensity factor /1/

$$K_{1c} = S\sqrt{(\pi a)} \qquad - (3)$$

Eq. (1) yields for the distribution, P, of the smallest strength, S, of a set of components or specimens:

$$P = 1-\exp-\{(V_K/V_o)(S/S_n)^m\} \qquad - (4)$$

where S_n is a material property and defines the strength of the unit volume at a fracture probability of 63 %. The strength of a ceramic thus depends on the stressed volume, i.e. specimen size. In general, the larger the specimen the weaker it is likely to be. However, this distribution only applies when the interaction of the stress field of each critical flaw with the surrounding microstructure in a specific component or specimen is the same in all cases.

This latter assumption means that the stress intensity factor K_{1c} of each crack, $a,.....,a_n$, is given as:

$$K_{1c} = S\sqrt{(\pi a)} = ... = S_n\sqrt{(\pi a_n)} \qquad - (5)$$

Thus K_{1c} is a material-specific property of each volume element of the material, which is a prerequisite of a unimodal flaw-size distribution, and implies unique values of the cohesion strength S_{mc} and size of process zone $2\psi_c$ for all parts of the material in question.

K_{1c} can therefore be expressed as

$$K_{1c} = S_{mc}\sqrt{(\pi\psi_c)}/2 \qquad - (6)$$

Eqs. (4) to (6) are based on the assumption that the ceramics being considered are linearly elastic. In this case, the size of microcracked material in front of a critical crack, especially the size of the process zone $2\psi_c$, has to be small compared to the uncracked ligament (small-scale elastic damage).

The distribution parameters S_n and m are consequently a measure of the magnitude and distribution of strength and, therefore, a measure of the "reliability" of the material. However, in reality, technological materials are often inhomogeneous and anisotropic and show a multimodal strength distribution. This has been found to be the case for a set of large tension specimens of a mullite refractory used as a thermal insulator in high-temperature processes. The tests were performed at the IMW, Freiburg, FRG, and are to be published elsewhere /2/. The multimodal strength distribution of this particular refractory is caused by fluctuations occurring during the manufacturing process. Density variations are the most common deficiency. Density influences the stress intensity factor K_{1c} and in Fig. 1 are shown the slopes of the multimodal strength distribution each being characterized by a specific K_{1c} value. Thus Eq. (5) is not unequivocally valid for this type of material.

Nominally, a multimodal strength distribution can be characterized by one least-square fit. However, this tends to give a low m-value and results in a bad measure of reliability for a material. To obtain better insight into the capabilities of the material just referred to, the multimodal strength distribution was separated into two sets of unimodal strength distributions, one set each for the upper and lower section of the bimodal strength distribution, as shown for two loading rates indicated on Fig. 4.1 (Z_A and Z_B). Each strength distribution is characteristic for a specific flaw size distribution manifesting a specific microstructure and thus each distribution must be bounded, additionally, by quantities which characterize the continuum of the distribution. It has been found that each set of strength distributions covers a distinct range of density distribution of the nominally identical tension specimens /2/.

Together with the tension tests, flexural tests on the same material were performed. These show only a unimodal strength distribution as a consequence of a narrow density distribution for the flexural specimens. This is a result of the sampling conditions. The relatively small bend specimens were machined from one of about five plates which were cut out of one brick, whereas each of the large tension specimens were machined out of one plate each, which means that the tension specimens were machined from many bricks.

Fig. 4.2 shows the tensile strength/density relationship of all specimens tested. It can be seen that some of the measured strength values are not narrow. This is a consequence of the different microstructures of the tested specimens. By eliminating outliers indicated by arrows in Fig. 4.2 (and labelled 2 and 3 in Fig. 4.1), unimodal strength distributions are obtained, showing improved m-values as can be seen in Fig. 4.1 (Z'_{Al} and Z''_{Al}). The outliers represent densities far from the mean of the respective groups. Thus the range of densities in Fig. 4.2 denotes the upper and lower bounds for the ranges of validity for the different strength distributions.

One can conclude, therefore, that by appropriately selecting specimens or components of nominally the same density from a batch, which can be done by measuring the dynamic Young's modulus, for example, the "variability" of a material can be constrained, that is the "reliability" can be enhanced. That this is so for the case under consideration can be verified by comparing strength data from tension and flexural tests on the same mullite refractory. As shown in Fig. 4.3 flexural (B_A, B_B) and tension (Z_A, Z_B) strength data can be transposed with respect to the different specific stressed volumina if the upper and lower bounds of the range of validity of the distribution functions are nearly the same. This can be seen by comparing the respective slopes in Fig. 4.3 with those in Fig. 4.1.

4.3 MECHANICAL PROPERTIES OF THERMAL CYCLED CERAMICS AND CEMENTITIOUS MATERIALS

In the previous section, it was indicated how the reliability of a nominally linear-elastic material can be assessed with parameters which characterize the strength distribution. Linear-elastic deformation arises from the assumption of small-scale

elastic damage, i.e. that the size of the process zone is small compared to the stressed volume. However, it has been shown that the size of the process zone increases with increasing standard deviation of grain size distribution and is related to the Weibull modulus /2/.

The m-value is a measure of the homogeneity of the material, especially of the microstructure, and is a function of the mean values of strength, S, and of flaw size, a, respectively, divided by the corresponding standard deviations:

$$m = f_1(\frac{S}{\partial S}) \; ; \; m = f_2(\frac{a}{\partial a}) \qquad - (7)$$

and because the microstructure determines the damage conditions of a brittle material, the m-value can provide useful damage-related information. Deformation becomes non-linear, non-elastic if the damage, i.e. microcracking, spreads out over the stressed volume. It is necessary, therefore, to now consider factors affecting the reliability of a brittle material under large-scale damage conditions.

Microcracking (damage) arises by the activation of crack nuclei. Crack nuclei are the consequence of volume constraints and shape changes which arise during fabrication and/or stressing of characteristically brittle materials. The volume constraints and shape changes build up internal stresses. These cannot be relaxed by plastic deformation, the consequence of the non-yielding nature of the constituents which determine the mechanical behaviour of the microstructure of these materials. Internal stresses act on stress concentrators, such as pores and triple points of grain boundaries and thus microcrack nuclei of different activation potential arise, depending on the magnitude of the internal stresses.

Here, the influence of microcracking on the integral mechanical parameters of brittle materials will be discussed and, as examples, the influence of microcracking on the integral mechanical parameters of a) highly insulating refractory brick, b) water-saturated concrete and mortar are considered. This is done from a macroscopic point of view, with data from the literature being discussed.

Specimens of a high alumina porous refractory were thermal-cycled between 1,050 °C and room temperature with two different cooling rates of 10 and 20 K/min. /3/ where it was found that the Young's

modulus decreased rapidly by about 5 to 10 % after the first 20 cycles, but remained nearly constant with further cycling, up to 50 cycles. A somewhat different mechanical behaviour during thermal cycling was observed with two types of water-saturated concretes cycled between room and various low temperatures (down to -170 °C) /4,5/. Fig. 4.4 shows measured values of degradation of compressive and tensile strength for these materials. In contrast to the refractory material, the slope of the drop is highest during the first five cycles. Furthermore, the degradation of strength is more pronounced when the cooling temperature goes down to -70 °C than when the cooling temperature goes down to -170 °C, when the slope of the degradation of strength is nearly constant. Generally, the tensile strengths, which were measured with a diametral compressive test, decrease more than the compressive strengths.

The degradation of compressive strength after cycling is remarkable but it is important to realize that microcracking affects Young's modulus more than strength. This can be seen from the mechanical behaviour of water-saturated mortar during cycling between room temperature and -170 °C /4,5/. From the stress-strain curves shown in Fig. 4.5, the Young's modulus was evaluated and compared with the corresponding compressive strength as a function of number of cycles. Fig. 4.6 shows the relative values and it can be seen that with increasing cycling, up to 9 cycles, the Young's modulus decreases more than the compressive strength. It is clear, therefore, that these two groups of materials - the highly insulating refractories and water-saturated cementitious materials - show some similarity during the beginning of thermal cyclic fatigue on one hand, but a pronounced difference during long-term cyclic fatigue, on the other. For both groups of materials, the degradation of mechanical behaviour commences with a steep slope. Then, after some thermal cycling for the refractory materials, the gradient of the degradation curve decreases to nearly zero, whereas for water-saturated cementitious materials, the gradient of the degradation curve diminishes but remains finite.

From the above-mentioned experimental observations and the fact that the bulk porosity increases during cycling, it must be concluded that the degradation of mechanical parameters is caused by microcracking. Microcracks originate from nuclei which have a characteristic residual stress-induced stress intensity factor or energy release rate G_{1r} given by:

$$G_{lr} = E\varepsilon^2 A^2 d/(24(1-\nu^2)) \qquad - (8)$$

where E and ν are the elastic constants of the material, d is the grain/inclusion/aggreggate size and ε, A are the residual strain and the anisotropy factor, respectively, which arise in a facet relative to the adjacent grains or phases.

Both types of materials discussed previously have a high density of microcrack nuclei which are activated through the imposed macroscopic thermal stresses. During the beginning of degradation by thermal cycling for both groups of materials, the density of microcrack nuclei diminishes sharply. For the refractory material, after some cycling, all microcrack nuclei with a distinct activation potential have nearly disappeared. This is a self-regulating feed-back process which is induced by the microcrack-reduced Young's modulus (Eq. (8)). For the water-saturated cementitious materials, the density of active microcrack nuclei also decreases during the early thermal cycles. However, the degradation rate becomes constant after the initial drop and thus a new group of microcrack nuclei is generated during each cycling.

This new group of microcrack nuclei are the water-filled microcracks generated during each cycle. Fig. 4.7 shows the differential distribution of pore radii before and during thermal cycling of water-saturated mortar /4,5/. In the as-received state, the distribution function of pores has a maximum at a pore radius of some 10^{-8} m. With increasing cycling, a new group of pores is generated with sizes larger than in the as-received state, whereas the density of small pores (especially with radii in the range of 10^{-8} m) decreases. Thus the total volume and the size of pores increase, with an increasing number of cycles, as shown in Fig. 4.8.

Generally, the strength of brittle materials is influenced most by the large pores. Fig. 4.9 shows the decrease of tensile strength with increasing pore volume, for pores larger than 0.1 µm. These pores are equivalent to the microcracks which were generated during each cycle, in the thermally cycled case considered earlier.

In conclusion, it can be stated that thermal fatigue of a high-alumina insulating refractory and of cementitious materials is caused by microcracking.

Microcracking affects both the elastic as well as the fracture behaviour of the material. However, the Young's modulus is more sensitive to microcracking than is strength. The "reliability" of these materials is diminished by thermal fatigue but, since this in turn is governed by the microstructure, it is necessary to look more closely at the relationship between microstructure and damage.

4.4 RELATIONS BETWEEN MICROSTRUCTURE AND DAMAGE

From the foregoing, it should be clear that microcracking is influenced by mechanical and microstructural parameters of brittle materials, especially the grain or inclusion size distribution. Generally, it is known from the literature /6,7/ that a critical grain/inclusion/aggregate size exists in these materials, above which microcracking will occur. This is primarily a consequence of the non-yielding nature of the constituents of this group of materials. Thus, residual strains will be built up during fabrication and stressing. This characteristic property determines the mechanisms of microcracking, which are here considered in more detail.

Residual strains arise in phase and grain boundaries of this group of materials as a consequence of volume constraints and shape changes, primarily during fabrication. The magnitude of the residual strains depends on the thermomechanical properties of the adjacent phases or grains in facets and on the orientation of their crystallographic axis with respect to the common facet.

The mechanisms of volume constraints and shape changes are very different in ceramics and cementitious materials. In ceramics they occur during cooling down from sintering temperature as a consequence of grain boundary mismatch and give rise to residual strains in facets; and phase changes enhance these effects. In cementitious materials, on the other hand, a volume contraction around hard aggregates occurs during hydration and gives rise to shrinkage of the cement matrix. Similarly, this produces residual strains in facets around aggregates. However, despite this difference in the mechanism of internal constraint operating within the two types of materials, the consequence is that the development of residual strains in phase or grain boundaries gives rise to the same end results. Therefore, the analytical modelling of the mechanisms of microcracking for this group of materials can be treated

from the standpoint of a common approach in a first approximation.

The problem was originally investigated by Clarke /8/. He quantified the anisotropic volume expansion and related phenomena of neutron-irradiated fine-grained ceramics like beryllia and alumina. Spontaneous intercrystalline microcracking in polycrystalline ceramics and cementitious materials occurs if the residual strain induced energy release rate G_{1r} equals the specific surface energy $2\gamma_s$ /8,9,10,11/:

$$G_{1r} \geqslant 2\gamma_s \qquad - (9)$$

In the case of cementitious materials ε (Eqn. (8)) is related to the amount of shrinkage of the cement matrix around an aggregate. For ceramics, especially fine-grained "one-phase" alumina, beryllia or silicon carbide ceramics, the residual strain is given by the difference of thermal expansion coefficients $\Delta\alpha$ of adjacent grains in a facet with respect to the angle of their crystallographic axis (anisotropic factor, $A \leqslant 1$) multiplied by the temperature difference between the freezing temperature, T_f, for internal stress-induced grain-boundary creep during cooling down from sintering temperature and the usual working (e.g. room) temperature, T_{rt}. Thus ε is given as

$$\varepsilon = \Delta\alpha(T_f - T_{rt})A = \varepsilon_o A \qquad - (10)$$

where $\varepsilon_o = \varepsilon_{max}$ is defined as the maximum residual strain which can arise in a facet (i.e. in the case of alumina or silicon carbide if the a and c axes of the respective grains are parallel to one another, then A = 1).

An external stress field with the stress intensity factor K_1 lowers the effective surface energy of microcracking to some extent in which case the microcrack criterion is given as

$$G_1 = K_1^2(1-\nu^2)/E + G_{1r} \geqslant 2\gamma_s \qquad - (11)$$

Eqs. (11) hold also for rocks with anisotropic properties of the constituent grains, for instance in the case of heating and stressing /10/.

The usefulness of Eqs. (11) to forecast the fracture behaviour of, for example, neutron irradiated beryllia for purposes as a moderator in high-temperature gas-cooled reactors has already been demonstrated over a decade ago /7/. Hilsdorf et al. /12/ have recently determined, with a formula equivalent to Eq. (9), the critical grain/aggregate size for spontaneous microcracking of concrete to be about $d \simeq 25$ mm. However, in both investigations the grain size distribution and the orientation of grains were not considered and these features are important in attempting to quantify the reliability of this class of material. Generally, due to the multiphase microstructure and multimodal grain size distributions of many ceramics and cementitious materials, the parameters of Eqs. (8,10) are not well quantified. To obtain insight into the influence of grain size and grain orientation dependency of microcracking on fracture behaviour, it is preferable to select a material with a simpler microstructure, such as fine-grained high-strength alumina. (The technological parameters, the microstructure and the grain size distribution of this type of alumina are discussed elsewhere /9/.)

Lack of space prevents any further discussion on the relationship between microstructure and the structural parameters of a microcrack system and the reader is referred to an extensive presentation elsewhere /11/.

4.5 CONCLUSIONS

In this brief survey, mechanical aspects relating to the reliability of nominally brittle materials have been discussed from the standpoint of:

- Relations between microstructural parameters and strength
- Influences of cyclic fatigue on mechanical parameters
- The relationship (without treating experimental details) between microstructure and damage (microcracking).

The grain and phase distribution of the raw materials (e.g. powder, sand) and mixing and forming conditions determine the mechanical behaviour and especially the critical flaw size of a brittle material. The size of the critical flaw is a stochastic parameter.

Using the stress intensity factor as a material-specific property, there can be derived a relationship between strength and critical flaw size which, however, includes a volume component. The local structural and the integral mechanical parameters of the material inside the "process zone" determine the strength and crack resistance of the material.

To obtain high mechanical reliability with this type of structural material it is important, therefore, to have not only a quantitative assessment of the range of critical flaw sizes but to ensure, by appropriate fabrication conditions, that the microstructure and the mechanical parameters (including fatigue behaviour) of the material volume preceding a critical flaw, in any batch of components, are similar: ideally, the microstructure should be as homogeneous as possible.

REFERENCES

/1/ Freudenthal A.M. - Fracture III, Academic Press, New York.

/2/ Meyer W., Buresch F.E - Internal Kfa Report (to be published).

/3/ Jung J., Mittenbuhler A., Reck A. - Verhalten keramischer Werkstoffe unter den Einsatzbedingungen in nuklearen Prozesswärmeanlagen, Jahrestagung Kerntechnik 80, Proceedings, pp. 641 - 644, 1980.

/4/ Rostasy F.S., Wiedemann G. - Festigkeit und Verformung von Beton bei sehr tiefen Temperaturen, Betontechnische Berichte, 2, 54, 1980.

/5/ Rostasy F.S, Weiss R., Wiedemann G. - Changes of Pore Structure of Cement and Mortars due to Temperature, Cement and Concrete Research, 10, 157 - 164, 1980.

/6/ Lange F.F. - Fracture Mechanics and Microstructural Design, Fracture Mechanics of Ceramics, Vol. 4, p. 799, R.C. Bradt and D.P.H. Hasselmann (eds.), Plenum Press, New York, 1978.

/7/ Buresch F.E, Hecker R., Rixen W. - The Effect of Cyclic Fast Neutron Irradiation Damage and Thermal Treatment on Modulus of Rupture of BeO, Science of Ceramics, 5, 195 - 218, 1970.

/8/ Clarke F.J.P - Residual Strain and the Fracture Stress-Grain Size Relationship in Brittle Solids, Acta Metallurgica, 12, 1964.

/9/ Buresch F.E. - Relations betwen Microstructure Fracture Toughness and Thermal-Shock Resistance of Ceramics, Science of Ceramics, 12, 513, 1983.

/10/ Davidge R.W., McLaren J.R., Titchell I. - Statistical Aspects of Grain Boundary Cracking in Ceramics and Rocks, Fracture Mechanics of Ceramics, Vol. 5, 594, 1983.

/11/ Buresch F.E. - Macrocrack Extension in Microcracked Dispersion-Toughened Ceramics, Zirconia 83, MPI Stuttgart (to be published in Advances in Ceramics).

/12/ Ziegeldorf S., Müller H.S., Hilsdorf H.K. - Effect of Aggregate Particle Size on Mechanical Properties of Concrete, ICF, Vol. 5, 2243, 1981.

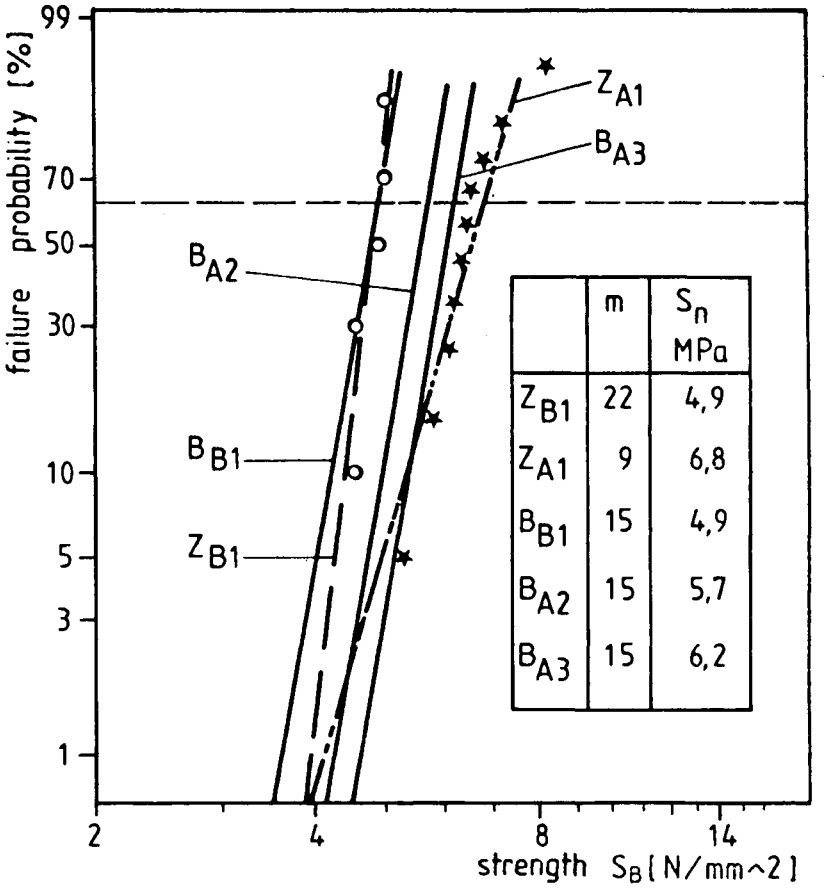

Figure 4.1: Bimodal Weibull Distributions of Tensile Strength Data for a Mullite Refractory. (Z_A = High Loading Rate; Z_B = Low Loading Rate)

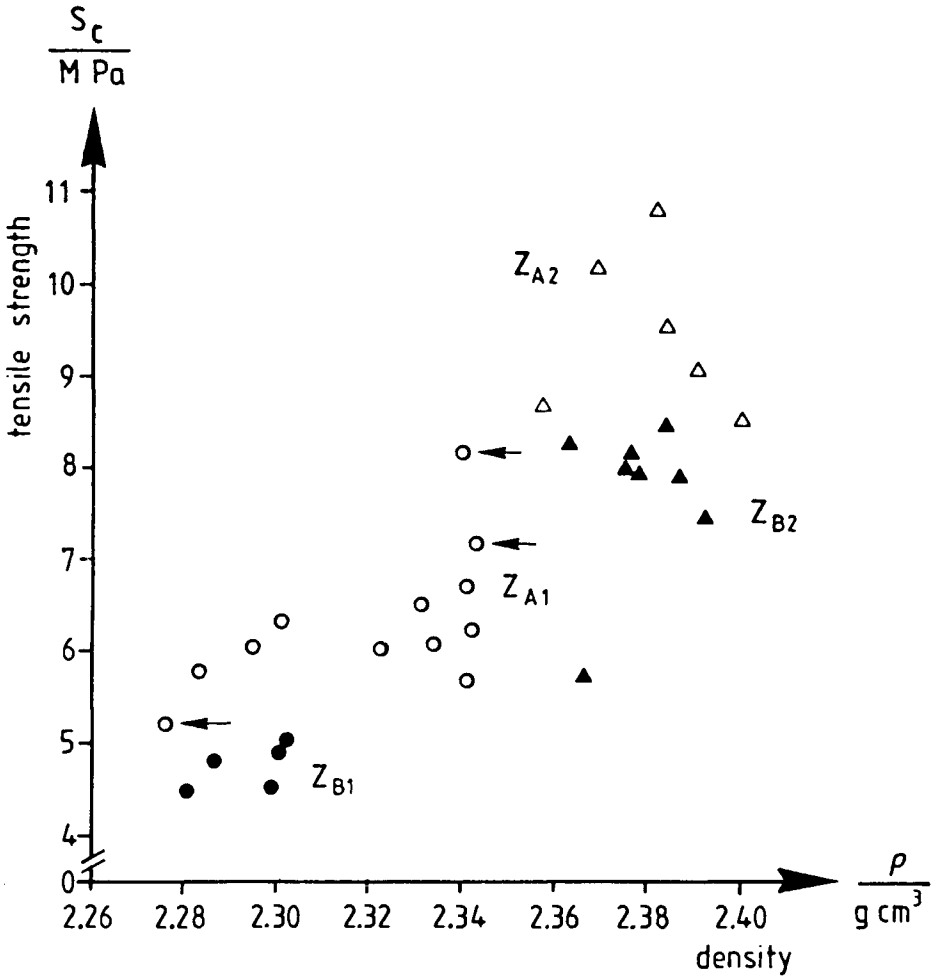

Figure 4.2: Distribution of Tensile Strength Versus Density for a Mullite Refractory. (Z_A = High Loading Rate: Z_B = Low Loading Rate, Arrows Indicate Outliers)

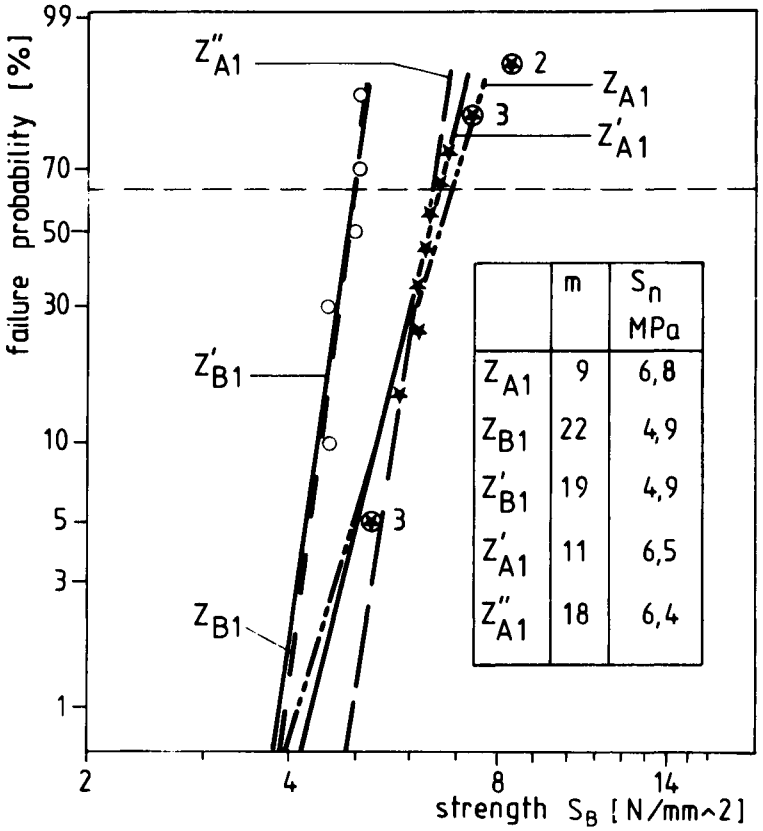

Figure 4.3: Analytical Correlations Between Tensile Strength and Bending Strength Data for a Mullite Refractory as Shown by Weibull Distributions (Z_A, B_A = High Loading Rate; Z_B, B_B = Low Loading Rate)

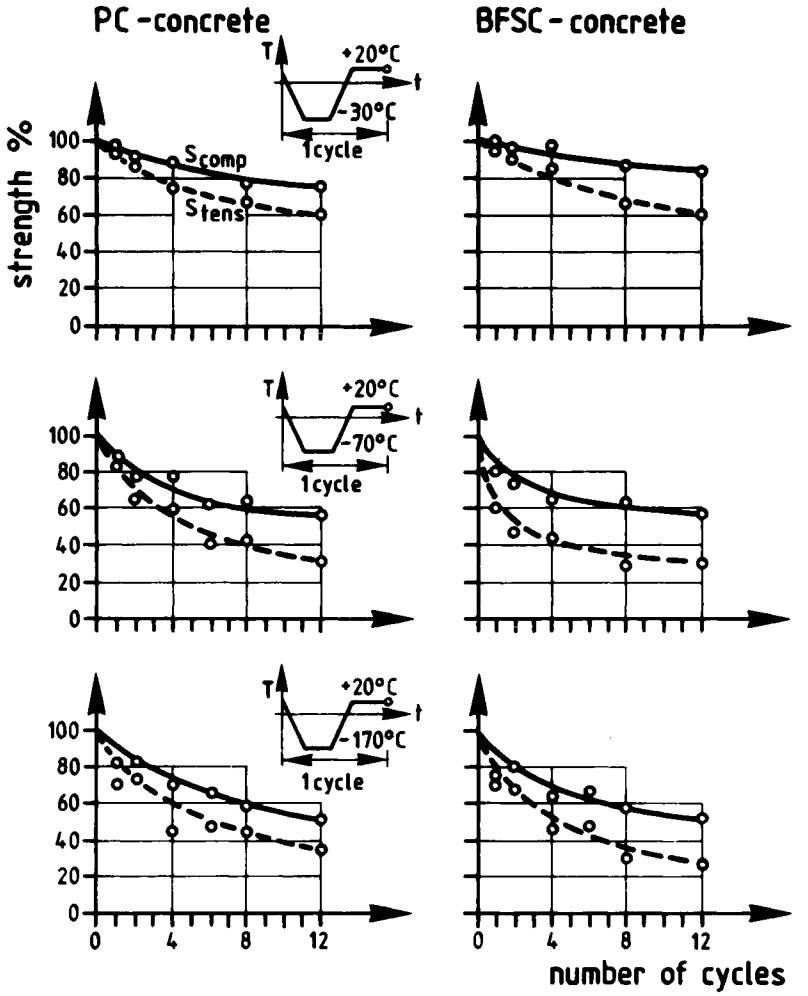

Figure 4.4 Dependence of Compressive and Tensile Strength of Water Saturated Concrete on Thermal Cycling Between 20 °C and Different Low Temperatures /4,5/

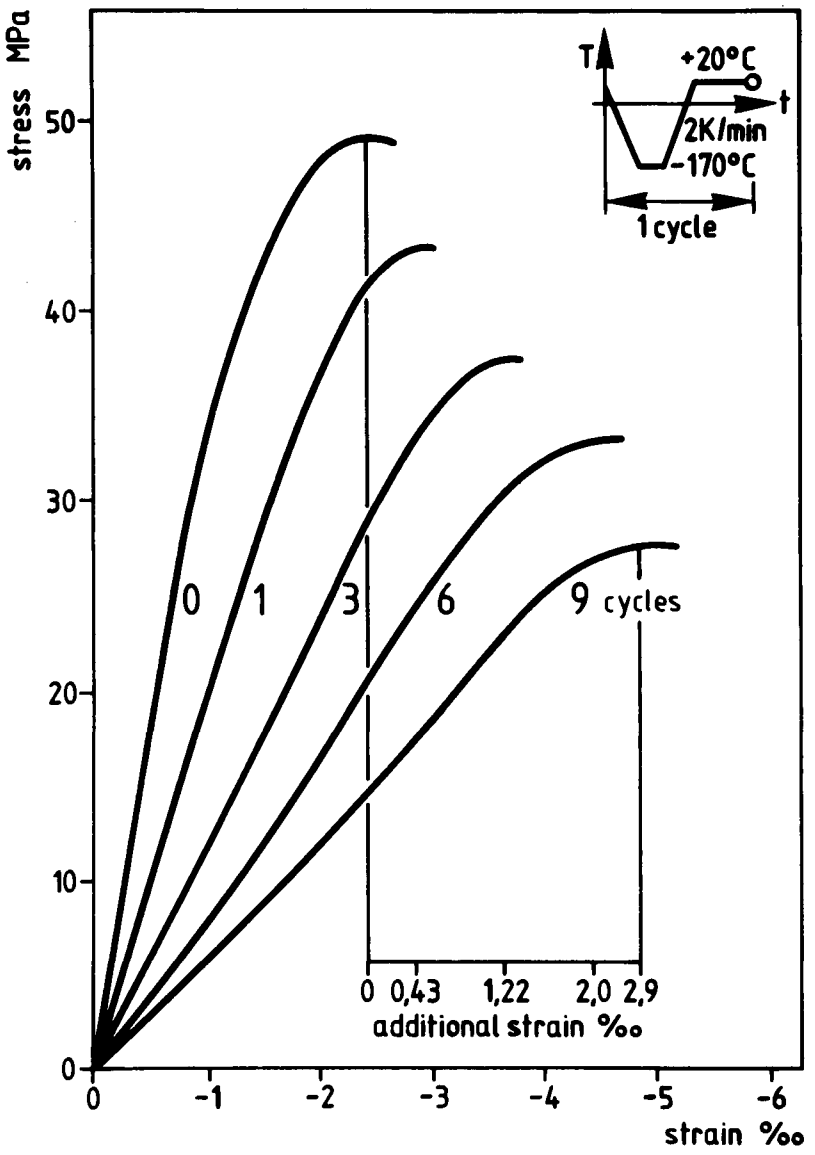

Figure 4.5: Compressive Stress - Strain Dependencies of Water Saturated Mortar on Thermal Cycling Between 20 °C and -170 °C /4,5/

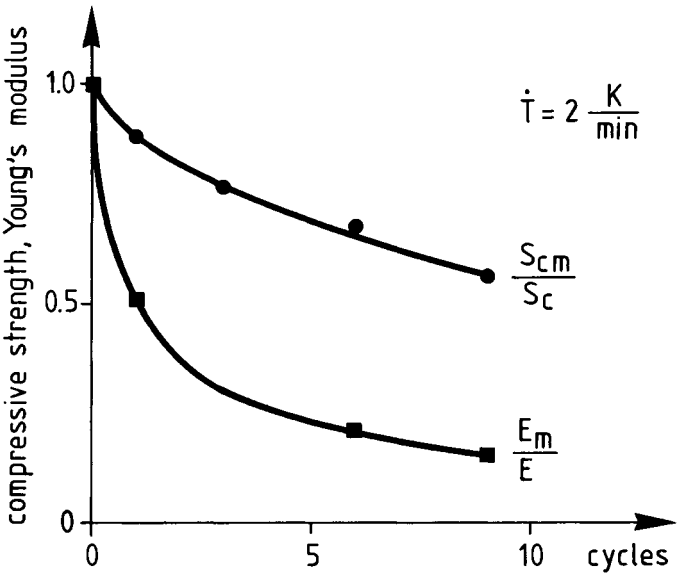

Figure 4.6: Dependence of Compressive Strength and Young's Modulus of Water Saturated Mortar on Thermal Cycling (Based on Figures 4.4 and 4.5)

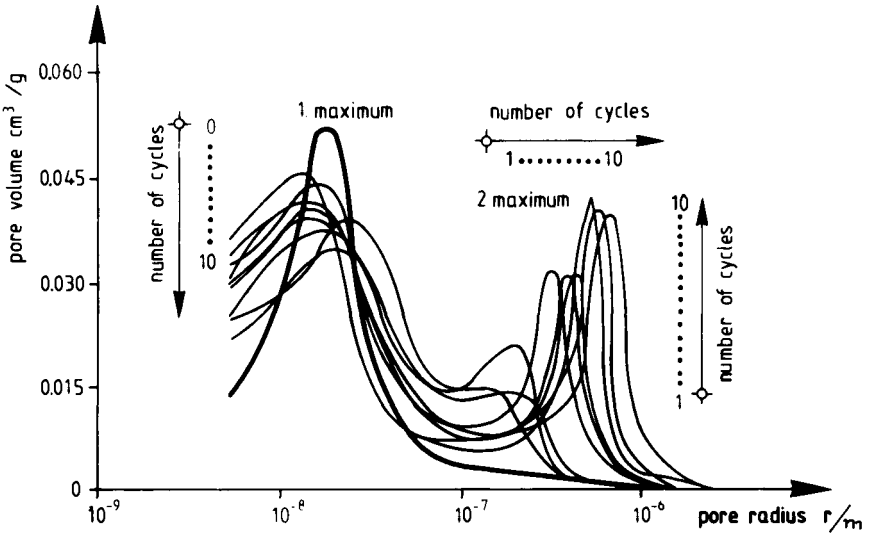

Figure 4.7: Differential Distribution of Pore Radii of Water Saturated Blast Furnace Slag Cement-Mortar After Thermal Cycling /4,5/

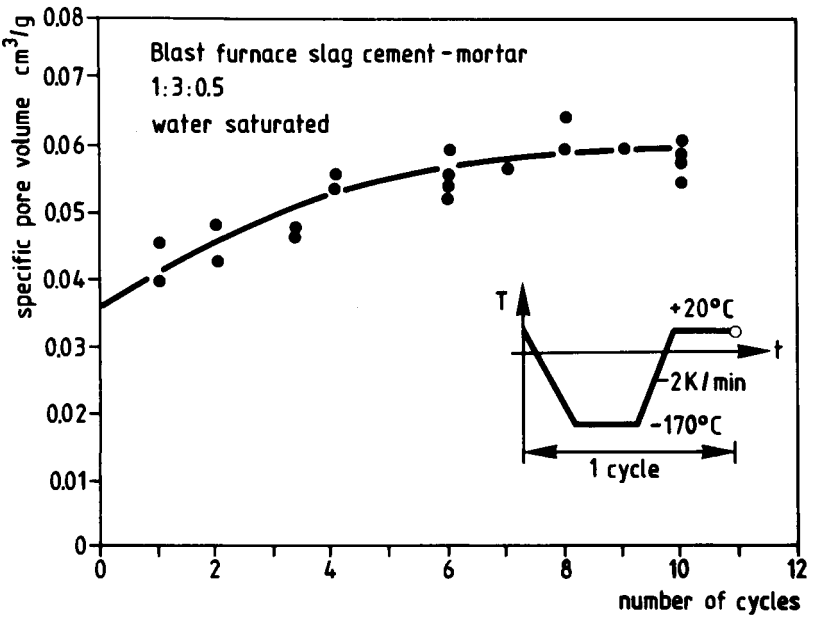

Figure 4.8: Pore Volume of Mortar After Thermal Cycling /4,5/

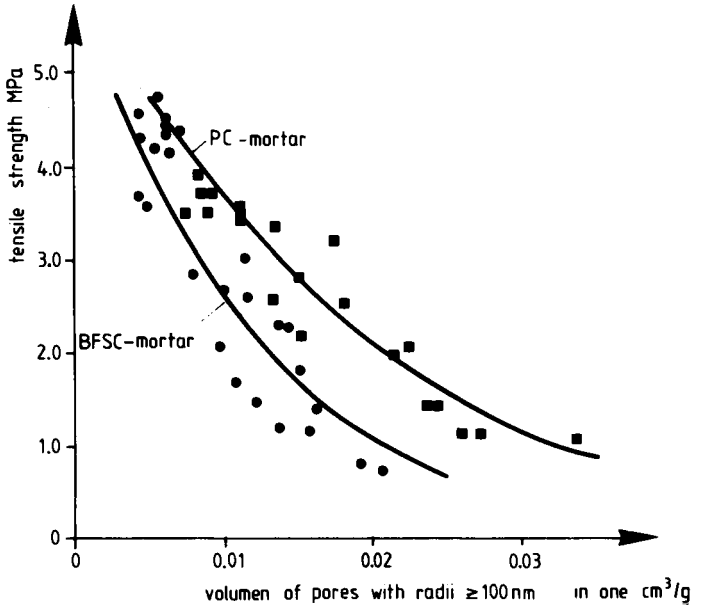

Figure 4.9: Dependence of Tensile Strength on Pore Volume for Two Water Saturated Mortars After Low Temperature Thermal Treatment /4,5/

5 METALLURGICAL FACTORS AFFECTING THE RELIABILITY OF MATERIALS IN HIGH-TEMPERATURE APPLICATIONS OF TURBINES

W. Hoffelner

Brown, Boveri & Cie., Baden, Switzerland

5.1 INTRODUCTION

Component reliability is a very complex problem area, dependent on many factors such as loading conditions, environment, surface and mechanical properties of the material in question. Present considerations will be confined to aspects concerning reliability from the standpoint of the mechanical properties of materials used for components in high temperature applications.

The components of concern here will be rotors and blades. The rotor materials which will be treated are low allow steels containing typically 1 % Cr, 1 % Mo and 0.25 % V. Such steels are used world-wide as rotor material in high pressure (HP) and intermediate pressure (IP) sections of steam turbines, as well as in stationary gas turbines. The most interesting mechanical parameters in such applications are creep strength and toughness. Creep stresses occur in steady-state operation due to centrifugal forces acting in rotor and blading. Startup and shutdown procedures lead to additional thermal stresses which can cause fatigue crack propagation from existing flaws, leading to brittle fracture of the rotor at low temperatures. This means that the toughness of the material is of importance, especially in situations where embrittlement during service can occur. Gas turbine blading materials, chosen as the second example, are nickel-base alloys often in the as-cast condition. Types of loading typical for this particular application are creep due to centrifugal forces and high cycle fatigue (HCF) due to blade vibrations.

The above-referred to materials show a certain "reliability" under the applicable loading conditions. Nevertheless, because of the complexity of the alloy systems, a variety of microstructures can develop, each showing very different response to mechanical loads. Due to the high temperatures in service, microstructures can also change with time of equipment operation. This means that mechanical

properties can become critical, thereby necessitating the regular renewal of parts operating, particularly, in situations of high risk. As has been discussed in the chapter by Buresch, the reliability of materials is strongly affected by their microstructure and their response to mechanical loading. The present chapter is aimed, therefore, at pointing out connections between microstructure and essential mechanical properties for the class of materials previously specified. Considerations will be confined mainly to such elementary properties as creep or fatigue. More complex problems such as creep-fatigue interactions, multi-axial loading conditions and environmental degradation cannot be discussed in the present context.

5.2 RELIABILITY OF MECHANICAL PROPERTIES

Many mechanical properties of materials are studied in the laboratory by determining the loading conditions under which failure or measurable damage (e.g. crack increments) of specimens occurs. Typical examples of this type include not only determination of yield strength σ_y, ultimate tensile strength σ_{uts}, stress rupture curves or S/N curves but also fracture mechanics quantities such as the fracture toughness K_{1c}, fatigue crack growth rates (da/dN) or creep crack growth rates (da/dt).

For loading conditions below the load leading to failure, the material is assumed to be safe whereas, for loading conditions higher than the load leading to failure, the material is assumed to be unsafe. The problem, however, is that normally the above-listed material parameters show a high amount of scatter. This is illustrated in Fig. 5.1, taking the stress rupture data of a typical rotor material (1 CrMoV steel) as an example. The data points separate regions of what might be termed high and low "reliability"; the scatterband can be treated as a "boundary of reliability". The further away from this boundary, the clearer the decision on safety or lack of safety becomes. However, the closer the boundary is approached, the higher the uncertainty regarding safety in the use of the material.

The judgement of material behaviour in the vicinity of a scatterband of the data should be performed on a probabilistic basis. The main reason why this is very often not done is that a proper statistical evaluation necessitates a large amount of data which does not normally exist in every case.

Therefore the data are often treated, without recourse to statistics, as mean values or as lower-bound values. For design purposes, the necessary safety is achieved by using lower-bound values together with safety factors /1/. However, especially with regard to reliability considerations of old equipment, where the actual scatterband of the data is reached, probabilistic methods for estimating "residual" life would be useful. Such methods, although in development, have not until recently been extensively used.

The "reliability boundary" is determined mainly by mean value and width of the scatterband. One problem is that, in the case of long-term properties, the curves must be extrapolated beyond existing experimental data. Such extrapolations are always difficult when time- and temperature-dependent changes of the strength of the material can be anticipated. This means that there is a degree of uncertainty in these types of reliability considerations whenever new materials are introduced. This behaviour is illustrated for a cast and a wrought steel in Fig. 5.2. In this figure, the minimum creep strength for 10^5 hours at 500 °C is plotted as a function of time /2/. During the first 10 - 12 years, this strength had to be reduced by 25 - 30 % as a result of increasing experience with these materials. Increasing laboratory and service experience can also lead to a reduction of the width of the expected scatterband. In the following sections, it will be demonstrated how metallurgical parameters can affect mean values and scatterbands and, therefore, influence material reliability.

5.3 ROTOR ALLOYS (1 CrMoV Steels)

Microstructure

The materials commonly used as rotors for steam and gas turbines are 1 CrMoV steels. These steels are some of the most economical high creep strength steels available and they have been used increasingly over the past 30 years in the power industry. The microstructural features of the material can be seen from the TTT diagram for continuously cooled specimens shown in Fig. 5.3 taken from /3/. A typical chemical composition is shown in Table 1.

Table 1: Typical Chemical Composition of a 1 CrMoV Rotor Steel (Mid-Seventies)

	A470 (1974) Class 8
Carbon	0.25 - 0.35
Manganese	1.00 max.
Phosphorous (max.)	0.015
Sulphur (max.)	0.018
Silicon	0.15 - 0.35
Nickel	0.75 max.
Chromium	0.90 - 1.50
Molybdenum	1.00 - 1.50
Vanadium	0.20 - 0.30
Iron	Balance

Depending upon the cooling rates, different microstructures can be expected: Martensite, which is a metastable phase formed by rapid cooling of hot austenitic steel to near room temperature; bainite, which is a decomposition product of austenite consisting of ferrite and carbide formed at temperatures higher than those at which martensite forms; pearlite, which is a lamellar aggregate of ferrite and cementite (Fe_3C) formed on slow cooling through the eutectoid transition temperature. The alloying elements Ni,Mn,Cr,Mo,V act as solid solution strengtheners and they also form carbide precipitates such as molybdenum and vanadium carbides improving, in consequence, the strength. (The role of tramp elements will be treated separately later.)

Creep Properties

Looking at the variety of microstructures which can be formed in this material, depending upon the cooling rate, one might expect rather different creep properties throughout a large forging. For a rotor forging, the expected microstructures are shown in Fig. 5.3. Much higher cooling rates, for example, can be achieved for the rim of the rotor body than can be achieved for the core. The creep behaviour of the different microstructures is shown in Fig. 5.4. In this figure, the strain is plotted as a function of the time at 550 °C and at a stress of 152 MPa.

The best creep rupture properties of CrMoV steels are achieved with a microstructure consisting of upper bainite /4/. A rotor should, however, combine good creep properties with high toughness and, therefore, other microstructures might be preferable (as discussed in the next section). It has been shown /3/ that the optimization of the microstructure considerably reduces the scatterband of the stress rupture data. Investigations of this type are certainly responsible for the demonstrated high reliability of those materials, here considered, during their successful application over the past 20 - 30 years.

There is, however, a pronounced trend towards extending the service life of already installed equipment, sometimes with changes in the operational modes. This leads to the necessity for estimating the remaining useful life of relevant components. Concepts for such residual-life calculations exist and are in use /1,2,5/. The problem of estimating creep properties in the vicininty of reliability boundaries can arise and, although in such situations a knowledge of microstructure and creep properties is very useful, the problem still remains that there could arise changes in the microstructure as a result of the very long preceding thermo-mechanical processes during service. One very severe difficulty in fact is the possibility of embrittlement /6/ which will be discussed in terms of toughness, in the following section.

Toughness of 1 CrMoV Steels

As previously mentioned, the toughness of rotors is a critical material parameter. There are different physical quantities describing the toughness of a material: the impact strength, the ductile-to-brittle fracture appearance transition temperature (FATT) and the fracture toughness, K_{1c}. The impact strength as well as K_{1c} should be high, whereas the FATT should be low. Like the creep properties, the toughness depends on the microstructure of the material. Unfortunately, there is an inverse relation between the creep rupture strength and the toughness /7/ as illustrated in Fig. 5.5. Increasing creep rupture strength is associated with increasing FATT which, in turn, implies decreased toughness. In microstructural terms, it can be stated that upper bainite has good creep properties but poor ductility, whereas lower bainite and martensite show good ductility combined with inferior creep strength.

Another factor affecting the toughness of rotor materials is the presence of tramp elements such as P, Sn, Mn, Si, As, Sb. These elements can segregate, during service at 320 - 550 °C, to grain boundaries and, consequently, embrittle the material /8,9,10,11/. This embrittlement is called temper embrittlement and it shows a very complex dependence on the trace impurities as discussed in, for example, /12/. Although 1 CrMoV steels do not show the same susceptibility to long-term temper embrittlement as the NiCrMoV steels used in low-pressure rotors, they nevertheless do show a tendency towards embrittlement. As an illustration of the correlation between grain boundary segregation and embrittlement, Fig. 5.6, taken from /13/, depicts embrittlement (expressed as Δ FATT) plotted against grain boundary impurity concentration. It is clear that impurity levels should be reduced. Trends in this reduction are shown in Fig. 5.7. In a recent assessment /13/, advanced melting technologies were investigated with respect to ultimate improved toughness. The toughness of low sulphur (LSC) material and eletroslag-remelted (ESR) material is compared with conventional CrMoV material in Fig. 5.8. It can be seen that the advanced technologies, with attendant higher purity levels, do indeed lead to improved fracture toughness.

As regards reliability of rotors one can say that, analogously to creep strength, toughness has also been improved over the last 30 years (refer to Figure 5.9) and the tendency for temper embrittlement to occur has decreased. Since, however, our present knowledge of toughness and embrittlement of the materials was not available when constructing the older plants, further equipment examinations and careful retirement programs are necessary.

5.4 BLADING ALLOYS FOR GAS TURBINES

Microstructure

Materials used for gas turbine blades must combine high strength at high temperatures with high hot-corrosion and oxidation resistance. This can be achieved with nickel-base alloys. A widely used gas turbine blading alloy is the cast material IN 738 LC. The typical chemical composition of this alloy is given in Table 2, together with the usual two-step heat treatment.

Table 2: Chemical Composition (Wt Pct) and Heat Treatment of the Cast Superalloy IN 738 LC

C	Cr	Co	Mo	W	Ta	Nb	Al	Ti	Zr	Ni
0.17	16.0	8.5	1.7	2.6	1.7	0.9	3.4	3.4	0.10	Bal.

Heat Treatment
2 Hours/1,120 °C AC + 24 Hours/845 °C AC
(AC = Air Cooling)

This alloy has an austenitic Ni-Cr matrix. Besides solid solution strengthening, a coherent γ'-phase $Ni_3(Al,Ti)$ acts as the hardening phase. A typical microstructure of this type of alloy is shown in Fig. 5.10. Primary carbides of MC-type occur at the grain boundaries and in the matrix. Along grain boundaries, $M_{23}C_6$-type carbides are formed. The high Cr content of the material is to prevent oxidation and corrosion attack. Such high Cr content can promote the formation of plate-like σ-phase which lowers the creep properties. The composition of present batches of IN 738 LC is optimised in this respect and does not show dangerous amounts of σ-phase even after long-term ageing. Besides the phases mentioned above, additional phases and phase reactions occur, mainly during the ageing process of the alloy /14,15/.

Creep Properties

Stress rupture is an essential parameter for the reliability considerations of gas turbine blades, as has already been mentioned. Analogously to the 1 CrMoV steels, for IN 738 LC the wide scatterband /16/ and the extrapolation of data, are problem areas. The latter may be illustrated by way of an example. One well-known method for presenting and extrapolating stress rupture data is the Larson-Miller parameter where the creep strength is treated as a function of a combination of test temperature and time to failure. Under the assumption that short testing times at enhanced temperatures should lead to results similar to long testing times at lower temperatures, the Larson-Miller parameter should provide a possibility for extrapolation of data. This method has been applied to different sets of creep data, and creep curves have been established for different temperatures /17/.

When sufficient long-term data were available, it turned out that the extrapolated values were much too optimistic /18/ as shown in Fig. 5.11. One reason for this behaviour is that the creep mechanisms can change as a function of stress and temperature. For IN 738 LC, for example, there is a tendency to γ'-cutting at high stresses and low temperatures, whereas dislocation climb is the predominant deformation mechanism at low stresses and high temperatures /19/. Besides these differences, purely thermally induced long-term changes in the γ'-phase affect the creep behaviour. Neither of these effects are accounted for in the Larson-Miller parameter applied to short-range data. Similar problems have also been found with other extrapolation methods /18/. In conclusion, one can say that all the parametrisation methods for creep rupture curves are able to represent an existing set of data, but they must be used extremely cautiously for data extrapolation.

The scatter band of the stress rupture curves is a result of a variety of microstructural parameters such as chemical composition (including residual elements), segregation, γ'-size and distribution, etc. The influence of these parameters on the creep properties has been discussed in detail elsewhere in the literature /16/.

High-Cycle Fatigue (HCF) Properties

High-cycle fatigue tests of cast nickel-base superalloys reveal, in almost all cases, casting pores as the origin of fracture /20,21/. These pores form during the solidification process at locations where different solidification fronts come together. They are, therefore, irregularly shaped with very sharp wedge-type edges. An attempt has been made to explain the HCF properties of these cast alloys in terms of crack growth parameters /22/. For this purpose, fatigue crack growth rates were measured. Since the fatigue failures started from internal pores, crack growth rates were measured in vacuum. The results are shown in Fig. 5.12 where the fatigue crack growth rates (da/dN) are plotted as a function of the cyclic stress intensity factor ΔK. The following relation exists between the applied load $\Delta\sigma$, the crack length, a, and ΔK:

$$\Delta K = \Delta\sigma\sqrt{(\pi a)}.T \qquad - (1)$$

T is a geometry-dependent function.

The fatigue crack growth curve shows typically three regions:

a) the threshold region where the curve drops to a fatigue threshold, ΔK_o below which no crack growth can be measured
b) a stage of power-law crack growth (Paris regime)
c) the stage of final fracture where the (cyclic) fracture toughness is reached.

Generally, one can write for the crack growth curve:

$$\frac{da}{dN} = f(\Delta K) \qquad - (2)$$

where $f(\Delta K)$ is a function of the cyclic stress intensity range ΔK . Integration of Eq. (2) gives:

$$N_f = \int_{a_i}^{a_f} \frac{da}{f(\Delta K)} \qquad - (3)$$

In this equation, a_i is the initial crack length, a_f the final crack length and N_f the number of cycles to reach the final crack length. Solving Eq. (3) numerically for the da/dN curve of IN 738 LC and inserting a_i as a characteristic pore diameter, the S/N curve can be derived /22/.

The calculated curve is shown in Fig. 5.13 together with the measured S/N values and shows a very good correlation. This means that size, location and distribution of casting defects govern the fatique properties. Taking into consideration, additionally, the fact that the fatigue threshold ΔK_o depends especially on microstructure, the high amount of scatter in the fatigue data is understandable. It should be mentioned that this straightforward calculation works only at high temperatures. At lower temperatures, the correlation becomes worse, because of the different fracture modes as discussed in /22/. The fact that fatigue fracture occurs in connection with casting porosity is, however, independent of the temperature.

In an effort to improve the reliability of the materials considered here, an attempt has been made to improve the fatigue properties by removing the porosity using hot isostatic pressing (HIP). It was able to be shown that HIP actually improves the HCF properties of the materials considered here /21/ and developments are underway to optimise the HIP treatment for these alloys.

5.5 CONCLUSIONS

Metallurgical factors affecting the reliability of essential material properties of alloys used in high-temperature applications have been summarized. The materials which have been considered are forged low-alloy steels (1 CrMoV), used world-wide as rotor material for rotor parts, both for steam turbines and gas turbines and a cast nickel-base superalloy IN 738 LC, which is a common gas turbine blading material.

Due to the very complex microstructures of these materials, the mechanical properties are influenced by alloy composition, trace elements, heat treatment, melting and casting technology and service exposure. This means that the mechanical properties can change drastically in one batch of material, or even in one component, simply as a result of the manufacturing process. Different parts of a large forging necessarily experience different cooling rates during heat treatment, leading to location-dependent creep properties or toughness. It is impossible to avoid casting defects, leading to fatigue failure in cast components, even with advanced casting facilities.

Years of research, development and experience with these materials have led to relatively good understanding of the basic material properties and with respect to these properties, the materials discussed can be considered as possessing high reliability. A real problem, however, still remains, namely the estimation of the useful remaining life in old equipment. This is partly due to the fact that present experience was not available when that equipment was installed in power plants. On the other hand, damage occurring during service is a very complicated combination of different damage processes including embrittlement, thermal fatigue, creep-fatigue interactions and environmental attack. A "reliable" judgement on the remaining life is not, therefore, always possible. Consequently, parts may have to be renewed without the benefit of a judgement on their residual lifetime being able to be made.

REFERENCES

/1/ Berg U., Melton K.N., Heiberger D. - Determining and Evaluating the Service Life of Steam Turbine Components, Brown Boveri Review, 68, December 1981.

/2/ Czeratzki A., Busse L., Stys Z. - Remaining Useful Lifetime of Older Steam Turbines, The American Power Conference, Chicago, Illinois, April 1983.

/3/ Norton J.F., Strong A. - Improvement of Creep and Rupture Properties of Large 1 % CrMoV Steam Turbine Rotor Forgings, J. of the Iron and Steel Inst., p. 193, February 1969.

/4/ Viswanathan R. - Strength and Ductility of CrMoV Steels in Creep at Elevated Temperatures, ASTM J. of Test Eval., 3, No. 2, p. 93, 1975.

/5/ Woodford D.A. - Creep Damage and the Remaining Life Concept, J. Eng. Material Technol., 101, p. 311, 1978.

/6/ Roman I., Rau C.A., Tetelman A.S., Ono K. - Fracture and Fatigue Properties of 1 % CrMoV Bainitic Turbine Rotor Steels, EPRI NP-1023 (Research Project 700-1), Technical Report, March 1979.

/7/ Batte A.D., Murphy M.C., Fischer K., Venkatesworln J. - The Production Heat Treatment of 1 % CrMoV Steam Turbine Rotors for Creep Resisting Service, Stahl und Eisen, 98, p. 34, 1978.

/8/ Viswanathan R., Joshi A. - Effect of Microstructure on the Temper Embrittlement of CrMoV Steels, Metall. Trans. A, 6A, p. 2289, 1975.

/9/ Takayama S., Ogura T., Shin-Chang Fu, McMahon C.J. - The Calculation of Transition Temperature Changes in Steels Due to Temper Embrittlement, Metall. Trans. A, 11A, p. 1513, 1980.

/10/ Qu Z., McMahon C.J. - The Effects of Tempering Reactions on Temper Embrittlement of Alloy Steels, Metall. Trans. A, 14A, 1983.

/11/ Jaffee R.I - Metallurgical Problems and Opportunities in Coal-Fired Steam Power Plants, Metall. Trans. A, 10A, p. 139, 1979.

/12/ Chen S.H., Takasugi T., Pope D.P. - The Effects of Trace Impurities on the Ductility of a CrMoV Steel at Elevated Temperatures, Metall. Trans. A, 14A, p. 571, 1983.

/13/ Viswanathan R., Jaffee R.I. - Toughness of CrMoV Steels for Steam Turbine Rotors, EPRI RD-2357-SR Special Report, April 1982.

/14/ Hoffelner W., Kny E., Stickler R., McCall W.J. - Effects of Aging Treatments on the Microstructure of the Ni-Base Superalloy IN-738, Z. Werkstofftechn., 10, p. 84, 1979.

/15/ Geiger T., Stickler R., White G.H. - The Structural Stability of NiCr-Base Superalloys during Long-Time Exposure at Elevated Temperatures, High-Temperature Alloys for Gas Turbines, p. 317, D. Coutsouradis et al. (eds.), Applied Science Publishers, London, 1978.

/16/ Lupinic V., Gibbons T.B. - Factors Influencing the Creep Behaviour of NiCr-Base Alloys, High-Temperature Alloys for Gas Turbines, p.335, D. Coutsouradis et al. (eds.), Applied Science Publishers, London, 1978.

/17/ Buchmayr B., Danzer R. - Creep and Fatigue Behaviour of IN 738 LC, COST 50, III, A3, Int. Rep. No. 1, Montan University, Leoben, Austria, 1981.

/18/ Martens H.J., Rosselet A., Walser B. - Creep Fatigue Interaction, COST 50, III, Chapter 5, Final Report, Sulzer AG, Switzerland.

/19/ Hoffelner W., Stickler R. - Unpublished Results, University of Vienna, 1977.

/20/ Hoffelner W., Tschegg E. - Gefügeuntersuchungen an Proben aus IN 939 nach Wechselverformung bei hohen Temperaturen, Z. Werkstofftechn., 12, p. 185, 1981.

/21/ Schneider K., Gnirss G., Türck B., Arnim G.V. - Mechanisms of High-Cycle Fatigue of Cast Nickel-Base Alloys in High-Temperature Alloys for Gas Turbines, p. 685, R. Brunetand et al. (eds.), D. Reidel Publishing Company, Dortrecht, 1982.

/22/ Hoffelner W. - High-Cycle Fatigue Life of the Cast Nickel-Base Super Alloys IN 738 LC and IN 939, Metall. Trans. A, 13A, p. 1245, 1982.

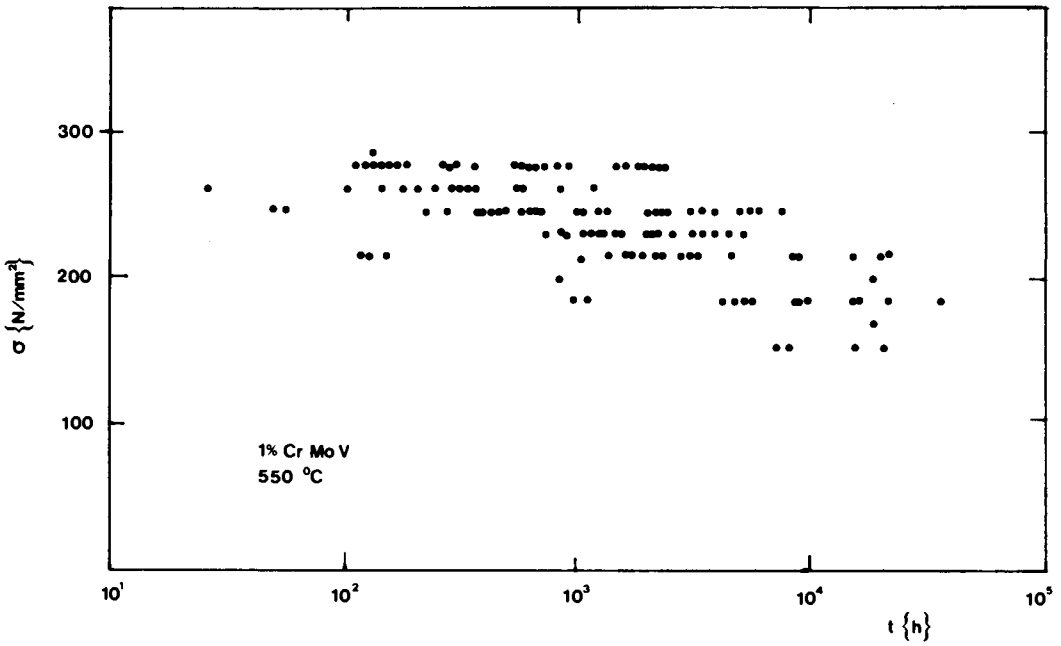

Figure 5.1: Stress Rupture Data for 1 % CrMoV Steel /3/

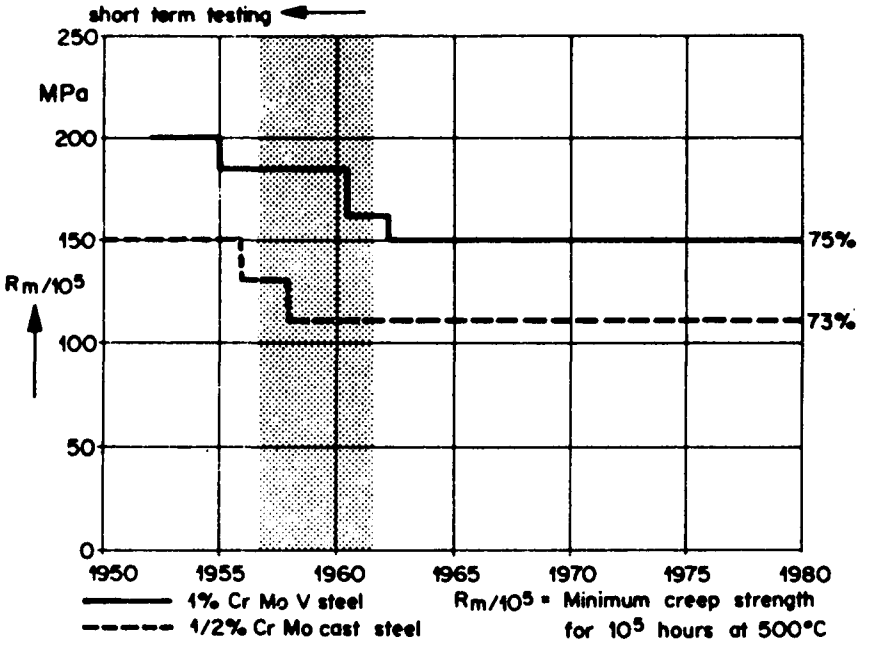

Figure 5.2: Reduction in Minimum Creep Strength for a Cast and a Wrought Steel over 1 Decade /2/

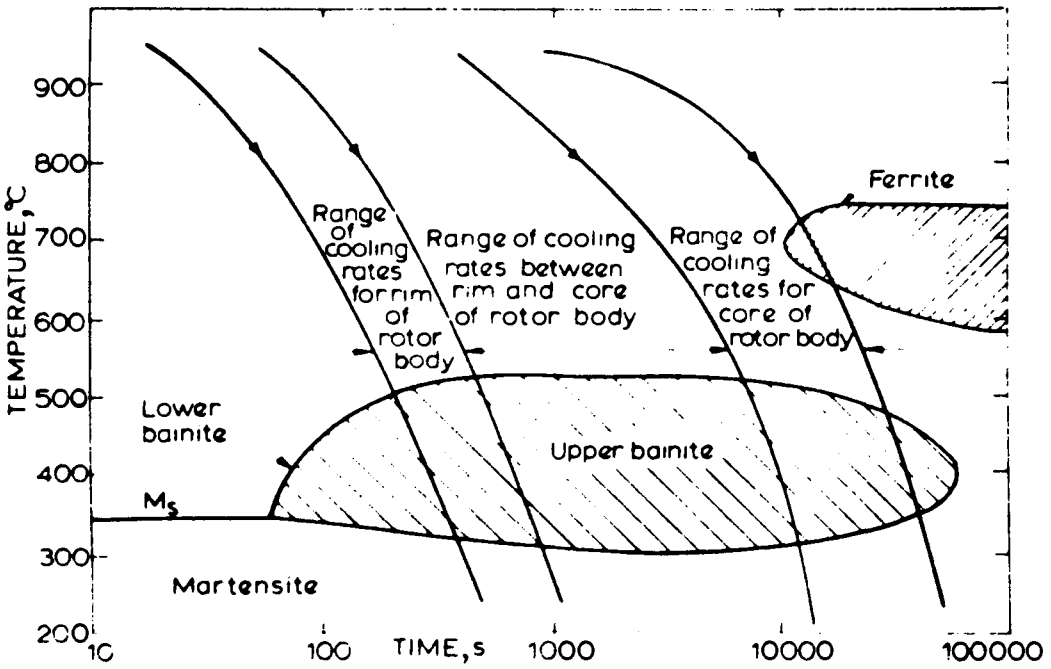

Figure 5.3: Ranges of Cooling Rates for Different Regions of a Rotor Forging /3/

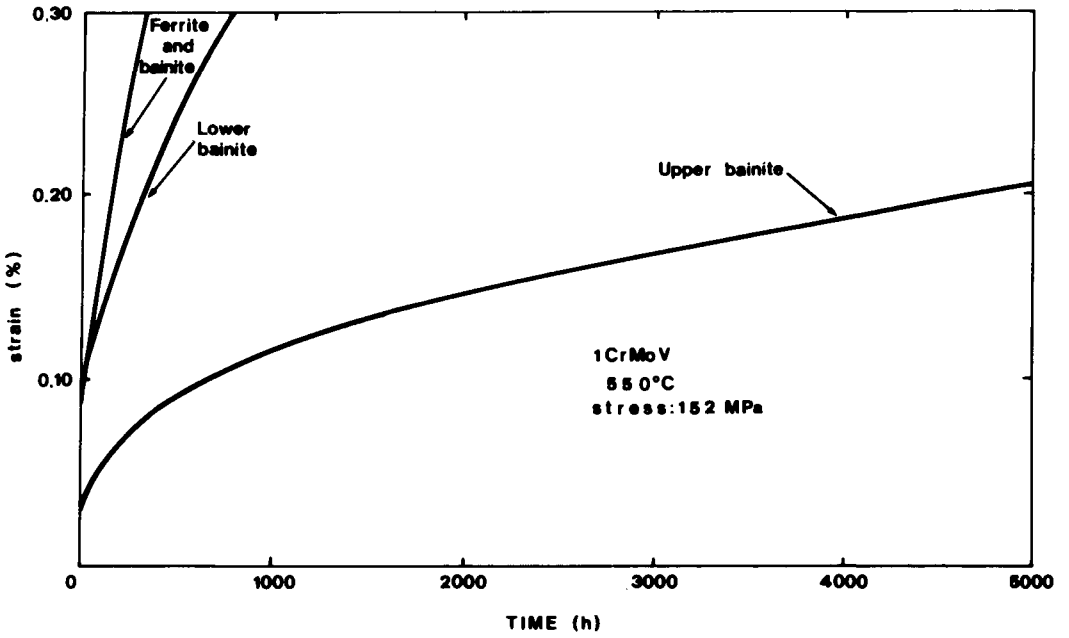

Figure 5.4: Creep Behaviour of Different Microstructures of 1 CrMoV /4/

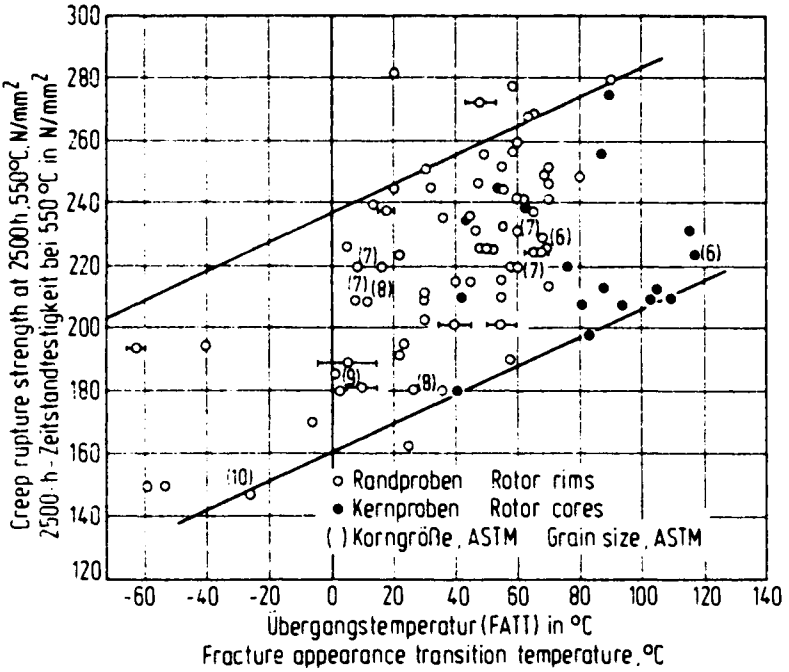

Figure 5.5: Relationship Between Creep Rupture Strength and Toughness /7/

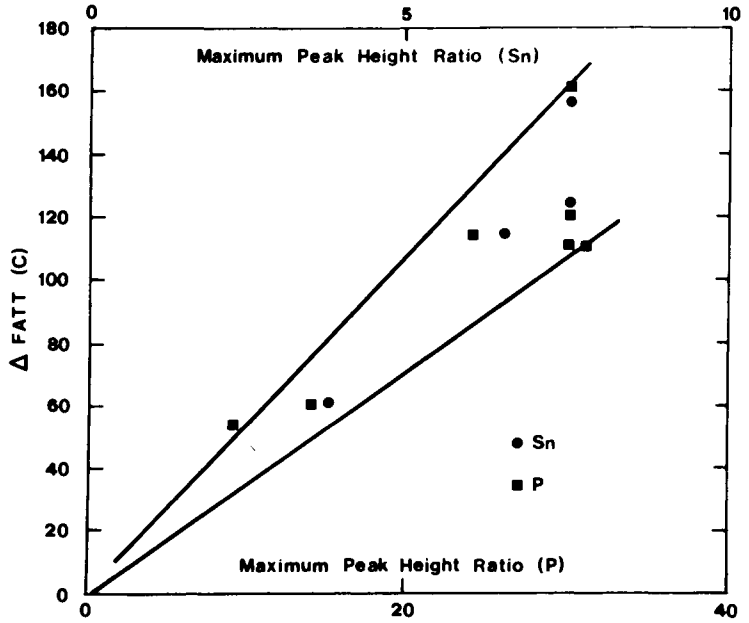

Figure 5.6: Relationship Between Embrittlement (Vertical Axis) and Grain Boundary Impurity Concentration (Horizontal Axis) /13/

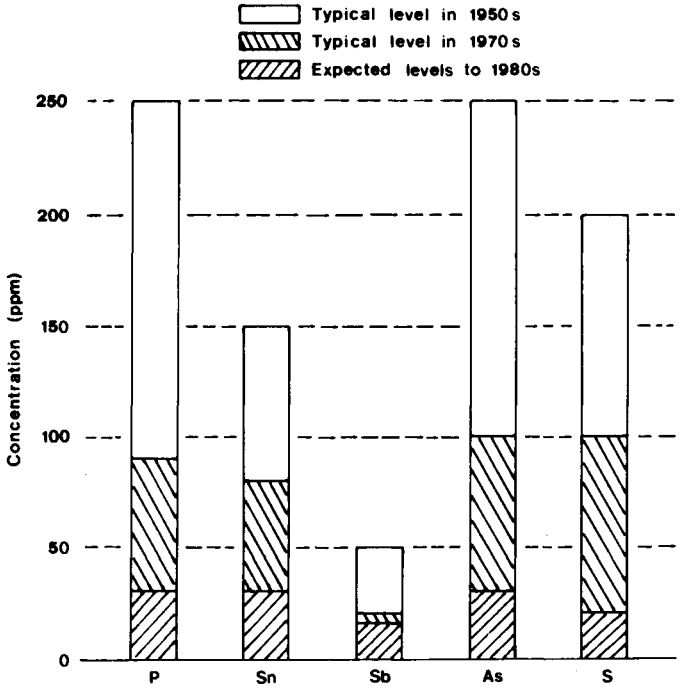

Figure 5.7: Reduction in Steel Impurity Levels Between 1950 and 1980 /13/

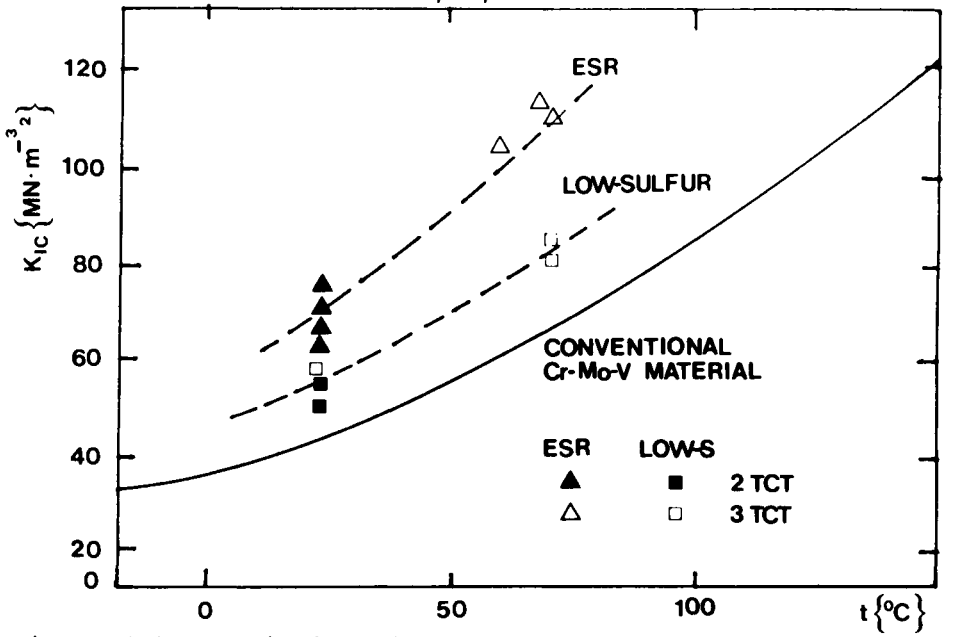

Figure 5.8: Variations in Toughness Between Low Sulphur and Electroslag-Remelted Materials and Conventional CrMoV Materials /13/

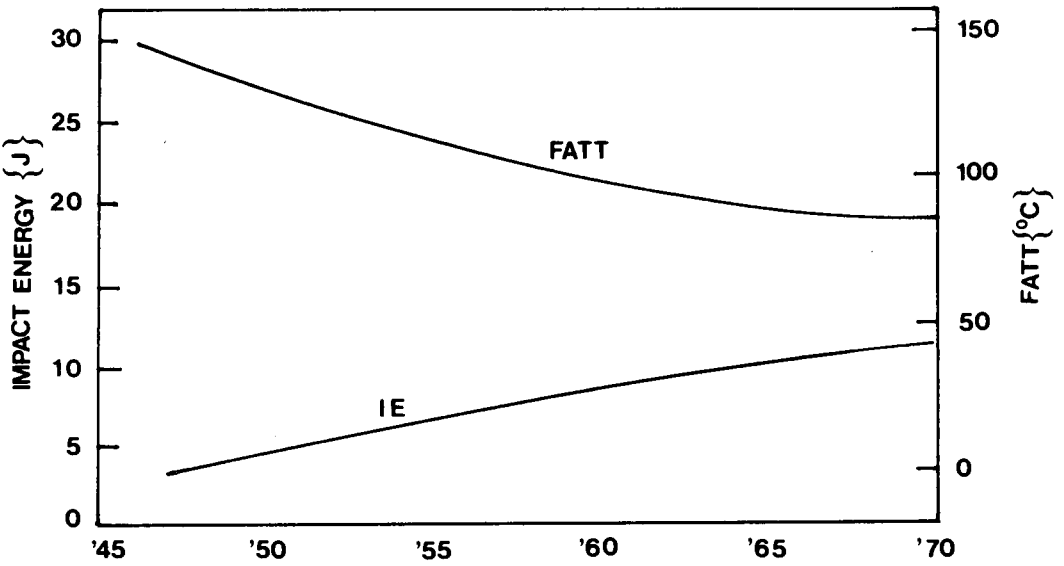

Figure 5.9: Changes in Toughness of Rotor Material with Improved Technology Over the Years 1945 - 70 /13/

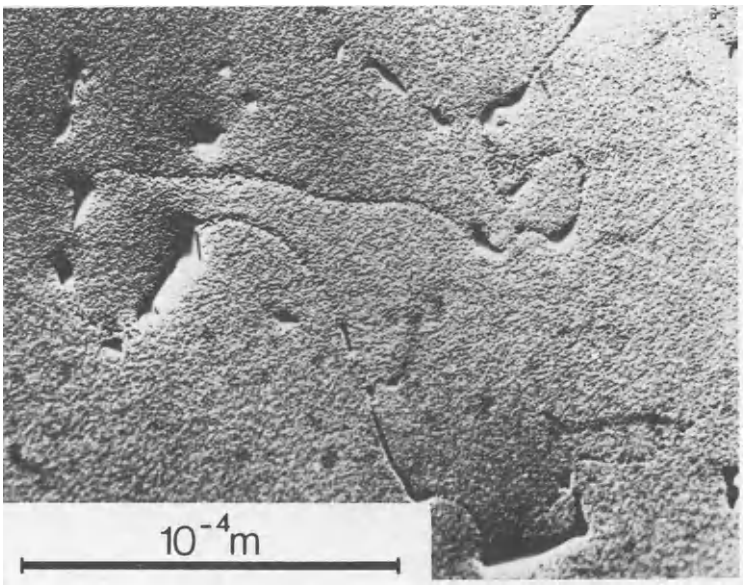

Figure 5.10: Typical Microstructure of the Cast Superalloy IN 738 LC

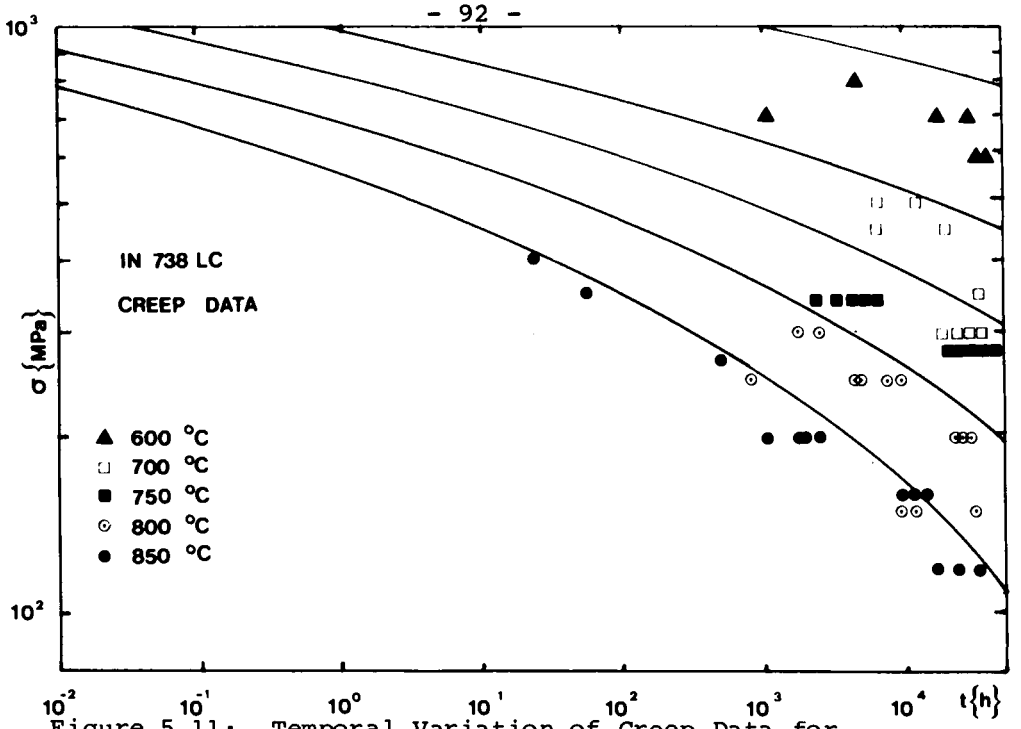

Figure 5.11: Temporal Variation of Creep Data for IN 738 LC (Extrapolated and Measured) /18/

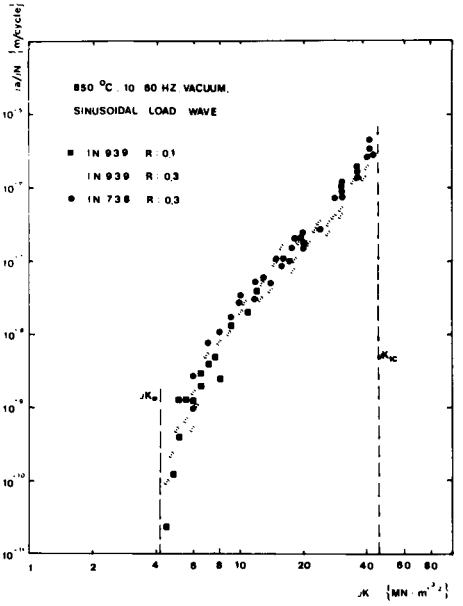

Figure 5.12: Fatigue Crack Growth Rates of the Cast Nickel-Base Alloys IN 738 LC and IN 939 in Vacuum at 850 °C

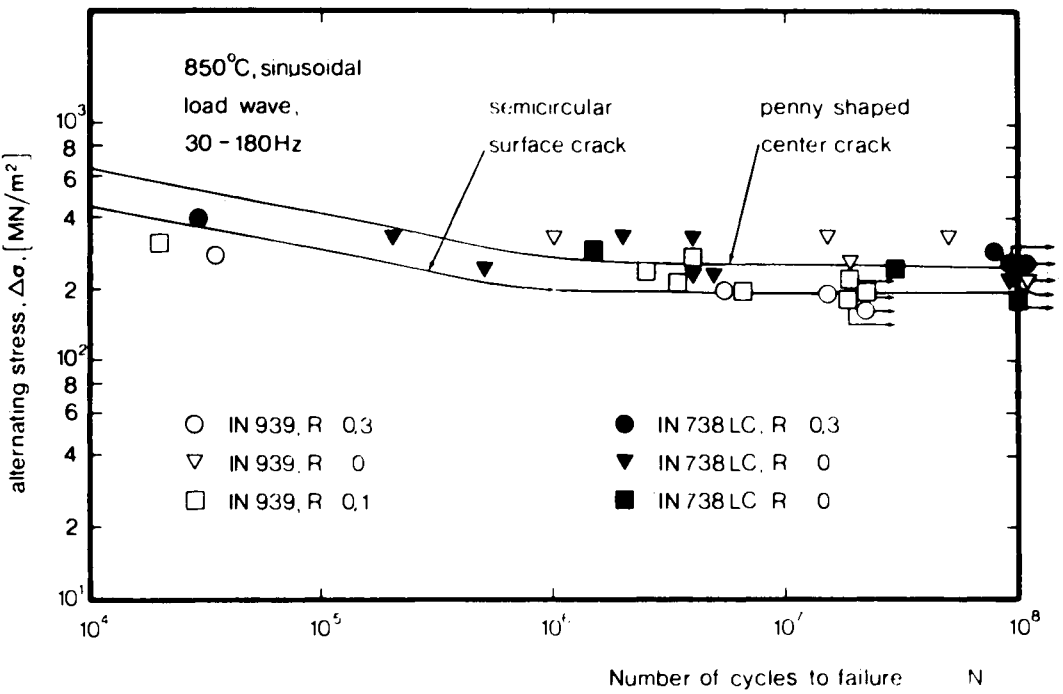

Figure 5.13: Calculated S/N Curves for IN 738 LC Together With Experimental Data Points /22/

6 MATERIALS PROPERTIES DATA BASES FOR MATERIALS RELIABILITY

H. Kröckel

Commission of the European Communities,
Joint Research Centre, Petten, the Netherlands

6.1 INTRODUCTION

Technical reliability has been investigated under this term since the end of World War II, and the classical fields in which reliability methodologies have been developed are electronics and aerospace technology. Energy production followed, in particular driven by the safety requirements of nuclear reactor technology, and many other fields actually apply these principles, among them land and sea transport, offshore technology and various other industrial activities in which product reliability is a major concern.

The main attention of this methodology is orientated firstly to phenomenological - statistical aspects, i.e., recording of events and their evaluation on the basis of statistical models, and secondly to mechanistic - analytical aspects which are linked with design, lifetime prediction and failure analysis methods.

The subject of present concern, engineering materials reliability, is mainly related to the second area, and so are materials properties data bases, the present subject of discussion. Obviously, materials data bases interlink with reliability methods in a similar way as with design and lifetime prediction methods. The usual reliability data bases on the other hand mostly support the statistical approach and prognostication on the basis of models.

In this light, it is of particular interest to review some aspects of materials data bases and their future potential, and to describe in greater detail the development by CEC-JRC of a mechanical properties data base which concentrates on materials for high-temperature applications.

6.2 TYPES OF PUBLICLY ACCESSIBLE ON-LINE DATA BASES

Broadly classifying computer-readable data bases which are currently available or coming into use via public telecommunication networks, one must distinguish two categories:

- Bibliographic data bases (reference files or reference data bases)

- Factual data bases (data files or data banks).

As a possible third category, there are the "full text journal systems" ("electronic journals"), a rather recently introduced alternative medium for the presentation of full-size articles, reports and journals by electronic transmission and display replacing hard copy or microfilm. They are not data bases, however, in the proper sense.

Genuine "data bases" have a feature lacking in the full text systems - the abstraction of the information which enables the rationalisation of the storage and access processes. The first two data base categories have seen a strong development over the past 25 years, which has recently been intensified by the integration of wide-band digital communication networks with better and cheaper computer terminals and more powerful computer software for data base management and data communication. The advent of mass communication systems like cable television and video text is preparing the ground for the introduction of data communication into all societal environments.

Computer readable, on-line reference (bibliographic) files are nowadays readily available and easy to access in nearly all fields of science and technology. The introduction of data files or data banks containing factual information generally started later and there is some divergence in their state of development, depending on the fields of application and the nature of their data. Marked differences can be noted in particular in the exactness, universality, standardisation and commercial sensitivity of the data information. Data on engineering materials are among the most difficult information for data banking, and materials data banks have, therefore, been very slow to come into common use by the public.

6.3 ENGINEERING MATERIALS DATA BANKS

Whilst the capability of computer and communication technology for the storage, retrieval, analysis, display and dissemination of data information undoubtedly exists, it is the nature of materials data itself which causes the fundamental problems in the conception and realisation of engineering materials data banks. The main barriers to enhanced development are the high cost and still unpredictable return of investment on materials data bases for engineering use. Such banks must provide access to a combination of physical, technical and commerical information such as basic properties, standard data, performance data, manufacturing data, availability and cost. Moreover, materials data are not only critical for technological progress and innovation but also to competition and they are, therefore, often subject to various restrictions and proprietary protection.

On the other hand, the concept of computerising materials data does not only offer to this complex system inherent advantages of comprehensiveness, currency and speed of access, but also opportunities for enhanced engineering capabilities. Computerised materials data are the ideal basis for "computer-aided engineering" (CAE) disciplines, CAD, CAM, CAT, multi-parameter handling, design algorithms (finite element analysis), lifetime prediction and performance and reliability analysis.

The use of computerised methods in all of these disciplines creates demands for computerised files of materials properties data which may, in future, result in a complete integration with certain of these methods. Obviously, in many parts of the world this has caused a strong drive to overcome the obstacles outlined above, to develop engineering materials data banks and to integrate these into publicly accessible information systems.

As an example, the advanced system development taking place in Germany can be quoted. The "Fachinformationszentrum Werkstoffe" has been established and charged with integrating geographically dispersed and independently developed materials (bibliographic) data bases and data banks /1/. These include:

- Bibliographic Data Bases:
  - SDIM 1 (Documentation and Information System Metallurgy), 1972 to August 1979
  - SDIM 2 (idem) from September 1979
  - Rheology/Tribology from Autumn 1982

- Factual Data Bases (Data Banks):
  . Material Data Base: Measured Properties of Steel
  . Material Data Base: Standard Properties of Steel
  . INFOS (Machinability Data Bank)

- Other Documentation and Information Services: Seven documentation centres, not (as yet) operating on line, which, in addition, cover the field measurements of mechanical quantities, welding technology, NDE, steel plants and processes, metallurgy and mining, foundry technology.

In the USA, some recent studies have examined the development of a co-ordinated system of materials data bases. These studies were commissioned by the Metals Properties Council and supported, among others, by the National Bureau of Standards (NBS), the National Materials Advisory Board, the Numerical Data Advisory Board of the National Academy of Sciences and CODATA. Their conclusions and recommendations /2/ suggest that the development of computerised systems of materials data is essentially driven by direct information needs and the advancement of computerised engineering and manufacturing systems.

Taking into account the actual adequacy of computer and telecommunication technology for remote access to a distributed network of independent data bases, the recommended concept for a materials property data system is based upon the connection of individual data bases of limited scope by a common "gateway" computer which will be the user access point and provide such features as standard support programs, an on-line master index to data sources, built-in tutorials and translation of protocols and formats /3/. Individual data bases would be developed and managed by expert groups and existing ones would be integrated into the system. This basic concept is the subject of further study by key government agencies and technical committees. In May 1983, the Metals Properties Council announced its plan for a "National Co-operative Materials Data System Based on Co-ordinating Existing Facilities", and subsequent development will undoubtedly be followed with interest.

Similar developments are under discussion or being implemented in other parts of the world. These efforts demonstrate - something that has been known for some time - that there have been many attempts to construct materials data banks, some of which have resulted in successful operation. It is also known that many of the large companies in Europe and the USA are operating computerised materials data banks for their internal use. Most of the systems, however, are small and narrowly focused and demonstrate minimal "user comfort". A widely usable, comprehensive system has to all intents and purposes not become publicly available yet, due in part to the lack of integration efforts and in part to the still-existing insufficiencies on already developed individual data bases. For Europe, it is of vital importance that the progress made in the important industrialised countries is carefully followed and an initiative, similar to that in the USA, be undertaken as soon as possible.

Table 1: Machine-Readable Data Bases of Materials Properties /4/

Material Property Field*	Total	Europe
Systems for Identification of Unknown Substances	19	7
Systems for Properties of Pure Substances and Mixtures	20	7
Systems for Metallurgical Calculations	5	4
Systems for Tables of Thermodynamic and Thermochemical Properties of Individual Substances	6	1
Properties of Plastics, etc.	2	-
Systems for Chemical Process Simulation and Design	11	3
Machine-Readable Files of Engineering Data on Materials	60	21

* A planned inclusion of data bases for nuclear, atomic and molecular properties is announced for a later extension of the directory.

One aspect which is of interest to note is the drive to commercialisation, wherever this appears feasible. Publishers are beginning to enter this market in the obvious conviction that the classical handbook functions may sooner or later be taken over by on-line systems.

A "Directory of Machine-Readable Data Bases of Material Properties" recently published /4/ shows that development of such systems is taking place all over the world. The numbers of relevant data bases listed in this directory are shown in Table 1 (the numbers of those associated in any respect with European countries have been derived). This survey must be qualified as being preliminary only and the figures shown are likely to be under-estimations.

Data bases relevant to materials and plant component reliability are mainly found among the engineering data files. They include mechanical properties and corrosion behaviour, as well as plant performance information. An interesting concept of a combination of such data bases is demonstrated by NBS (USA) in the form of the "Fossil Energy Materials Performance and Properties Data Centre" /5/ including:

- A materials and components plant performance data base

- A materials properties data base.

The first of these is computerised and both together contain a wealth of data information for practical engineering use, including reliability research.

A final data base of materials properties information which can be mentioned here is the METADEX/ METALS DATAFILE base operated by Metals Information (American Society for Metals in the USA and The Metals Society in Britain).

6.4 THE HIGH-TEMPERATURE MATERIALS DATA BANK DEVELOPED BY THE JOINT RESEARCH CENTRE (JRC)

The JRC has been involved in a high temperature materials research programme since 1975 at the Petten Establishment in the Netherlands. Since 1980, this research has included a project undertaking the development of a data bank within the scope of this programme.

The High-Temperature Materials Data Bank is being developed by the Petten and Ispra Establishments of the CEC JRC as a research and pilot concept for a European on-line information system which should, in future, cover the engineering requirements for factual data information on the properties of high-temperature materials. The general scope of the system comprises mechanical properties and corrosion performance of materials used in technical applications at temperatures above 600 °C.

In order to satisfy the research objective of the programme, it was defined that the data to be collected and held in the bank should be "original test results", i.e., measured or raw data as defined by the following data hierarchy:

- Measured data (as reported)
- Evaluated data (assessed by experts, committees)
- Typical data (generally accepted, handbook-type data)
- Standard data (specifications).

This ensures that the data bank should be suited to, and can be used for, the evaluation of data, one of the objectives of the project.

In order to maintain feasibility in the potentially large goal area of the project, it was, furthermore, decided that during the pilot phase the general scope should be restricted to three groups of mechanical properties and one type of material, namely the Alloy 800 group of alloys (21Cr,32Ni,Ti,Al, bal.Fe).

Structure

The (pilot) scope of mechanical properties thus comprises /6/:

- Tensile test results (tensile strength, elongation, reduction of area, proof strength, stress-strain curves)

- Creep test results (rupture strength, elongation, reduction of area, minimum creep rate, creep curves)

- Fatigue test results (isothermal endurance, cyclic stress-strain curves, thermal fatigue, fatigue crack growth).

These - at present - 3 groups of "test results" are available in association with the following "characterisation" files:

- Material characterisation (identification, fabrication, form, composition, thermal, thermo-mechanical and mechanical history)

- Specimen characterisation (test configuration, surface finish, thermal, thermo-mechanical and mechanical history, description of fabrication or machining)

- Test condition/method characterisation (test temperature, test environment, load, stress or strain, test method)

- Test result origin and data source.

The basic structure of these files allows the extension of the data bank to other materials and properties, a feature mainly enabled by the adaptability of the data base management software (ADABAS) which governs data bank operations such as file definition, data input, data storage, data updating and retrieval.

Links of test results with characterising parameters and of these with each other can be multiple, as dictated by the complex nature of the data. Moreover, data can be values (numbers), text, curves or "relations" and often combinations of these which must not only be taken into account for storage but also for the specific retrieval and display requirements at the output end. An example of the fields making up the "materials file" is shown in Fig. 6.1.

The operation structure of the data bank is depicted in Fig. 6.2 and, with reference to this, the following aspects can be commented on.

Data Formatting

Data are prepared for data bank input by a formatting procedure making use of so-called "data collection forms". These forms, which enable the extraction of data from any type of source document, take up data in the standard format required by the "data input and updating program".

Software

The data files and data bank software are implemented at the computing centre of JRC Ispra in Italy and operate from a Petten terminal via the Euronet data transmission network. The main data bank software system is thus at Ispra while the Petten "intelligent" terminal operates some local processing software for the formatting of the numerical and graphical output.

- The Data Base Management System (DBMS):
  The DBMS - ADABAS - is a commercially available, generalised DBMS, for multi-user systems with terminal facilities operating on-line concurrently with batch processing.

- The Data Input and Updating Program:
  Data formatted on the "data collection forms" are transferred to magnetic tape and input to the computer via the "input and updating program". The program controls the loading of information into the data bank and the interrogation of the stored data for display and checking purposes.

- Data Checking (Document Reporting Program):
  The purpose of this program is to produce reports of the content of defined sets of source documents using batch operation. It serves as a basis for batch mode data checking and updating.

- Output Formatting and Data Display Software:
  Various application software components developed or currently in use are associated with the operation of the data bank, in particular the "common command language" (ADACCL), parts of the computer graphics software GRAPHIT(GINO-F), and many other modules of the Ispra program library. A number of routines are being developed for the special on-line requirements of Ispra/Petten, mainly for data search operations. A "numerical display" makes visible, and enables printing of, the content of a searched interim file, according to pre-defined output pages such as bibliographic, test result, test method, etc. A "graphical display" permits the two-dimensional presentation of each x/y data couple held in an interim file.

- Computation Software (Standard Evaluation Programs):
  These programs enable statistical evaluation of data, interpolation, regression and probability analysis and display (including graphical presentation). These software components will be supplemented by future extensions.

- Petten Terminal Software:
  While the above programs are housed at Ispra, there is some local software on the Petten terminal, the main components of which, at present, are:
  . Data Receive Mode
  . Graphic Routines
  . Digitising Routine
  . Source Document Administration
  . Data Sheet Format Routines.

Hardware

The hardware comprises the terminal facilities at JRC Petten and the Amdahl 470/V8 computer associated with the various ancillary units of the computing centre of JRC Ispra, linked via Euronet by a fully synchronous (X-25) 2400 bit/sec connection which uses leased telephone lines between Petten and the Euronet multiplexer in Amsterdam, and Ispra and the Euronet multiplexer in Rome, respectively (refer to Fig. 6.3).

The Petten terminal comprises a Tektronix 4025A graphical terminal, a Tektronix 4054 graphics computer with data communication interface, file manager (twin floppy disc) and the following peripherals:

- A Qume Sprint 5 RO line printer
- A Mannesmann-Tally MT 162KSR matrix printer
- A Tektronix 4956 digitiser
- A Versatec V80 hard copy unit.

The linkage of these units with each other and the other equipment of the Petten and Ispra Stations is depicted in Fig. 6.4.

The Present Data Content

The main sources from which the present data have been acquired are publicly available literature, the HTM Programme of JRC Petten and a contracted transfer by an external laboratory. The High-Temperature Materials Data Bank at present stores about 10,000 data records. Figs. 6.5 and 6.6 show details of the distribution and characteristics of these data. Fig. 6.5 gives the number of all "test result" values stored and their quantitative distribution over the reported test temperature ranges; it is valid for all test environments and materials. Fig. 6.6 gives the number of test results stored for different Alloy 800 "grades" and heat treatments. The classification of the alloy 800 group into material sub-categories can best be made by carbon content ranges instead of the historical grades or the coded specifications. The carbon content ranges shown sub-divide the alloy into the main classes 800L, 800H and 802 which also represent different application areas. The further classification by heat treatment uses an average value of the "grain coarsening temperature" (1,120 °C) as a limit between two groups representing different microstructural, property and application characteristics.

Data Searching

Searches through the data bank can be made utilising the versatile search procedures which cover a wide range of possible queries. A query can range from simple structured overviews, e.g., all tensile tests conducted on a material within its specification, to scientific investigations on the effect of particular metallurgical parameters on material properties in a particular experimental environment.

The versatility of the search procedures is enabled by particular features such as:

- Easy file inversion and a rather comprehensive range of parameters useable as search variables

- Storage of individual test results combined with fully retrievable correlated information including the data origin

- Features enabling reconstruction of original figures or tables as an "experiment report" related to special investigations.

Data Display

The response of the data bank to a completed search (which in a dialogue session consists of many successive question-and-answer steps) is a set of data which can be processed in the form of tabular or graphical displays or as text without format conditions. Usually, the purely numerical data which have an x/y correlation structure are shown in graphical format; other structured output is usually in the form of tables or inserts in the appropriate figure. An example of a graphical display obtained from the data bank is shown in Fig. 6.7.

6.5 CONCLUSIONS

The long-term objectives of the project can be summarised as follows:

- The interactive dissemination of numerical and graphical materials data information accessible by the R & D public through the information market.

- The provision of a query service handling data searches via telephone, telex or letter and publication of data sheets and topical reports assembled from processed data.

- The evaluation and critical assessment of data for the benefit of industry, research, standardisation organisations and European Community institutions.

- The provision of research management services for the identification of areas where data generation requires stimulus.

- The data bank is now operative and holds mechanical property data on Alloy 800. All the stored data are accessible through any form of search profile within the data scope. This scope will be extended to other materials and/or other properties after sufficient experience has been gained during the pilot phase and the feasibility and utility of the concept have been demonstrated.

- The planned on-line availability for external users will be preceded by additional development on the user interface (query language) which, as yet, does not possess adequate comfort for those who are not familiar with the present expert formalisms. This phase will extend to 1984/1985, and in 1985/1986 an experimental phase of direct access operation will be established for the first time.

REFERENCES

/1/ Fachinformationszentrum Werkstoffe - Hüttenkunde, Werkstoffe, Metallbearbeitung, Publication by FIZ Werkstoffe bei der BAM, Berlin, April 1982.

/2/ Westbrook J.H., Rumble Jr J.R. - Computerized Materials Data Systems, Proceedings of a Workshop Held at Fairfield Glade, Tennessee, USA, November 7 - 11, 1982.

/3/ Hampel V.E. - Fact Retrieval for the 1980s, In Proc. Techn. Inform. Panel AGARD Conf., CPP-304, 1981.

/4/ Hampel V.E. et al. - A Directory of Data Bases for Material Properties, UCAR 10099, Rev. 1, Lawrence Livermore Nat. Lab., August 1983.

/5/ Ondik H. et al. - Construction Materials for Coal Conversion - Performance and Properties Data, NBS SP 642, US Dept. Commerce, Nat. Bur. of Standards, September 1982.

/6/ Commission of the European Communities, Joint Research Centre, High Temperature Materials Programme, Data Bank Project - First Demonstration Report on the High Temperature Materials Data Bank of JRC, EUR 8817 ENfs, September 1983.

Title	Parameters	Remarks
Material class		e.g. high Fe superalloys
Material designation	alloy name; trade name; standard designation; material number; material data sheet number	
Material production	name of producer; melting and refining; forming procedures; product form	
Batch number		
Grain size		metric or ASTM
Chemical composition	element; min. content; max. content; quality type	up to 20 elements; "quality type" refers to actual or nominal
Hardness	hardness test method; hardness value	
Thermomechanical treatment (TMT), 1st	type; min. temp.; max. temp.; time; heating/cooling rate; quenching medium; environment; degree of deformation; rate of deformation; rank of step	
TMT, 2nd	idem	
TMT, 3rd	idem	
TMT, 4th	idem	
Melting range	upper temp.; lower temp.	
Electrical resistivity	value; temperature	up to 7 couples
Lin. thermal expansion	value; temperature	idem
Thermal conductivity	value; temperature	idem
Young's modulus	value; temperature	idem
Density	value at room temperature	
Specific heat	value at room temperature	
Magnetic permeability	value at room temperature	

Figure 6.1: File MATERIALS

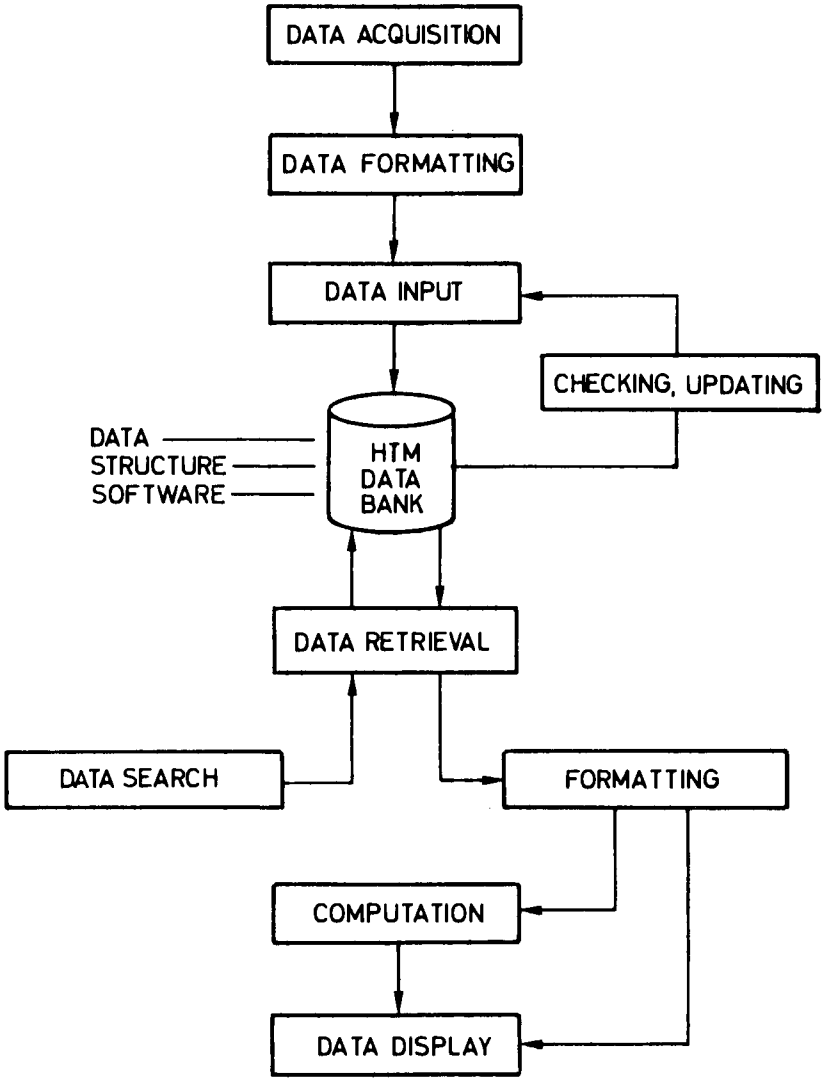

Figure 6.2: Data Bank Operation Structure

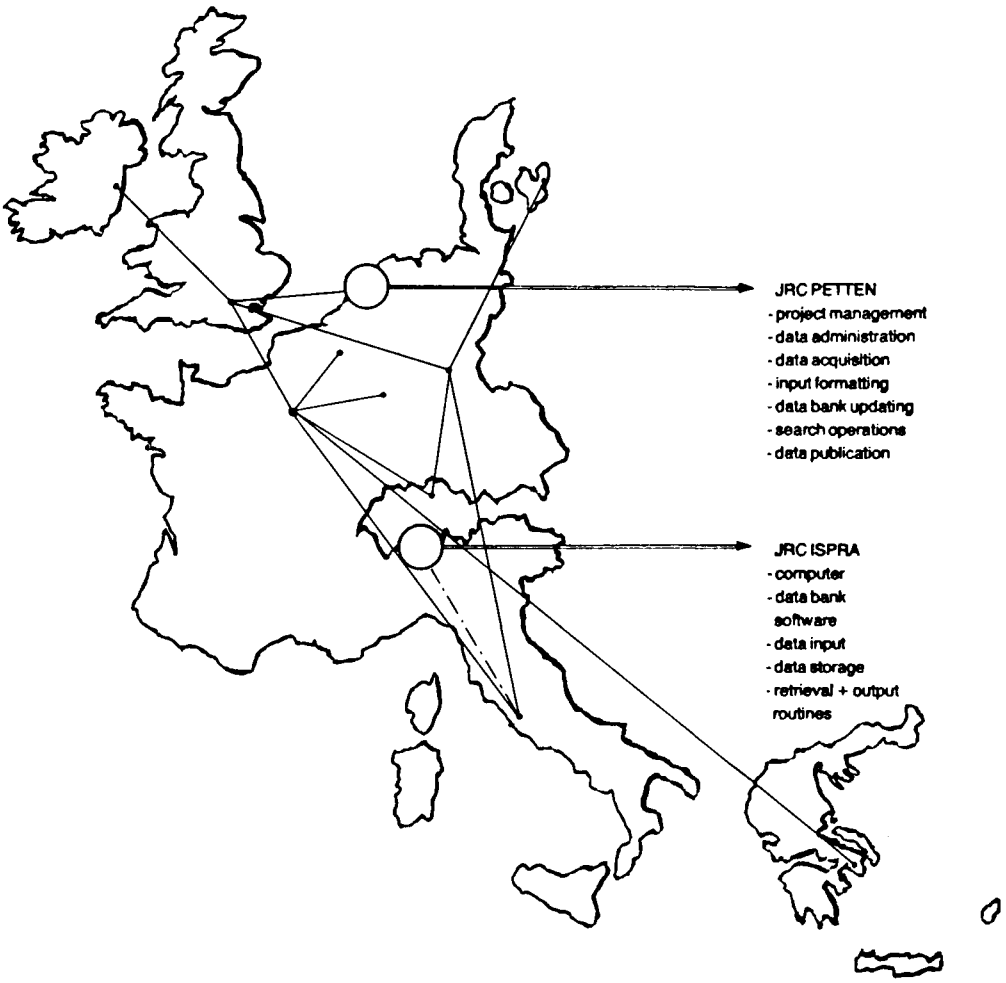

Figure 6.3: Euronet Linking JRC Petten and JRC Ispra

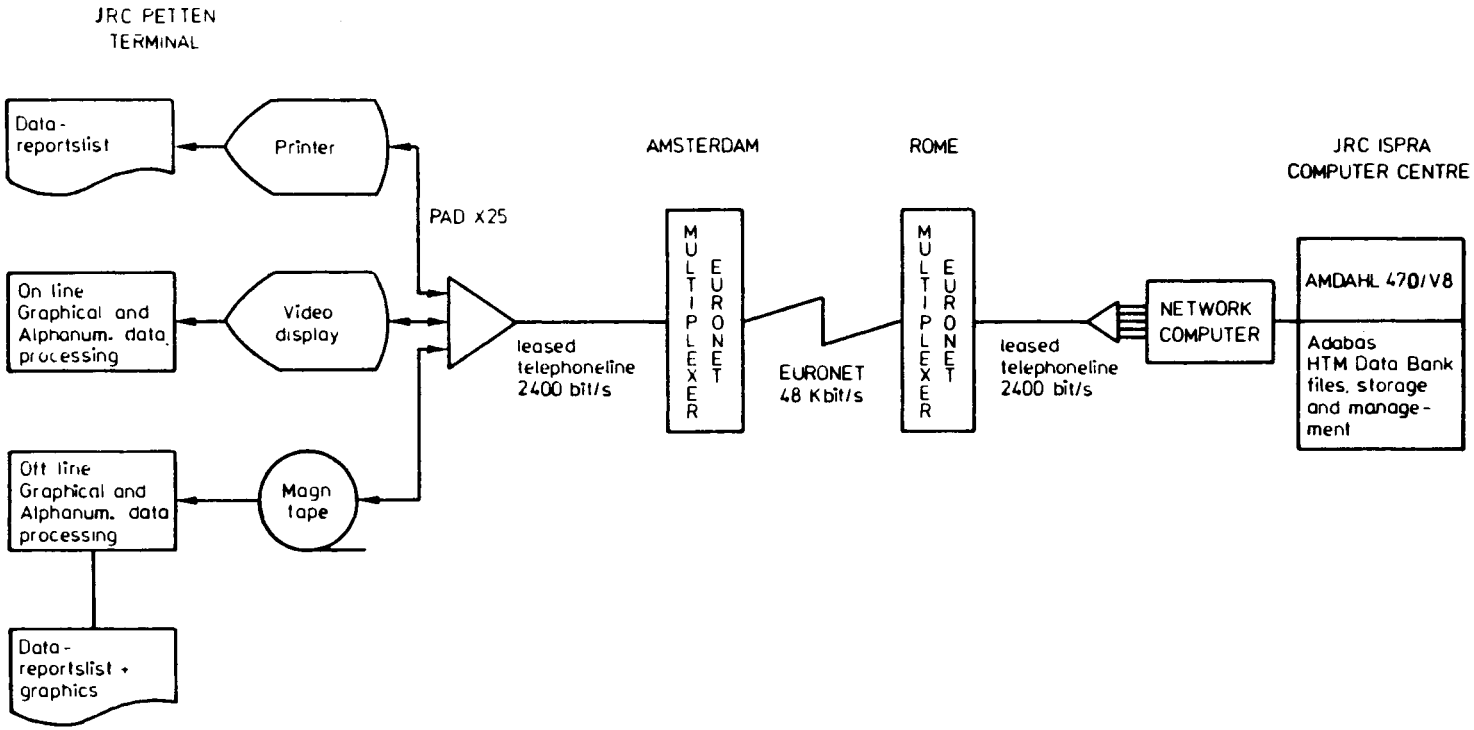

Figure 6.4: HTM Data Bank Facilities, Data Transmission System

	Total	Temperature Range (°C)												
		RT - 99	100 - 199	200 - 299	300 - 399	400 - 499	500 - 599	600 - 699	700 - 799	800 - 899	900 - 999	1,000 - 1,099	1,100 - 1,199	1,200 and above
TENSILE TEST														
Tensile Strength	764	210	30	59	43	67	86	85	62	45	29	28	8	12
Elongation after Fracture	718	204	27	56	40	63	81	69	56	45	29	28	8	12
Reduction of Area after Fracture	629	133	27	56	40	58	61	71	61	45	29	28	8	12
Proof Strength	2,631	484	129	273	185	270	273	307	228	161	107	127	34	53
Yield Strength	562	93	28	69	47	73	45	62	46	31	28	32	6	2
Tensile Stress-Strain Curve	25	3				1	14	2	1	4				
CREEP TEST														
Creep Curve	103						38	41	11	4		8	1	
Creep Strength	357						80	129	133	15				
Minimum Creep Rate	298						111	112	75					
Creep Rupture Strength	2,362*						376	1,042	587	185	48	18		
Elongation after Fracture	1,247						282	494	352	79	40			
Reduction of Area after Fracture	978						188	455	238	67	30			
FATIGUE TEST														
Cyclic Stress-Strain Curve	7	1				1	2	1	2					
Isothermal Endurance	650	69				11	221	165	161	9	14			
Fatigue Crack Growth	79						28	51						

* total includes 106 Larson-Miller correlated values

Figure 6.5: Number of Test Results Stored, All Test Enviroments

Carbon content: Alloy Specifications:	C<0.05 % 800/800L/(801)			0.05 % ⩽ C ⩽ 0.10 % 800/800H/(801)			C>0.10 % 802
Heat Treatment Temperature:	all	< 1,120 °C	⩾ 1,120 °C	all	< 1,120 °C	⩾ 1,120 °C	all
TENSILE TEST							
Tensile Strength	298	150	135	388	71	213	8
Elongation after Fracture	253	121	119	358	71	206	37
Reduction of Area after Fracture	210	123	74	353	91	213	8
Proof Strength	882	471	388	1,577	374	1,021	8
Yield Strength	226	148	78	257	197	53	1
Tensile Stress-Strain Curve	14	3	10	7			
CREEP TEST							
Creep Curve	46	34	9	45	6	39	1
Creep Strength	105	32	73	224	14	19	10
Minimum Creep Rate	172	136	36	99	8	11	
Creep Rupture Strength	1,290	597	524	629	83	174	89
Elongation after Fracture	713	370	295	324	78	161	31
Reduction of Area after Fracture	626	332	294	195	67	113	
FATIGUE TEST							
Cyclic Stress-Strain Curve				7		7	
Isothermal Endurance	45	16	18	435	2	49	
Fatigue Crack Growth	79						

Figure 6.6: Number of Test Results Stored for Different Alloy 800 "Grades" and Heat Treatments

-Test Environment : Air
-Compositional
  Restrictions [%]: None
-Heat Treatment
  Temperature [°C]: >1100
-Pre-Treatment : No cold work or aging

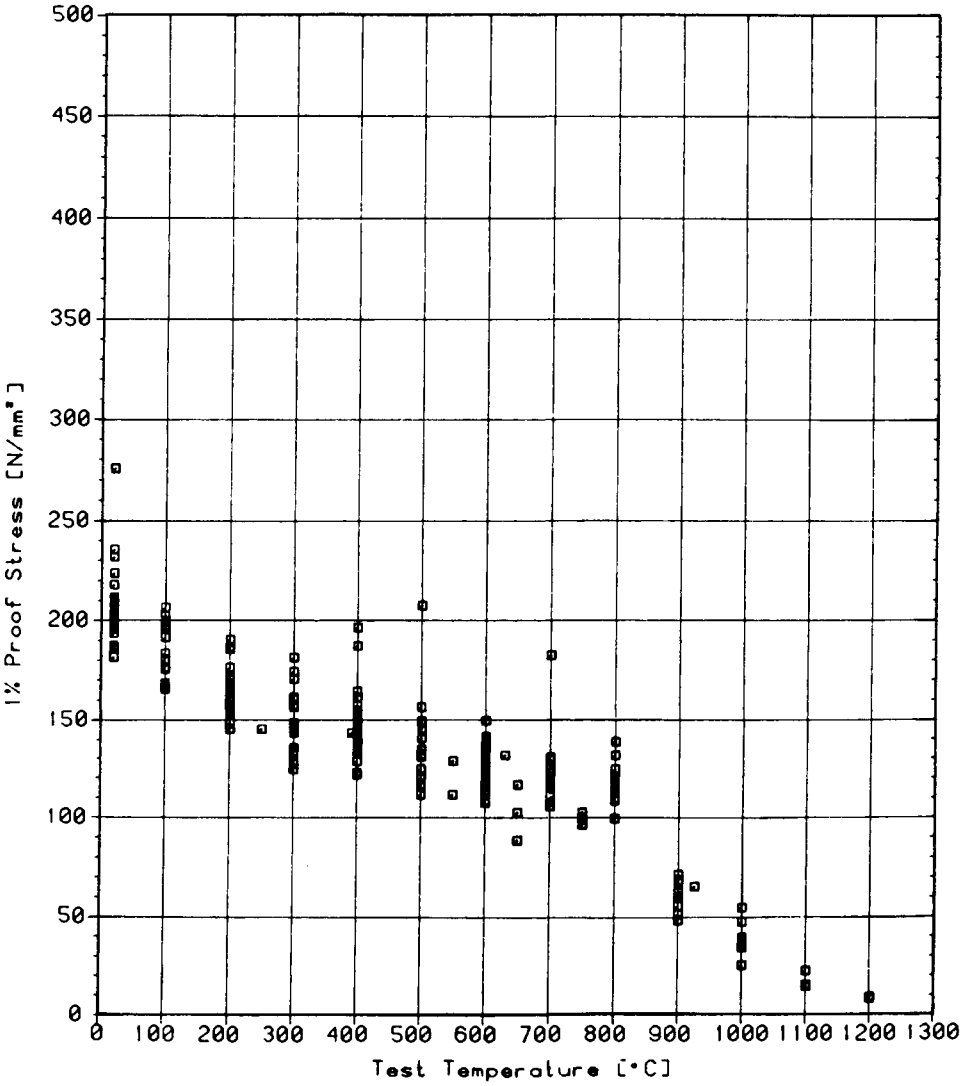

Figure 6.7 Specimen Data Sheet Obtained from the HTM Data Bank

7 MATERIALS RELIABILITY DATA BANKING - AN EXAMPLE FROM THE CHEMICAL INDUSTRIES

G. Gavelli

Istituto Guido Donegani, Novara, Italy

C. Scala and V. Colombari

ENI, S. Donato Milanese, Italy

7.1 INTRODUCTION

In the chapter by Kröckel it was pointed out that reliability data banks may be broadly classified into those concerned with phenomenological - statistical information and those concerned with mechanistic - analytical information. Materials properties data bases belong to the second class of bank. A further type of data base which belongs to the second class of bank is one which is often found in the chemical industries where a large number of different materials are utilized under a large number of different operating regimes and come into contact with an equally large number of different chemical environments.

The data usually come from items of equipment which do not function repetitively under minimally changing operating conditions (i.e. do not have repetitive characteristics). Frequently the items of equipment are uniquely fabricated for one particular function and even when there are a large number of similarly fabricated items, this functioning is often differentiated by differences in the operating conditions. The stored data in such cases refer to equipment failures, primarily damages caused by corrosion or thermal stresses; damages caused by mechanical stresses are less frequent. Here, the Corrosion Data Bank of the Department of Corrosion and Electrochemistry of the Istituto Guido Donegani is presented. This bank is directly accessible by ENI and the latter company has undertaken a large number of studies, utilizing the accessible data, one of which is outlined subsequently.

7.2 INFORMATION STORED IN THE DATA BANK

The information stored in the data bank consists of data relating to equipment or structural failure events in chemical plants. The factors causing failure of the equipment or structural material which are taken into consideration are corrosive, thermal, thermomechanical and mechanical. Additionally, information relating to problems of material selection for new plants or modifications to plants already in operation, to corrosion tests and to literature of technological interest, is also stored in the bank.

Data storage in the computer follows the five steps:

Event ⟶ technical report/inspection sheet ⟶ summary form (specially devised) ⟶ coding for computer ⟶ memory input.

The coding procedure takes the following information into account:

- factory
- progressive numbering of summary form
- initials of the document
- issuing office
- date of issue of the document
- type and characteristics of the document
- process
- type of equipment or part of equipment
- materials
- environment
- pH
- temperature and pressure
- process fluid speed
- absence or presence of aeration
- mechanical stresses
- anti-corrosion measures already taken
- present situation and damages occurred
- results of investigation
- proposed remedies
- adopted remedies

When extracting information from the data bank during the analysis of any particular problem, it is often necessary to return to the original documents and examine these in order to be able to interpret the historical information in the correct manner for adaptation to new operating conditions which may be similar, but hardly ever identical, to those in the stored data. This is a very common problem encountered with this type of data bank.

Whilst the above method of utilizing the bank is the most usual, with the large number of reports included over the years, some statistical analyses of the data content of the bank are possible. These are next considered, bearing in mind that for obvious practical reasons relating to the acquisition of data, the population of stored events can never be considered a representative sample of all the failure events occurring in even the plants participating in this system.

7.3 ANALYSES OF DATA CONTENT OF THE BANK

Presently 2,269 reports are stored in the bank, of which 75 % relate to "behavioural" aspects of materials. These approximately 1,730 items comprise the following:

- Investigations on causes of failure 72 %
- Non-destructive examination 20 %
- Material studies, testing procedures, etc. 8 %

The results from the first category above (investigations on causes of failure) and which comprise 1,115 "events" relate primarily to corrosion damage and, irrespective of the type of damage process (failure mode), the causes of failure are as follows:

- Errors in manufacturing/fabrication techniques 24 %
- Inadequate specifications or materials selection 17 %
- Errors in equipment or structural design 6 %
- Assembly/erection mistakes 7 %
- Accidental and unclearly identified causes 46 %

The damage processes (failure modes) exhibit the following percentage distribution:

- Stress corrosion cracking (SSC) 21 %
- General or uniform corrosion 20 %
- Fatigue 18 %

- Pitting corrosion or craters 10 %
- Erosion corrosion 7 %
- Crevice corrosion 6 %
- High-temperature corrosion 6 %
- Creep 4 %
- Intergranular corrosion 3 %
- Hydrogen damage 1 %
- Galvanic corrosion 1 %
- Impingement 1 %
- Other types of corrosion 2 %

Three failure modes (stress corrosion cracking, general or uniform corrosion and fatigue) together account for over half of the reported failures to date. It is worthwhile analysing the causes of the failures which occurred by some of these modes, and this is done in Table 1 for SSC, fatigue and pitting.

Table 1: Causes of Failure for 3 Common Failure Modes

Causes of Failure	Failure Mode (% of Total Events)		
	SSC	Fatigue	Pitting/ Craters
Accidental/unclearly identified	39	32	52
Errors in manufacturing technique	22	34	10
Inadequate specs./materials	24	10	15
Design errors	3	18	1
Errors in maintenance procedures	2	-	13
Insufficient testing	3	2	2
Insufficient cleaning	1	1	1
Incorrect operation of plant	6	3	6

The figures indicate the following:

- Fatigue damage occurs more often than SSC or pitting as a result of errors in manufacturing techniques or design.

- Pitting occurs more often than SSC or fatigue (which does not occur) as a result of errors in maintenance procedures.

- SSC occurs more often than pitting or fatigue as a result of inadquate specifications or materials selection.

One can conclude, therefore, that fatigue problems in general can be greatly reduced by paying proper attention at the design and manufacturing stage. On the other hand, SSC can be, to a certain extent, reduced by care in the selection of materials whilst careful maintenance can contribute towards reducing pitting and crater problems.

As a final analysis, the failure modes encountered for heat exchangers incorporated in the data bank can be detailed as follows:

- Crevice corrosion, differential aeration, bacterial corrosion, scaling	16 %
- Pitting corrosion	14 %
- Stress corrosion cracking (SSC)	12 %
- Defective material or welding	11 %
- Fatigue	8 %
- High-temperature modification of material	6 %
- Erosion, erosion corrosion, cavitation	6 %
- General corrosion	6 %
- Thermal or mechanical modification of the material during manufacturing	5 %
- Other types of attack	16 %

From the above figures it can be seen that the greatest contributors to failure are crevice corrosion, differential aeration, bacterial corrosion and scaling, which suggests that all too often water treatment and circulation outside of the tubes are inadequate. In addition, together with pitting, SSC

and material deficiencies (previously shown to be a contributor to SSC) and defective welding, these failure modes account for the majority of failures. In fact, the figures indicate just how important are decisions taken at the project or manufacturing stages. Careful attention needs to be paid to possible problems, such as tube vibration (which could give rise to fatigue), mechanical assembly (in particular welding), cooling-water flow-rates and treatment (conditioning).

7.4 THE USE OF TITANIUM AND ZIRCONIUM IN UREA SYNTHESIS REACTORS

Data, such as accessible in the above described bank were uilized to investigate the feasibility and capabilities of titanium and zirconium as materials in urea synthesis reactors and the results of this investigation are here presented.

The industrial synthesis of urea is based on the exothermic reaction of ammonia with carbon dioxide to produce ammonium carbamate with a simultaneous partial dehydration to urea:

$$2NH_3 + CO_2 \longrightarrow NH_4CO_2NH_2 \longrightarrow H_2O + NH_2CONH_2$$

The most usual processes operate at temperatures between 160 - 205 °C and employ a compressor to recycle the carbamate solution which, at the upper temperature, however, is extremely aggressive and causes frequent replacement of the recycle compressor and other materials with attendant high operating costs. The only way in the past of attempting to reduce these costs (and enabling the use of 300 series stainless steels, for example) has been by lowering the operating temperature which then, however, considerably reduces the conversion index of CO_2 into NH_2CONH_2 and lowers the urea yield. This approach has, nevertheless, been the traditional one, the reactors being lined with stainless steel and protected by oxygen (the presence of which serves to moderate attack by reforming the passivation film which is destroyed during the process). The limiting temperature in this case is 190 °C.

A process has been licensed, however, which eliminates the recycling of carbamate solution (but recovering and recycling the unconverted ammonia and

carbon dioxide) which, at the same time, gives urea yields of 85 % as compared with the traditional 65 - 70 %. On the other hand, a higher reactor temperature is required (230 °C) and the use of traditional materials in process equipment is virtually impossible. The attractiveness of the process is its improved yield and reduction of investment costs by eliminating the carbamate recycle compressor stage.

Information from the data bank has substantiated the potential for titanium and zirconium as materials to be utilized in such a process. The former metal is virtually inert to attack by ammonium carbamate but, nevertheless, still requires a limitation of process temperature to $\simeq$ 205 °C. One negative factor regarding titanium is the ready deterioration of the oxide passivation film which still forms the basis for this material's resistance to chemical attack. Vibration, for example, can cause deterioration of this film. The passivation film is also readily damaged by the presence of traces of iron or iron oxide and hence manufacturing, inspection and maintenance operations necessitate the introduction of special techniques.

Zirconium, on the other hand, despite posing metallurgical problems, can be utilized at process temperatures up to 230 °C and, what is more, the necessity for oxygen injection (such as is required with stainless steels and titanium) falls away when this metal is used for the reactor lining. There is an attendant improved efficiency in the CO_2 compressor and a reduction in volume of the reactor. Despite the higher price of the material, overall process costs are considerably reduced, especially when one takes into account the decreased maintenance requirements and shorter shut-down periods for repairs.

In consequence, steps are being taken to introduce the use of zirconium in this alternative process and the next stage is to ensure satisfactory "management" of the material by appropriate fabrication, manufacturing, etc. through the utilization of staff thoroughly familiar with zirconium and its properties.

7.5 CONCLUSIONS

A data bank established for use by the chemical industries has been described. The class of data bank to which this particular bank belongs precludes the use of the information in statistical failure-rate/lifetime predictions. On the other hand, useful materials behavioural information can, and has been, incorporated into the bank and has been utilized in, for example, the selection of materials of improved "reliability" for applications in the chemical industry. Analyses of the data content of the bank have also provided useful information on causes of failure which can be utilized in an effort to reduce the number of future failures. It would be of benefit to the whole European chemical industry if greater exchange of such data could be implemented on a much wider scale and on a continual basis.

8 THE RELIABILITY OF MATERIALS IN HEAT-EXCHANGER APPLICATIONS

R.O. Müller

Brown, Boveri & Cie., Baden, Switzerland

8.1 INTRODUCTION

Condensers and other heat exchangers have a profound influence on the availability of power plants. As outage costs of big units are very high, there is great concern to reduce outage time /1-3/. So it is worthwhile to look at the reliability of a condenser and see how it is influenced by different parameters. To give some idea of scale, for a power plant of 1,000 MW, the condenser may contain 50,000 tubes, each 12 m long, with an inner diameter of 22 mm and a wall thickness of 0.5 - 1 mm. Even if, for example, two 100 % capacity heat exchangers have been installed and reliability may not seem so important in view of the redundancy, since the repair costs from potential damages resulting from tube failure may exceed many times the cost of the heat exchanger, the reliability of the tubes is still of great concern. What is more, the problem with power plant condensers is the fact that corrosion attack will cause leaks and even one leak will result in a forced outage or a load reduction and repair measures having to be implemented.

Table 1: Failure Rate of Different Tube Materials

	Al-Brass	CuNi10Fe	CuNi30Fe	Titanium
Beavers /2/	0.17-0.29	0.04-0.10	0.05	0.02
Dechema /4/	0.33	0.05	0.06	< 0.01
BBC experience:				
10 years of service	0.004-0.005	-	-	-
2 years of service	< 0.005	-	< 0.005	< 0.001

As a measure for the performance of heat exchanger tubes, the failure rate (FR) has been introduced. It is defined as the percentage of perforated tubes, divided by the service hours times 10^{-4}:

$$FR = \frac{\text{\% of perforated tubes}}{\text{service hours} \cdot 10^{-4}} \qquad - (1)$$

In Table 1 are listed the failure rates of different tube materials as reported in the literature. Beavers has found for Al-brass 0.1 to 0.29, Dechema has reported 0.33 and our own experience yields values of 0.004 to 0.005 for Al-brass for 10 years in river water, and less than 0.005 for Al-brass in sea water for the first 2 years of service. Titanium has a lower failure rate, 0.02 to less than 0.01, as reported in the literature. In BBC condensers, tubed with titanium, a failure rate below 0.001 has been experienced. Thus, one observes a spread in the FR values.

Table 2: Time until 10 % of the Tubes are Perforated /4/

Tube Material	Time (years)
Al-brass	2 - 16
CuNi10Fe	2.5 - 20
CuNi30Fe	3 - 30

In Table 2 are indicated the times until 10 % of the tubes are perforated, for different materials, as quoted in the literature. Al-brass has a life expectancy of 2-16 years, CuNi 3-30 years. The values of FR and the statistical life expectancies of the tubes demonstrate a broad spread. This indicates that the failure rate is obviously dependent upon parameters which are either unknown or have not been considered. In fact, the failure rate does not give any information about the modes of failure and causes of the attack and, for this reason, one needs to go deeper into the details of heat exchanger reliability.

It is first necessary to provide definitions of some reliability parameters. The mean up-time (MUT) is defined as the time whilst the unit is running; the mean down-time (MDT) is defined as the sum of all repair times and is related to the mean time-to-repair (MTTR) which may vary between one hour and a few days, depending on how fast the leak can be detected and the affected tube plugged. In addition, a failure of the heat exchanger will be defined as a single leak above 20 ml/h, or a power loss of the plant, due to the condenser, of more than 10 %. Finally, the mean time between failures (MTBF), which is of primary concern here since it has a direct influence on MUT, can be expressed in terms of failure rate (FR) and total number of tubes (n) as:

$$MTBF = \frac{100}{FR \cdot n \cdot 10^{-4}} \qquad - (2)$$

One can see immediately that the MTBF is inversely proportional to the number of tubes. For this reason, with a given FR, a small unit will have a higher reliability than a large unit. Having established this, it is now necessary to consider the connections between MTBF and the modes of failure, primarily corrosion, and their causes. In DIN 50 50930 /5/ where the corrosion behaviour of construction metals in water is given, one only finds probabilities concerning corrosion resistance, which does not help that much. However, our experience has shown that the MTBF of condensers is a function of:

- The tube material (composition, heat treatment and fabrication)

- The water composition (pH, oxygen content, chloride-sulphate, calcium, sodium, ammonia content) and chemical oxygen demand, for instance

- Factors such as temperature, maintenance, cooling system and overall design.

These aspects are considered below.

8.2 POSSIBLE FAILURE MODES

Since different alloys, which may suffer different types of corrosion attack, are in use in heat exchangers, the MTBF can best be discussed in the context of a consideration of all the possible failure modes. As can be seen from Table 3, different alloys are prone to various types of attack. The higher chemical stability of titanium is obvious. The greater number of failure modes for copper alloys shows that, for these, more effects need to be considered and be kept under control. Thus, copper alloy condensers have to be designed and treated more carefully than other condenser types. It is also obvious that even titanium tubes may fail mechanically, if the condenser is not designed properly. The typical failure modes presented in Table 3 will be discussed in more detail below by considering each of the alloys in turn.

Table 3: Typical Condenser Tube Materials and Possible Failure Modes

Failure Modes	Material			
	Al-brass CuZn20Al	CuNi10Fe CuNi30Fe	Stainless Steels	Titanium
Pitting	x	x	x	-
Crevice corrosion	x	x	x	-
Erosion) tube middle	x	x	-	-
corrosion) inlet	x	x	-	-
Stress corrosion cracking	x	-	(x)	-
Steam side-) NH_3/O_2 attack)	(x)	-	-	-
Tube vibration	x	x	x	x
Steam side erosion	x	x	x	x

x = failures possible; - = no failures known

Copper Alloys

Copper alloys have many advantages /6/. Their good thermal conductivities, ease of fabrication, biocidic action which reduces biofouling and acceptable general corrosion resistance has led to numerous applications in the last 200 years. However, these alloys also have limitations. They are prone to pitting and crevice corrosion in aerated, sulphide-containing waters and Al-brass suffers stress corrosion cracking in stagnant, NH_3-containing, air. Pitting and crevice corrosion of copper alloys occur in aerated, sulphide-containing water /7,8/. Although there exists some controversy in the literature, claims that at least some copper alloys resist aerated sulphide-containing sea water /9-12/, present unconvincing arguments against the facts which demonstrate that copper alloys will definitely be attacked when sulphide is present /13-18/.

Some experimental results can here be presented to illustrate the action of sulphide on copper alloys /8/. It can be seen from Fig. 8.1, which depicts the free corrosion potential of Al-brass as a function of time, for exposure to sea waters with differing sulphide content, that the free corrosion potential in clean, sulphide-free sea water stays at about -30 mV (SHE). In water slightly contaminated with sulphide (content about 0.01 mg/l) the free corrosion potential rises to +30 mV. With higher amounts of sulphide, namely 0.5 mg/l, after 2 - 3 days the free corrosion potential exceeds 120 mV. At these high potentials, pitting and crevice corrosion take place /7/.

Fig. 8.2 shows current-potential curves as a function of time, measured with a rotating cylinder of Al-brass in sea water. At the beginning, the polarization resistance is low and gradually, after 20 - 30 days, the resistance starts to increase and reaches about 80 $k\Omega cm^2$. All the time the free corrosion potential stays low, at -50 to +30 mV. On the other hand, when sulphide is present (Fig. 8.3), after a few days the free corrosion potential rises to above +150 mV while the polarization resistance is still very low. The effect of the sulphide has been to make the surface very noble, while the polarization resistance was still low. Fig. 8.4 illustrates the pitting that can develop in an aggressive (sulphide contaminated) water below an intact iron-hydroxide layer.

Sometimes blockages occur in the tubes. These blockages can be caused by, for example, dead mussels, shellfish or sea weed. In such cases, two types of attack are possible:

- Around the foreign objects, water jets will cause erosion corrosion or pitting attack, such as shown in Fig. 8.5.

- On the other hand, if the foreign objects consist of putrifying organic material, the water composition down flow from these objects will be changed, and contain deposition products such as sulphides. In this way, the water will become aggressive for copper alloys and general pitting attack will occur, as shown in Fig. 8.6.

Another type of attack is erosion-corrosion at the tube inlets, caused by too high a water velocity. An example is shown in Fig. 8.7 (2.9 m/s). This attack is distinctly different from the tube-inlet attack which occurs in slightly aggressive cooling water when there is no cathodic protection (an example of which is shown in Fig. 8.8). In this last case, in spite of a normal water velocity ($v = 1.8$ m/s) heavy pitting attack developed at the tube inlet which could have been eliminated by the use of a cathodic protection system with sacrificial anodes. Since tube ends can easily be protected cathodically by either iron anodes or external current systems, it is standard practice to do so.

When tube inlets are cathodically protected the question arises how far into the tubes the cathodic protection will reach. According to Uhlig /19/ the potential distribution can be expressed by the following differential equation:

$$\frac{\partial^2 U}{\partial x^2} - \frac{4D\Lambda}{\kappa} U = 0 \qquad - (3)$$

where $U(x)$ is the potential in the tube at location x, measured from the end of the tube, D is the tube diameter, Λ is the specific surface conductivity $(1/R_p)$, with R_p the polarization resistance and κ is the conductivity. Other used symbols are U_H, the free corrosion potential (referred to the normal hydrogen electrode) and α, given by $2\sqrt{D\Lambda/\kappa}$.

With an Al-brass tube of length 10 m, $D = 0.022$ m, $R_p = 1.3 \Omega m^2$, $\kappa = 4.4$ S/m (for water of pH = 8), the potential distribution is as shown in Fig. 8.9 and it can be seen that, for Al-brass tubes, whilst tube ends can be cathodically protected, the same is not true for the tube centre.

Finally, some remaining comments on failure modes can be made:

- Stress corrosion cracking can occur, with Al-brass, by the action of ammonia. Attack in humid NH_3- containing air causes stress corrosion cracks within a very short time (24 h). Stress corrosion cracking in heat exchanger tubes may occur during shut-down, when organic matter in water boxes decomposes and releases ammonia. Good maintenance procedures can help to overcome this type of attack.

- Steam side ammonia attack has occurred in the air cooler section of some condensers of other than BBC design. Good condenser design prevents these attacks completely.

- Tube vibration has to be restricted by the proper choice of the free-tube length.

- Steam impingement may attack the upper row of tubes which are exposed to water droplets of high velocity. Properly designed condenser necks will reduce the collection and development of large droplets, which are especially harmful, and can go a long way towards resolving steam-impingement problems.

Stainless Steels

These form a large class of different alloys, with differing compositions and corrosion resistances /20,21/. In general, the composition ranges are as follows:

Cr content : 12 - 28 %
Ni content : 0 - 25 %
Mo content : 0 - 6 %

For instance, 304 (DIN 1.4301), named X5CrNi189, is not resistant to sea water. 316 (DIN 1.4401), named X5CrNiMo1810 is stable in sea water if cathodic protection is provided, but is unsuitable for long tubes.

The most severe problem experienced by stainless steels is crevice corrosion under deposits /22,23/. Since it is always possible that in a few heat exchanger tubes sand or other deposits accumulate, concentration cells will occur (Fig. 8.10) accompanied by crevices.

Because the stainless steel surface is exposed to anodic and cathodic conditions at different locations, both reactions have been separately investigated and a crevice corrosion test developed /24,25/ These investigations are here summarized. The cathodic reaction was investigated by measuring the free corrosion potential (U_H) of the passive, unpitted surface as a function of different parameters. In a special crevice corrosion test cell the critical potential for crevice corrosion (U_S) was measured. U_S is, in fact, a repassivation potential of an actively corroding crevice. Some of the results of the investigation are presented in Figs. 8.11, and 8.12.

In Fig. 8.11, where the free corrosion potential is shown as a function of water pH, it is obvious that the stainless steel surface acts in a broad range of pH, between 8 and 5, as a nearly perfect pH electrode. (This means that at pH 8 its free corrosion potential is +250 mV, while it is much higher, namely +400 mV, at pH 5.) In Fig. 8.12 the critical potential for crevice corrosion (lower curve) versus chloride content is plotted, together with the critical potential for pitting corrosion (upper curve). At potential and chloride values left of the critical potential for crevice corrosion, the material is stable to corrosive attacks. Right of the critical potential for crevice corrosion (i.e. at higher chloride levels or higher potentials) crevice corrosion is possible. At even higher potentials (above the critical line for pitting corrosion) pitting corrosion may occur. If the free corrosion potentials are combined with the chloride potential diagram, limiting values for the chloride content are found, below which the material will be stable to crevice corrosion. This has been done for a large number of stainless steels, the result being that only a few very highly alloyed stainless steels are found to be stable in aerated, cold sea water. This is confirmed by crevice exposure tests, as reported in the literature /26,27/. These sea water resistant stainless steels are listed in Table 4.

Table 4: Name and Composition of Sea Water Resistant Stainless Steels

Name	Designation/ Supplier	C	Cr	Ni	Mo	Other
Monit	Nyby, Sweden	<0.025	24.5 - 26.0	3.5 - 4.5	3.8 - 4.3	Ti 0.3-0.6
DIN 1.4575	X1CrNiMoNb2842	<0.015	26.0 - 30.0	3.0 - 4.5	1.8 - 2.5	Nb > 12xC <1.2
Sea cure	Trent, USA	0.01	25.6	2.1	3.1	Ti 0.5
Al 29-4c	Allegheny, USA	0.01	28.8	0.8	3.8	Ti 0.6

Monit, 1.4575, sea cure and Al 29-4c are all ferrites with a very high chromium content (between 25 and 29 %) and at least 2 % molybdenum.

Titanium

Titanium is a very resistant material for heat exchanger tubes. At temperatures < 120 °C titanium tubes are completely resistant against attack in sea water. No attack will occur in the presence of ammonia nor in polluted, sulphide-containing water.

Thinner wall thickness is possible with titanium, resulting in better heat transfer properties. However, vibration and steam impingement need to be taken into consideration and thin-walled titanium tubes need more support plates than copper-alloy tubes for example. This is the material of the future and BBC has, to date, over 10 years' good experience in the use of this material.

8.3 WATER TREATMENT

In order to avoid macrofouling in the system, which could lead to blocked tubes or deposits of organic matter which would release sulphide harmful to copper alloys, and to avoid biological fouling, which could cause trouble by blocking tubes, the water has to be treated. For this reason, the cooling water system must be fitted with a coarse and a

fine screen at the intake. The cooling water system must be free of settling ponds and anti-fouling actions have to be taken. One possibility is the thermal shock treatment, where the cooling water temperature is raised above 40 or 50 °C for a short time. The other possibility is intermittent dosing of sodium hypochlorite or chlorine, to eliminate biological fouling by mussels or barnacles. For copper alloy tubed condensers, an iron sulphate dosing would need to be additionally provided.

8.4 OPERATING EXPERIENCE

Between the time an offer for supply of a system including condensers is placed and the erection of the plant, there can be a time lag of 5 - 15 years. During preparation of the offer, certain information is often lacking. Time is limited and a selection of materials has to be made which will ensure the lowest possible price. When an order is finally placed, the selection of materials is again investigated and, very often, the water quality has changed from the assumptions made for the initial offer. The cooling system may even be different too. So, adaptions are necessary. During erection and running-in, BBC operates a remote corrosion control through tube examinations /28/. This permits final adjustments to ensure an optimal solution. Some examples of the findings of such examinations are worthwhile including here.

Attack at the Tube Inlet

When investigating tubes removed from a power plant, attack was observed right at the inlet of the tube which meant that the cathodic protection system was not working. On further investigation, the iron anodes were found lying on the ground, near to the water box. The brackets for mounting the anodes had not been delivered; they had been ordered but had not yet arrived. The situation was corrected by appropriately mounting the anodes and the tubes are now still in good shape.

Cooling Water Intake Structure

In Fig. 8.13 (top) a cooling water intake structure which was designed to unload heavy components is depicted. In this way a harbour was formed which would act as a settling pond where three units would have their water intake. This meant, however, that the system would be fouled with deposits of organic matter and, as all three units would take their water out of this small harbour, one could not drain the system and clean it (since one unit had always to be operational). The design was altered with a proposal to stream-line the cooling system, but it could still not be emptied for cleaning. So a third proposal was made, with dividing walls. Each cooling system could thus be closed off at the intake, emptied and cleaned. This solution was eventually developed into a fourth proposal with very short channels, because the long distance between cooling water pump and the open sea was no longer necessary. The system has been built according to the bottom picture in Fig. 8.13 and it works perfectly.

Damping Pond

In another project there was very clean Atlantic water available, so copper alloys were selected. When a drawing of the cooling water intake, Fig. 8.14 was presented, the proposed settling pond could not be accepted for the following reason. The pond had to smooth out waves - about 20 m high. The residence time of the water in this system would be 10 minutes to 1 hour and consequent biological fouling would preclude the use of copper-alloy tubes. The lower part of the figure shows a system with small internal volume, direct lines from the sea into the pumps, chlorination right at the intake, the whole system capable of staying free from biological fouling thereby ensuring no sulphides to attack the copper alloys. This alternative water intake would, however, have been so much more expensive than the first one, even allowing for replacement of the copper-alloy tubes by titanium tubes in the first case, that the system was built as originally designed (with the damping pond) but using titanium instead of copper alloys.

8.5 ECONOMIC CONSIDERATIONS

When selecting tube materials, price is naturally a very important factor.

Table 5: Approximate (1983) Market Prices for Tube Materials (Inner Diameter 22 mm)

Material	Wall-thickness (mm)	Cost of Tube in SFr./m
Al-brass	1	4.50 - 6.00
Titanium	0.5 - 0.7	8.00 - 10.50
1.4575	0.7	6.20
Monit	0.7	7.70
CuNi10Fe	1.0	7.70

In Table 5 are given approximate 1983 market prices for tube materials (inner diameter 22 mm). One can calculate the influence on the condenser of the cost of the tubes:

Unit : 1,000 MW, 50,000 tubes, 12 m length
Al-brass : 5 x 50,000 x 12 = 3 mio SFr.
Titanium : 10 x 50,000 x 12 = 6 mio SFr.

Titanium tubes in a typical condenser therefore cost about double the price of Al-brass. On the other hand, a 1,000 MW unit would have current outage costs of 0.5 - 1 mio SFr./d. Current replacement costs are 1 - 2 mio SFr./d. So, the extra cost of titanium is well invested, which explains the trend towards titanium tubes for large condensers in modern units.

8.6 CONCLUSIONS

It has been shown that the MTBF of heat exchangers is a complex function of many parameters. The following rating, in order of importance, can be given to these parameters:

- Material (In order of "reliability":
  . Titanium
  . Special stainless steels (e.g. 1.4575)
  . Cupronickel
  . Al-brass)
- Design of components
- Design of the cooling system
- Water quality
- Operation of the cooling system.

Since it is very difficult to derive precise values for the MTBF depending on the above criteria, an individual evaluation needs to be made in every case. However, trends towards ensuring higher reliability in the future will result in the following:

- In sea-water-cooled condensers, the trend towards using titanium will continue.

- In river-water-cooled systems, stainless steels will replace copper alloys.

- For small coolers, copper alloys will still be a good choice since they do not need mechanical tube cleaning, due to their biocidic action.

- An optimal systems approach, based on long experience, will ensure the best chance of fulfilling the exacting reliability requirements placed on the condenser, by ensuring optimal reliability of the cooling system as a whole.

REFERENCES

/1/ Bell R.J., Diaz-Tos I.A. - Performance of Condenser Tube Materials in the Electric Utility Industry, ASME, 82-JPGC-Pwr-12, New York, 1982.

/2/ Beavers J.A., Agrawal A.K., Berry W.E. - EPRI-NP-1468, TPS 79-730, Corrosion-Related Failures in Power Plant Condensers, prepared by Battelle, Columbus, 1980.

/3/ Lawrence W.B. - EPRI-NP-481, Research Project 621-1, Steam Plant Surface Condenser Leakage Study, prepared by Bechtel Corp, March 1977.

/4/ Dechema-Werkstofftabellen, Meerwasser, Blatt 25, 1975.

/5/ DIN 50 50930, Korrosionsverhalten metallischer Werkstoffe gegenüber Wasser, 1980.

/6/ Hibbard D.S. - Copper Alloy Tube Applications in Power Plant Condensers, Power Engineering, 85, 70-73, 1981.

/7/ Müller R.O. - Corrosion in Sea Water Cooling System and Corrosion Tests with Al-Brass in Sulphide and Iron-Containing Water, Metallic Corrosion, Proceedings, 8th Int. Congr. on Met. Corr. 1981, publ. by DECHEMA, Frankfurt a.M., 1981.

/8/ Müller R.O., Scheidegger R. - Korrosionsverhalten meerwassergekühlter Kondensatorrohre aus Buntmetall, El. Wirtsch., 80, 139-146, 1981.

/9/ Poppleweel J.M., Thiele E.A. - Blockage Erosion Resistance of the New Copper Nickel Alloy CA 722, NACE National Conference, Chicago, paper 170.30, 1980.

/10/ Gilbert P.T. - A Review of Recent Work on Corrosion Behaviour of Copper Alloys in Sea Water, Mat. Perf., NACE, 21, 47-53, February 1982.

/11/ Barbery J., Pepin Donat Ch. - Rohre aus Kupferlegierungen für Wärmeaustauscher, Metall, 36, 1181-1184, 1982.

/12/ Gaffoglio C.J. - A New Copper Alloy for Utility Condenser Tubes, Power Engineering, 86, 60-62, August 1982.

/13/ De Sanchez S.R., Schiffrin D.J. - The Flow Corrosion Mechanism of Copper Base Alloys in Sea Water in the Presence of Sulphide Contamination, Corr. Sci., 22, 585-607, 1982.

/14/ Angenend F.J. - Korrosion von Kondensatorrohren als Folge eines gestörten Deckschichtausbaus, VGB Kraftwerkstechnik, 61, 561-568, 1981.

/15/ Lee T.S., Hack H.P., Tipton D.G. - The Effect of Velocity on Sulphide-Induced Sea Water Corrosion of Copper-Base Condenser Alloys in Aerated Sea Water, 5th Int. Congress on Marine Corrosion and Fouling, Barcelona 1980: Corrosion, 274-291, 1980.

/16/ Syrett B.C. - The Mechanism of Accelerated Corrosion of Copper-Nickel Alloys in Sulphide-Polluted Sea Water, Corr. Sci., 21, 187-209, 1981.

/17/ Syrett B.C., Coit R.L. - Causes and Prevention of Power Plant Condenser Tube Failures, Materials Performance, 22, 44-50, February 1983.

/18/ Eiselstein L.E., Syrett B.C., Wing S.S., Caligiuri R.D. - The Accelerated Corrosion of Cu-Ni Alloys in Sulphide-Polluted Sea Water: Mechanism No. 2, Corr. Sci., 23, 223-239, 1983.

/19/ Uhlig H. - Corrosion and Corrosion Control, John Wiley & Sons Inc., 1963.

/20/ Advanced Stainless Steels for Sea Water Application. Proceedings of the Symposium, Piacenca, Italy, February 18, 1980. H. Marrow III (ed.) (Climax Molybdenum Company).

/21/ Bock H.E., Kugler A., Lennartz G., Michel E. - Schiff und Hafen, 18-23, February 1983.

/22/ Jessling F.P.I. - Electromechanical Methods in Crevice Corrosion Testing, Br. Corr. J., 15, 51-69, 1980.

/23/ ASTM G 48-76.

/24/ Scheidegger R., Müller R.O. - Loch- und Spaltkorrosion von Chrom- und Chromnickelstählen in chloridhaltigen Lösungen, Werkst. u. Korr., 31, 387-393, 1980.

/25/ Müller R.O. - Crevice Corrosion Test for Stainless Steels in Chloride Solutions, 5th Internat. Symposium on Passivity, Extended Abstracts, Soc. de Chimie Physique, Bombannes, France, 136-138, 1983.

/26/ Hack H.P. - Crevice Corrosion Behaviour of Molybdenum-Containing Stainless Steels in Sea Water, Materials Performance, 22, 24-30, June 1983.

/27/ Streicher M.A. - Analysis of Crevice Corrosion Data from Two Sea Water Exposure Tests on Stainless Alloys, Materials Performance, 22, 37-50, May 1983.

/28/ Müller R.O. - Improving the Resistance of Condensers to Corrosion by Systematic Examination of the State of the Tubes, Brown Boveri Review, 65, 516-522, 1978.

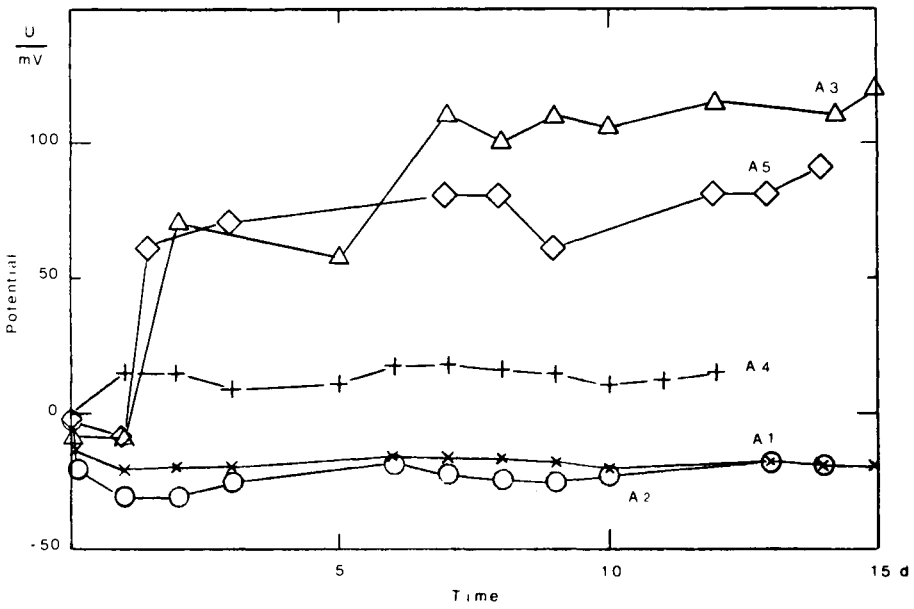

Test run	ρ (S^{--}) mg/l, 8 h/24 h	ρ (Fe^{++}) mg/l, cont.
× A1	0	0
○ A2	0	1
△ A3	1.5	0
+ A4	0.03	0
◇ A5	1.5	1

Figure 8.1: Free Corrosion Potential of Al-Brass as a Function of Time and Sulphide Content of Sea Water to Which it was Exposed

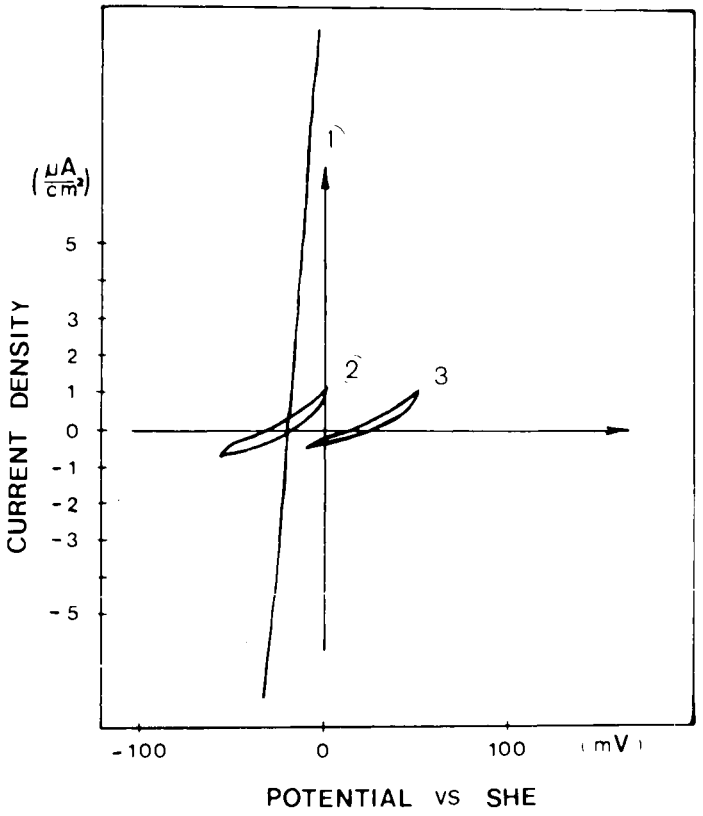

	Exposure-time	R_p $\Omega \cdot cm^2$
①	1 h	$0.7 \cdot 10^3$
②	26 d	$40 \cdot 10^3$
③	45 d	$80 \cdot 10^3$

Figure 8.2: Current-Potential Curves of Al-Brass as a Function of Time (Rotating Al-Brass Cylinders in Sea Water. No. S^{--}, ρ (Fe^{++}) = 1 mg/l)

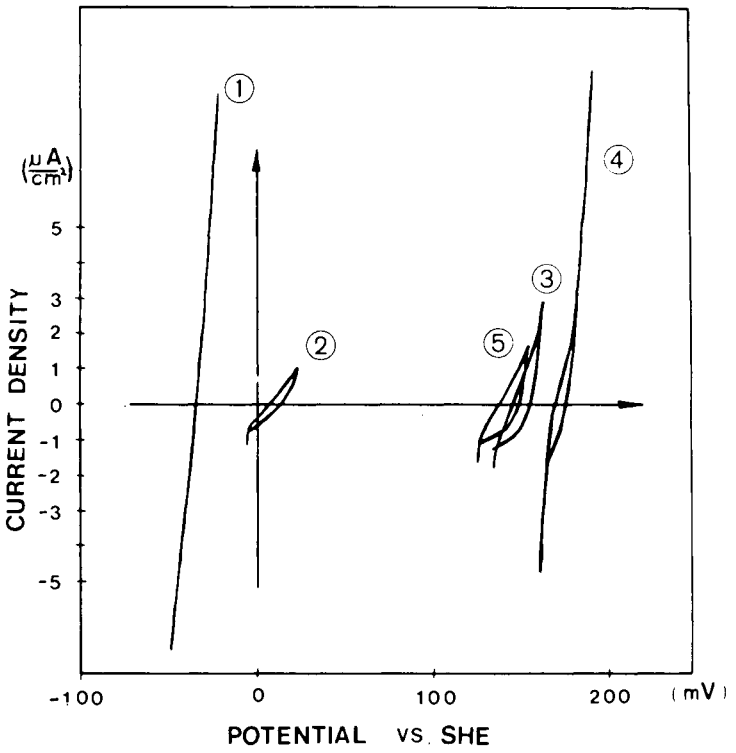

	Exposure-time	R_p $\Omega \cdot cm^2$
①	1 h	10^3
②	1 d	$1.7 \cdot 10^3$
③	4 d	$6.25 \cdot 10^3$
④	8 d	$2.14 \cdot 10^3$
⑤*	8 d*	$12 \cdot 10^3$

* After injection of S^{--}.

Figure 8.3: Behaviour of the Same Al-Brass Cylinder Considered in Figure 8.2 when in Sea Water Contaminated with Sulphide (Concentration = 0.2 mg/l)

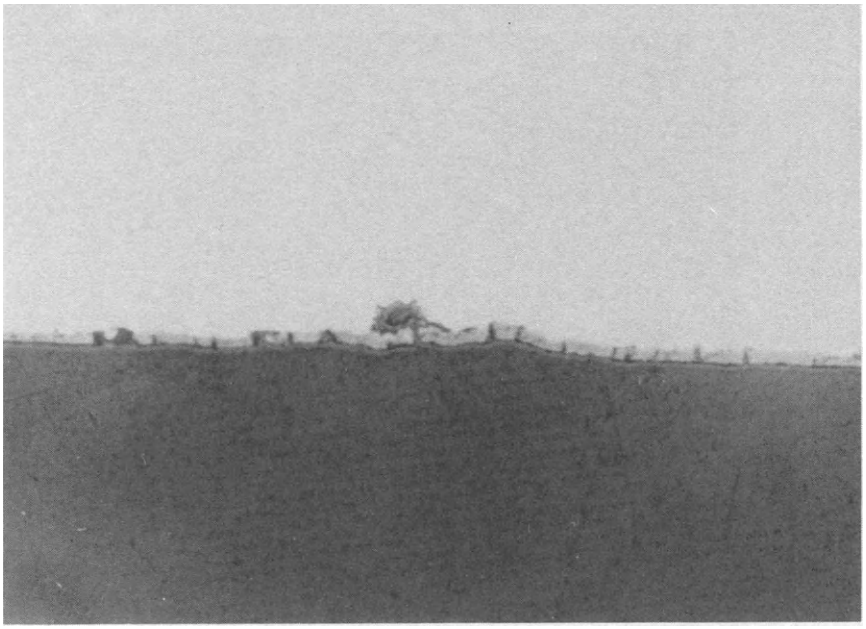

Figure 8.4: Pitting Below an Intact Iron-Hydroxide Surface Layer (Light Microscope x 500)

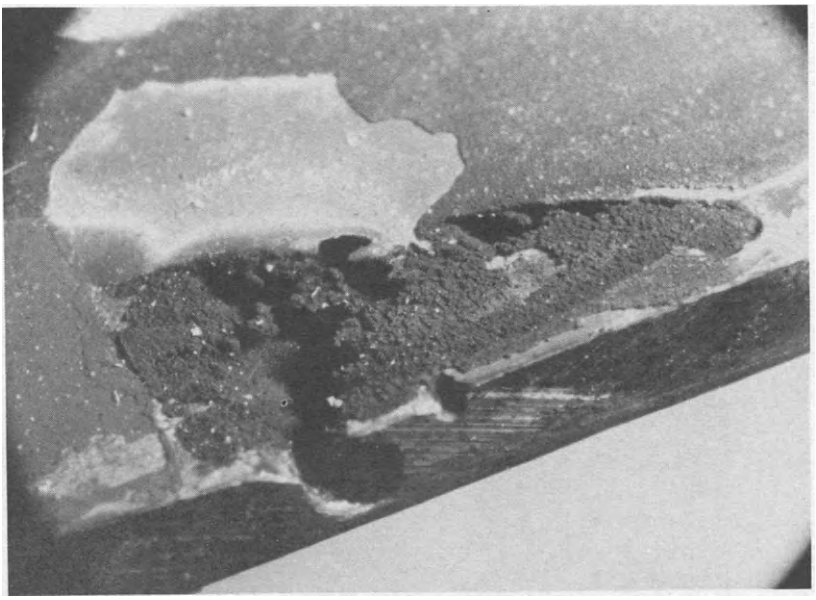

Figure 8.5: Pitting Attack Around an Obstacle

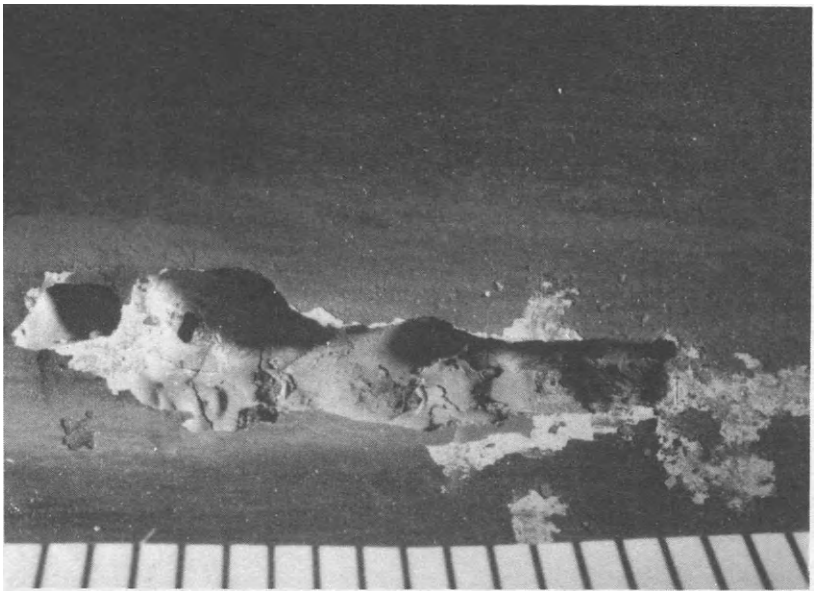

Figure 8.6: Pitting in Aggressive Sulphide-Containing Water

Figure 8.7: Erosion-Corrosion Attack at Tube Inlet Caused by Too High a Water Velocity

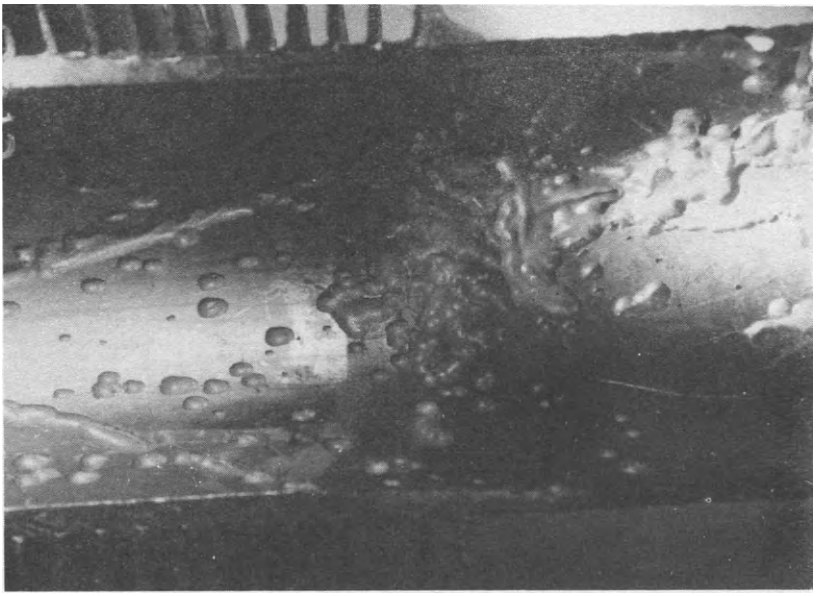

Figure 8.8: Corrosion at Tube Inlet Due to Missing Anodes

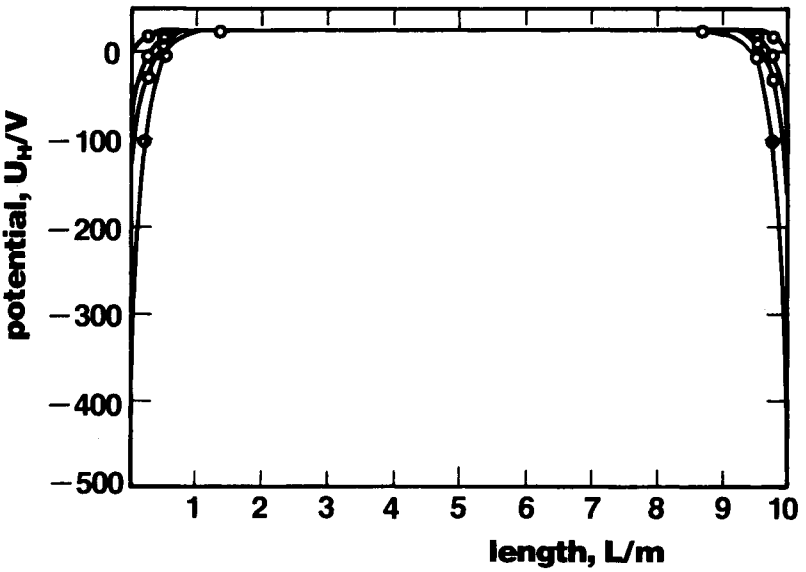

Figure 8.9: Potential Distribution in an Al-Brass Tube with External Cathodic Protection (See Text)

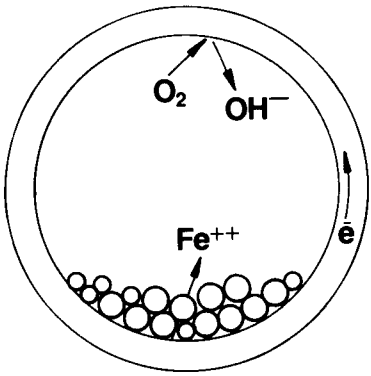

Anodic reaction: $Me \rightarrow Me^{+n} + n\bar{e}$

Cathodic reaction: $O_2 + 2\,H_2O + n\,e^- \rightarrow 4\,OH^-$

Figure 8.10: Heat-Exchanger Tube Containing a Deposit of Sand Produces a Concentration Cell

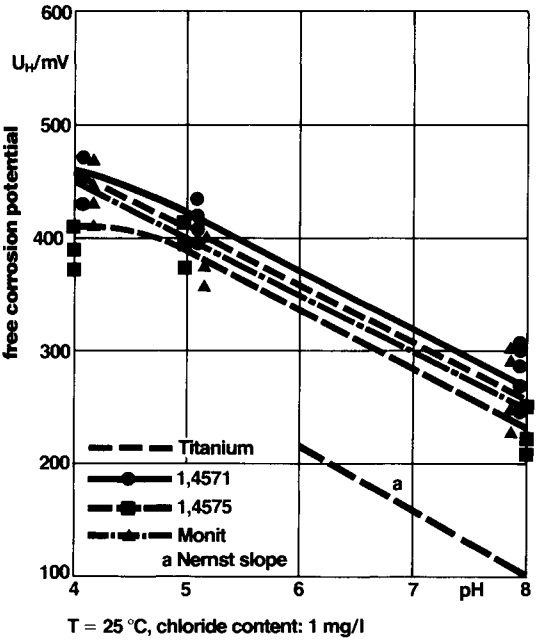

Figure 8.11: Free Corrosion Potential in Function of pH

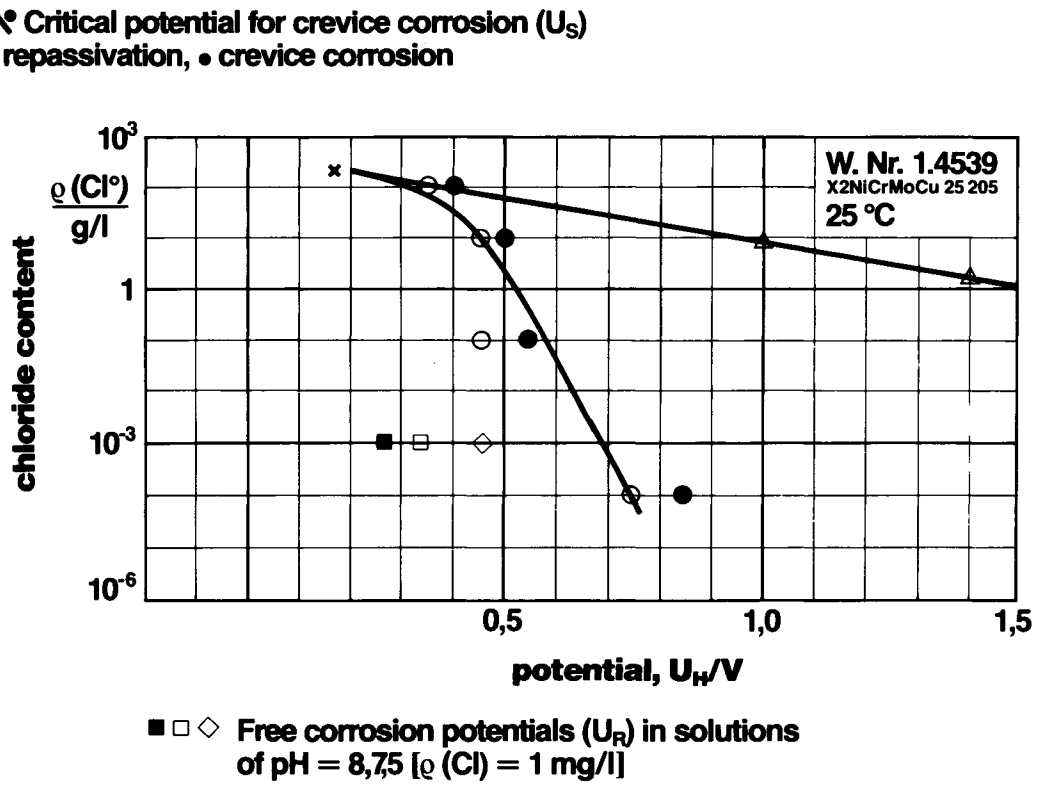

Figure 8.12: Chloride Potential Diagram (See Text)

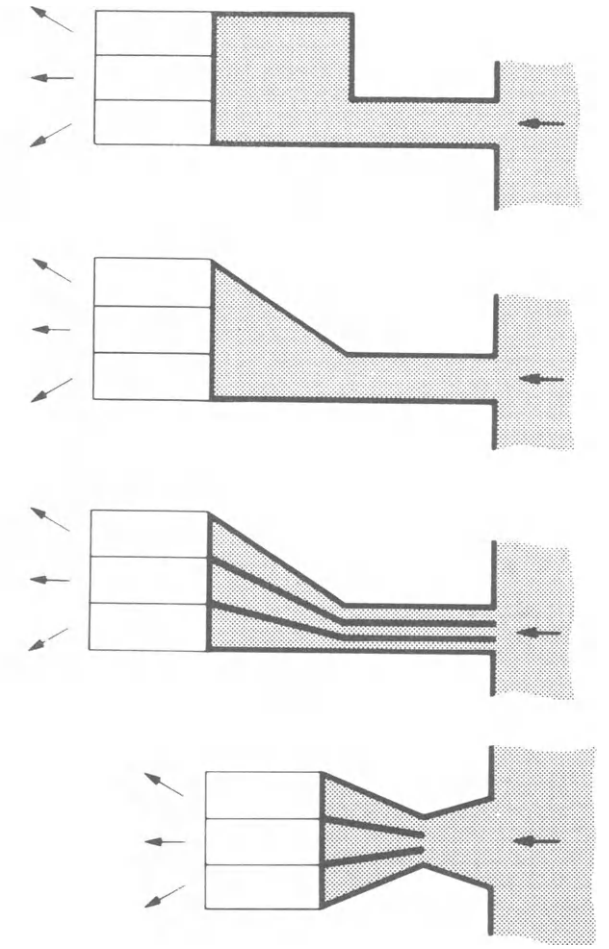

Figure 8.13: Alternative Cooling Water Intake Structures

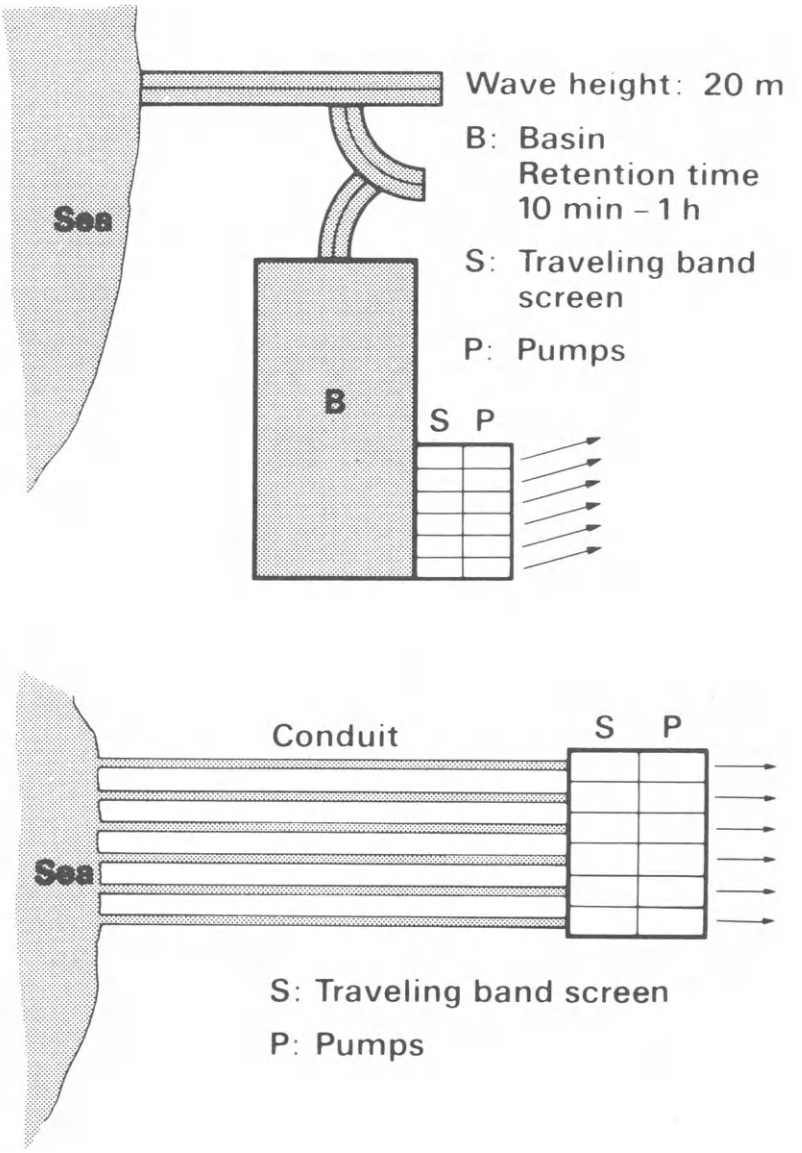

Figure 8.14: Clean Water Damping Pond